NTNU

Norwegian University of
Science and Technology

Process Integration Potentials in Coal-based Power Plants using Oxy-combustion

Tore Hatleskog Zeiner

Master of Energy and Environmental Engineering
Submission date: Januar 2012
Supervisor: Truls Gundersen, EPT
Co-supervisor: Fu Chao, EPT

Norwegian University of Science and Technology
Department of Energy and Process Engineering

NTNU

Norwegian University
of Science and Technology

Department of Energy
and Process Engineering

EPT-M-2011-68

MASTER THESIS

for

Student Tore Hatleskog Zeiner

Fall 2011

Process Integration Potentials in Coal-based Power Plants using Oxy-combustion

Potensialer for Prosessintegrasjon i Kullbaserte Kraftverk med Oksygenforbrenning

Background

Coal will continue to be a dominant energy source in the near future timeframe, in particular in China, USA and India, although it is the most carbon intensive fuel. Carbon capture and storage (CCS) is an important way to mitigate CO_2 emissions from fossil fuel based power plants. The power efficiency penalty and the cost related to CCS are the two biggest barriers from an economic point of view. The practical and economic solution to the CO_2 capture problem for such plants must be found as soon as possible to mitigate global warming. At the same time, of course, there is a need to solve problems related to transportation and storage of CO_2.

In the Department of Energy and Process Engineering, a PhD project was started in 2008 with focus on process integration of oxy-combustion processes for coal-based power plants with CO_2 capture. Oxy-combustion is a promising option for CO_2 capture especially for coal-fired power plants, since the reduction in efficiency is less than for natural gas based power plants. In an oxy-combustion process, the efficiency penalty is mainly caused by the air separation process (a cryogenic Air Separation Unit – ASU) and the CO_2 conditioning process (Compression and Purification Unit – CPU). Research in the mentioned PhD project has identified improvement opportunities both in the ASU and the CPU. This Master thesis should study process integration opportunities between the various sub-processes of a coal-based power plant, including but not limited to the ASU and CPU.

The Master thesis is a continuation of a last year Project during the fall of 2010, where simulation models were developed for the CO_2 conditioning process, and where some preliminary ideas for process integration were discussed.

Objective

The main objective of this Master thesis is to establish potentials for energy savings by process (heating/cooling) integration in a coal-based power plant where oxy-combustion is used as the route to CO_2 capture. One particular issue is to study the integration of compression heat from the ASU and the CPU with the power cycle, however, other process integration opportunities for the entire power plant should be considered.

The following tasks are to be considered:

1. Build knowledge about the complex steam cycles used in coal-based power plants by combining textbooks in thermodynamics with relevant literature.

2. Briefly describe the overall power plant with its sub-sections (ASU, combustion section, steam cycle and power production, CPU, etc.)

3. Describe and modify the Aspen Plus simulation model that has been developed for the power plant. A more detailed model is required for the hot side (gas side) of the steam boiler in order to make the study more accurate.

4. Study opportunities for improving the energy efficiency of the coal-based power plant through increased process integration. Such opportunities could be:
   - Integration of compression heat (from ASU and CPU) with the steam cycle (i.e. to use adiabatic compression).
   - Integration of compression heat with the regeneration of molecular sieves in the ASU and the CPU.
   - Using compression heat to preheat the recycled flue gas and oxygen prior to combustion.
   - Integration of compression heat and the low temperature heat from the flue gas with a new CO_2 Rankine cycle.
   - Any other integration options the candidate may discover.

5. Discuss to what extent the recent discoveries about energy savings caused by design modifications in the ASU and the CPU will affect the scope for process integration in the entire power plant. Do any of these modifications create new scope for integration?

6. Discuss the practical and economical aspects of any proposed process integration schemes resulting from task 4. Here, the economical analysis should not include cost estimations, only a qualitative discussion about the major economic effects of the changes in design (equipment count, added complexity, main units from a cost point of view).

7. Conclude by proposing a ranked list of process integration projects, while indicating to what extent these projects are related or in conflict.

-- ” --

Within 14 days of receiving the written text on the master thesis, the candidate shall submit a research plan for his project to the department.

When the thesis is evaluated, emphasis is put on processing of the results, and that they are presented in tabular and/or graphic form in a clear manner, and that they are analyzed carefully.

The thesis should be formulated as a research report with summary both in English and Norwegian, conclusion, literature references, table of contents etc. During the preparation of the text, the candidate should make an effort to produce a well-structured and easily readable report. In order to ease the evaluation of the thesis, it is important that the cross-references are correct.

In the making of the report, strong emphasis should be placed on both a thorough discussion of the results and an orderly presentation.

The candidate is requested to initiate and keep close contact with his/her academic supervisor(s) throughout the working period. The candidate must follow the rules and regulations of NTNU as well as passive directions given by the Department of Energy and Process Engineering.

Risk assessment of the candidate's work shall be carried out according to the department's procedures. The risk assessment must be documented and included as part of the final report. Events related to the candidate's work adversely affecting the health, safety or security, must be documented and included as part of the final report.

Pursuant to "Regulations concerning the supplementary provisions to the technology study program/Master of Science" at NTNU §20, the Department reserves the permission to utilize all the results and data for teaching and research purposes as well as in future publications.

The final report is to be submitted digitally in DAIM. An executive summary of the thesis including title, student's name, supervisor's name, year, department name, and NTNU's logo and name, shall be submitted to the department as a separate pdf file. Based on an agreement with the supervisor, the final report and other material and documents may be given to the supervisor in digital format.

Department of Energy and Process Engineering, 8 September 2011

Olav Bolland
Department Head

Truls Gundersen
Academic Supervisor

Research Advisors:

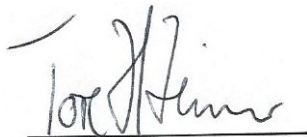PhD student Chao Fu, Department of Energy and Process Engineering, NTNU

Preface

This master thesis ends my five and a half years at Energy and Enviromental Engineering at NTNU. The thesis was written at the Department of Energy and Process Engineering.

Working on this thesis was challenging and exciting, and the technology discussed in this report may play a significant role in the future. Even though this master thesis presents many results, the work is far from finished, and there are many possibilities yet to explore. Hopefully this report can serve as a starting point for future student projects.

I would like to thank my supervisor Truls Gundersen and my research advisor Fu Chao for all the advice and help they have given during the process.

Any questions regarding the contents of the report can be sent to my e-mail address: tore.zeiner@gmail.com

Oslo, January 27, 2012

Tore Hatleskog Zeiner

Abstract

Oxy-combustion is a promising technology for capturing CO_2 from coal based power plants. In a coal based oxy-combustion power plant coal is combusted with high purity oxygen in order to produce steam for power production. The flue gas from this combustion consists mainly of H_2O and CO_2, but it will also be polluted with other components due to in-leakage of air, impurities in the coal, excess oxygen in the combustion and diluted oxygen supply. The main separation processes in such a power plant takes place in an air separation unit (ASU) where oxygen is separated from nitrogen, and in the compression and purification unit (CPU) where the CO_2 in the flue gas is separated from the H_2O and the other pollutants and compressed for transportation and storage. The introduction of these two units causes an efficiency penalty to the power plant.

In this master thesis it is studied if and how heat integration of low temperature heat can decrease the efficiency penalty related to the ASU and CPU. The base case power plant is a coal based oxy-combustion power plant with a 567MW net power output and a thermal efficiency 31,32%. The heat sources considered are the heat which is removed by intercoolers in the compressors in the ASU and CPU, and waste heat from the flue gas exiting the steam generator. It is also studied if lifting the temperature level of the compression heat by compressing adiabatically will increase the potential for heat integration.

Three main cases are considered for integration; integrating compression heat and waste heat from the flue gas with the feedwater system in the steam cycle of the power plant, integrating compression heat or flue gas heat to increase preheat of the recycled flue gas and oxygen entering the combustion, and integrating waste heat from the flue gas with a CO_2 Rankine Cycle. It was found that integration of compression heat with the feedwater can increase the thermal efficiency of the power plant by 1,19% if the compressors are operated with intercooling and 1,49% if adiabatic compression is utilized. If the flue gas heat is also integrated, the efficiency increases by 1,72% with intercooled compression and 1,96% with adiabatic compression. Utilizing flue gas heat to preheat the recycled flue gas and oxygen can give efficiency increases in the region of 0,3-0,7%. The same applies if compression heat is utilized for this preheating. Since the temperature level of the recycled flue gas and oxygen is low, it is not necessary to compress adiabatically. If the waste heat in the flue gas is integrated with a CO_2 Rankine cycle, efficiency improvements in the region of 0,47 to 0,51% can be obtained.

The integration projects discussed in this report will increase the complexity of the system and may increase equipment costs. It is necessary to do a more detailed analysis of the heat exchanger networks required to reach the energy targets and heat exchanger surface area requirements in order to properly estimate the costs and choose the optimal configuration for integration. However it is recommended that future studies focus on the use of adiabatic compression heat as it has been shown to give significant increases in efficiency. Whether or not to include the flue gas in the integration depends on whether or not it is cost-efficient to introduce corrosion resistant heat exchangers to cool it below the acidic dew point.

Sammendrag

Oksy-forbrenning er en lovende teknologi for å fange CO_2 fra kullbaserte kraftverk. I et kullbasert oksy-forbrenningskraftverk brennes kull med nesten rent oksygen for å produsere damp til kraftproduksjon. Avgassen fra denne forbrenningen består hovedsakelig av CO_2 og H_2O, men vil også være forurenset med andre gasser grunnet lekkasje av luft inn i forbrenningen, urenheter i kullet, oksygenoverskudd i forbrenningen og forurensninger i oksygenet som blir tilført til forbrenningen. Separasjonsprosessene i et slikt kraftverk vil hovedsakelig finne sted i en luftseparasjonsenhet (ASU) hvor oksygen blir separert fra nitrogen og i en CO_2 foredling- og kompresjonsenhet (CPU) hvor CO_2 separeres ut fra avgassen og komprimeres for transport og lagring. På grunn av disse to enhetene vil et oksy-forbrenningskraftverk ha dårligere virkningsgrad enn et standard kullkraftverk.

I denne masteroppgave blir det utredet om og hvordan varmeintegrasjon av lavtemperaturvarme kan redusere tapet i virkningsgrad forårsaket av ASU og CPU. Referansekraftverket er et kullbasert oksy-forbrenningskraftverk som leverer 567MW, og har en termisk virkningsgrad på 31,32%. Varmekildene som evalueres er kompresjonsvarme som fjernes i mellomkjølerene til kompressorene i ASU og CPU, og spillvarme fra avgassen fra forbrenningen. Det blir i tillegg utredet om det er gunstig å løfte temperaturen til kompresjonsvarmen ved å komprimere adiabatisk vil øke potensialet for varmeintegrasjon.

Tre hovedscenarioer blir evaluert for integrasjon; integrasjon av kompresjonsvarme og spillvarme fra avgass med fødevannsforvarmingen i kraftverkets dampsyklus, integrasjon av kompresjonsvarme eller spillvarme fra avgass for å forvarme oksygen og resirkulert avgass inn til forbrenningen, og bruk av spillvarme fra avgass med en CO_2 Rankine syklus. Det ble funnet at integrasjon av kompresjonsvarme med fødevannsforvarmingen kan øke virkningsgraden til kraftverket med 1,19% med mellomkjølt kompresjon, og 1,49% med adiabatisk kompresjon. Dersom spillvarme fra avgass også integreres vil økningen i virkningsgrad bli 1,72% med mellomkjølt kompresjon og 1,96% med adiabatisk kompresjon. Bruk av spillvarme fra avgass til å forvarme oksygen og resirkulert avgass kan gi en økning i virkningsgrad rundt 0,3-0,6%. De samme tallene oppnås dersom kompresjonsvarme brukes til denne forvarmingen. Siden temperaturen til strømmen med resirkulert avgass og oksygen er lav, er det ikke nødvendig å bruke adiabatisk kompresjon for å gjennomføre denne forvarmingen. Dersom spillvarmen i avgassen benyttes med en CO_2 Rankine syklus vil økningen i virkningsgrad være rundt 0,47-0,51%.

Integrasjonsprosjektene diskutert i denne rapporten vil øke kompleksiteten til kraftverket og kan medføre ekstra investeringskostnader. Det er nødvendig å gjennomføre en detaljert analyse av varmevekslernettverkene som kreves for å nå de satte målene for energiforbruk og kravene til areal i varmevekslerne for å kunne estimere kostnadene og velge den optimale konfigurasjonen av kraftverket. For fremtidige studier anbefales det å fokusere på adiabatisk kompresjon ettersom det har vist seg å gi betydelige økninger i kraftverkets virkningsgrad. Om avgassen skal brukes til varmegjenvinning avhenger av om det er lønnsomt å investere i rustfrie varmevekslere for å kjøle den under syreduggpunktet.

X

Nomenclature

Abbreviations

ASU	Air separation unit
CCS	CO_2 capture and storage
CPU	Conditioning and purification unit
FWH	Feedwater heater
GCC	Grand composite curve
HHV	Higher heating value
HP	Higher pressure
IP	Intermediate pressure
LHV	Lower heating value
LP	Low pressure

Greek letters

η - efficiency

Roman letters

A	Area	[m^2]
CP	Heat capacity flow rate	[kW/K]
k	Isentropic exponent	[-]
h	Specific enthalpy	[kJ/kg]
h_C	Cold side film heat transfer coefficient	[kW/m^{2}K]
h_H	Hot side film heat transfer coefficient	[kW/m^{2}K]
LHV	Lower heating value	[kJ/kg]
$\dot{m}$	Mass flow	[kg/s]
N	Number of streams	[-]
n	Isentropic exponent	[-]
$O_{2,excess}$	Excess oxygen	[kg/s]
p	Pressure	[bar]
$\dot{Q}$	Heat flow	[kW]
R	Gas constant	[kJ/kgK]
T	Temperature	[K]
ΔT	Temperature difference	[K]
ΔT_{LM}	Logarithmic mean temperature difference	[K]
ΔT_{min}	Minimum temperature difference	[K]
U	Overall heat transfer coefficient	[W/m^{2}K]
u_{min}	Minimum number of heat exchange units	[-]
v	Specific volume	[m^3/kg]
$\dot{W}$	Work rate	[kW]
$\Delta\dot{W}$	Work rate increase	[kW]

Subscripts

AD	Adiabatic
AI	Air in-leakage
aux	Auxiliary
C	Compressor
ex	Steam extraction
F	Fan
f	Fuel
FD	Forced draft
gen	Generator
IC	Intercooled
ID	Induced Draft
mech	Mechanical
P	Pump
p	Polytropic
RC	Recycle
SG	Steam generator
stoi	Stoichiometric
S	Steam
s	Supply
T	Turbine
t	Target
th	thermal

1 Introduction

1.1 Background

There is an agreement among scientists that the increase in the average global temperature is a result of man-made emissions of greenhouse gases such as CO_2. In order to reduce future CO_2 emissions from power plants fired by fossil fuels, CO_2 capture and storage (CCS) may be used to mitigate CO_2 emissions. Léandri et al. (2011) have found CCS to be cost competitive with other low carbon alternatives for power production, and states that CCS is a necessity if future reductions of CO_2 emissions are to be achieved. One of the potential problems with CCS is the efficiency penalty related to separation and compression of CO_2.

There are three main paths to capturing CO_2 from power plants: Post combustion, pre combustion and oxy-combustion. In this report CCS from a pulverized coal fired oxy-combustion power plant will be studied. IEAGHG (2007) and Kanniche et al. (2010) mentions oxy-combustion as a promising option of capturing CO_2 from coal based power plants as the investment costs and efficiency penalty related to CO_2 capture are lower than for natural gas based power plants. The efficiency penalty in an oxy-combustion power plant is mainly caused by the air separation unit (ASU) and the CO_2 compression and purification unit (CPU). Since it is likely that coal will continue to be a dominant energy source in the near future, future developments within oxy-combustion are to be expected.

1.2 Motivation

In order for the oxy-combustion technology to become more cost-efficient and competitive, improvements in efficiency should be made. In this report the potential for process integration through heat recovery is studied. The focus is on heat recovery from compression streams in the ASU and CPU, and from the flue gas exiting steam generator. One topic of particular interest will be whether to use adiabatic or intercooled compression heat with the steam power cycle in the power plant.

1.4 Methodology

After building knowledge on oxy-combustion, coal based power plants and heat integration, the performance of a pulverized coal fired oxy-combustion power plant will be established through simulations in Aspen Plus. From these simulations stream data will be extracted in order to

evaluate the potential for integrating compression and/or flue gas heat. Simulations of integration projects will be performed in order to evaluate the potential.

1.3   Limitations of Study

In this report only the potential of recovery of the low temperature heat from compression and the flue gas is studied. Process integration will results in reduction of both cooling and heating, but this report will focus only on heating. Since both the ASU and CPU operate at sub-ambient temperature levels, there may be some potential for integration of cold energy, but this potential will not be evaluated in this report. Cost calculations, heat exchanger network design and heat exchanger area calculations are not a part of this report. However the factors which may affect the costs and complexity of the system will be briefly discussed. Pressure drops and heat losses are not accounted for in the integration study.

1.4   Report Outline

The report is organized in 9 chapters including this introduction. In **Chapter 2** some basic theory regarding oxy-combustion, coal fired power plants, compression and heat integration will be given. The theory presented is the basis for the modeling and heat integration performed later in the report. In **Chapter 3** a description of a coal fired oxy-combustion power plant is given and the performance of the power plant is determined through an Aspen Plus simulation. In **Chapter 4** an introduction to the heat sources and possibilities for integration is given. In **Chapters 5** to **7**, 7 separate integration cases are evaluated and the performance of the integrated designs is established through simulations. **Chapter 8** gives a discussion and comparison of the proposed integrations. **Chapter 9** is the conclusion of the report, and some suggestions for further work are given.

2 Theory and definitions

2.1 What is Oxy-Combustion?

The basic idea of oxy-combustion is to have combustion take place with pure or almost pure oxygen and to have close to zero excess oxygen in the combustion (Bolland, 2010), instead of using air. The main reactions when coal is combusted with pure oxygen are as follows:

$$C + O_2 \rightarrow CO_2$$

(2.1)

$$2H_2 + O_2 \rightarrow 2H_2O$$

(2.2)

As can be seen from equations 2.1 and 2.2, the main combustion products are CO_2 and H_2O. In order to avoid excessively high temperatures in the combustion, cooled flue gas is recycled back into the combustion together with the oxygen supply in order to keep the temperature down. Recycling of the flue gas can be done before or after flue gas cleaning and treatment. Flue gas cleaning and treatment includes ash removal, drying and flue gas desulfurization. The configuration and design of the flue gas recycle depend on the coal composition, feasible limits of dust, sulfur oxides and water vapour (Kather and Klostermann, 2011). In this report a power plant with treated recycle will be studied.

The oxygen is supplied from an Air Separation Unit (ASU). Due to the high quantities of oxygen required, cryogenic air separation is currently the only feasible method of separating oxygen from nitrogen. Cryogenic air separation has already been applied throughout several decades on a commercial scale, and is a mature technology (Kather and Klostermann, 2011). The oxygen can be supplied at purities up to 99,5%, but due to the high energy requirements for high purity oxygen it seems optimal to choose purities around 96,5% (Tranier and Perrin, 2011). A detailed description of the ASU used in this study is given in Chapter 3.3.

Due to in-leakage of air, impurities in the coal, excess oxygen in the combustion and diluted oxygen from ASU, the flue gas will be diluted with more components than H_2O and CO_2. In order to reach storage specifications for the CO_2 the flue gas will need to be cleaned and compressed in a compression and purification unit (CPU). Sulfur, nitrogen-oxides, water vapour and dust can be removed by the same technology as for conventional power plants. Components with low boiling points, such as nitrogen, argon and oxygen, need to be removed by compression

and refrigeration (Kather and Klostermann, 2011). A detailed description of the CPU used in this study is given in Chapter 3.4.

2.2   Condensation Power Plants

Power production from coal can be achieved through combustion of the coal and heat rejection to a steam cycle or by gasification and combustion in a gas turbine system, with the primary being the most common. This report will focus on power plants with a pulverized coal fired steam generator, a so-called condensation power plant. In this chapter a basic description of coal based power plants will be given. Since the steam cycle is a topic for the heat integration projects in Chapter 5, a more detailed description of steam cycles and steam generators will be given.

2.2.1 Overview

A schematic of a pulverized coal air-fired power plant is shown in Figure 1. Coal is fed to the mills where it is pulverized. It is then mixed with preheated combustion air and introduced to the furnace where it is mixed with more preheated air. The combustion flue gas is used to produce steam in a steam generator. The produced steam is expanded through turbines in a steam cycle in order to produce work. After passing through the turbines, the steam is condensed in a condenser, pumped up and reintroduced to the steam generator. The flue gas exiting the steam generator is used to preheat the combustion air after NO_x removal. It is then introduced to an electrostatic precipitator where dust is removed. After the dust is removed the flue gas is led by the induced-draught (ID) fans into a desulfurization unit. The desulfurized flue gas is led to the stack where it is vented to the atmosphere.

In a pulverized coal power plant with oxy-combustion some modifications are made. The oxygen is supplied from an ASU and instead of being mixed with combustion air; the coal is being mixed with recycled flue gas and oxygen in the combustion process. The flue gas which is not recycled is led to the CPU where CO_2 is separated and compressed for storage. The introduction of an ASU and CPU reduces the efficiency of the power plant. A detailed description of the oxy-combustion power plant in this study is available in Chapter 3.
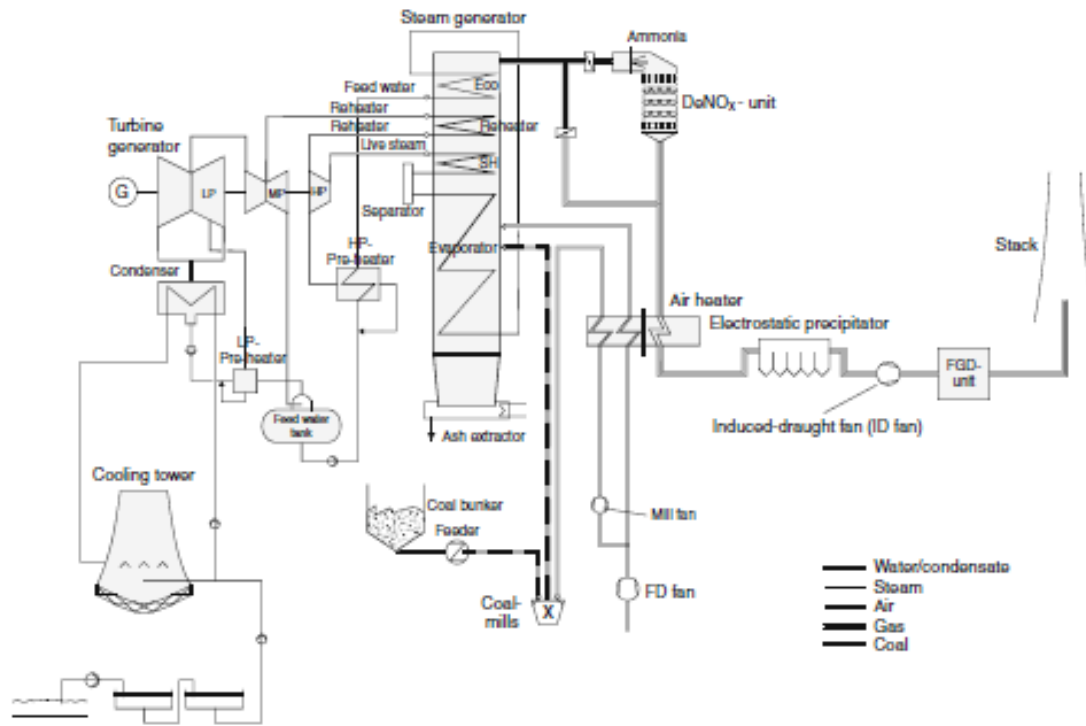
Figure 1 – Schematic of an Air-Fired Pulverized Coal Power Plant

2.2.2 Ideal Rankine Cycle
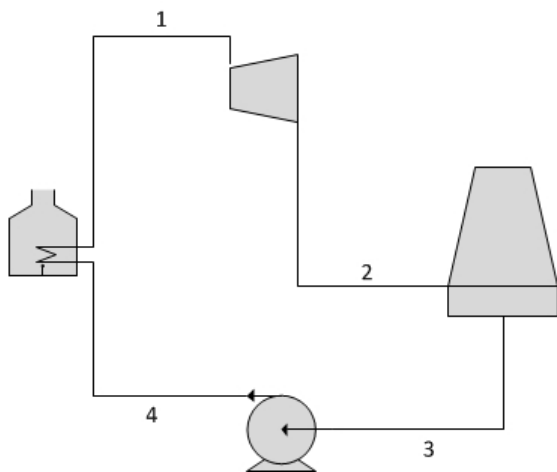
Figure 2 – Flow Diagram of Ideal Rankine Cycle
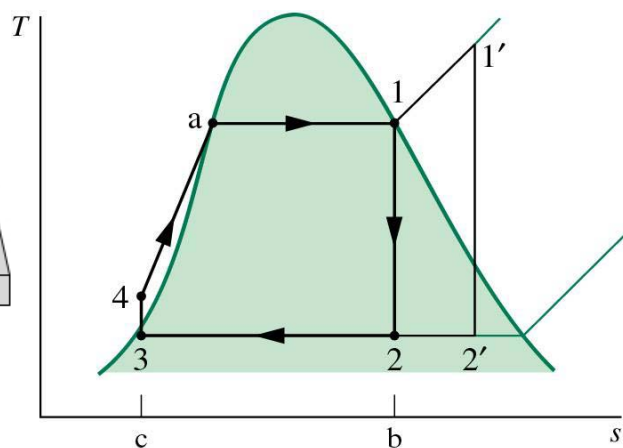
Figure 3 – T-S Diagram of Ideal Rankine Cycle (Moran and Shapiro, 2006)

A flowsheet and T-S diagram of an ideal Rankine cycle is shown in Figure 2 and Figure 3 respectively. From 1 to 2 an isentropic expansion is performed through a turbine from saturated vapor to the condenser pressure. Water droplets can erode the turbine blades, and it is therefore desirable to keep the outlet steam quality as high as possible. It is standard practice to keep the

steam quality above 90% at the outlet (Moran and Shapiro, 2006, p. 340). The steam quality at the outlet is therefore a decisive factor when determining the condenser pressure. From 2 to 3 the two-phase mixture is condensed to saturated liquid by cooling water in a cooling tower. The condensate is then pumped isentropically from 3 to 4 before being evaporated to saturated vapor from 4 to 1. The heat is most commonly supplied by the combustion of coal or a nuclear reactor. It is possible to superheat the steam in order to improve performance. State 1 will then be replaced by 1' and state 2 by 2' in the T-S diagram. Superheat increases the steam quality at the outlet and the work output from the turbine. This can be seen through the increased area in the T-S diagram.

2.2.3 Improvements on Rankine Cycle

There are several improvements that can improve the performance of the Rankine Cycle. In Spliethoff (2010), p. 142 it is stated that: "Improvements of thermal cycles aim at attaining a high mean temperature of the heat addition and a low mean temperature of the heat extraction". In this chapter methods to increase the average temperature of heat addition and to lower the mean temperature of heat extraction are discussed.

Raising Temperature of Heat Addition

By raising the live steam pressure[1] the boiling temperature of the water is raised, and the average temperature of heat addition in the steam generator is consequently increased. This tends to improve the thermal efficiency. However, by raising the pressure, one increases the pump work required for the feedwater pumps. The effect of increasing the pressure will therefore diminish at high pressures. At one point the increase in efficiency will stop, and further increases in pressure will have a negative impact on the efficiency. The pressure at where the increase in efficiency stops is however considerably higher than the pressures allowed by current material technology (Spliethoff, 2010, p. 142-143).

The increase in pressure shifts the steam conditions to the left in the T-S diagram. If the exhaust pressure is kept constant, this will increase the steam quality at the outlet. If the steam quality decreases below the 90% stated in chapter 2.2.2, water droplets may cause erosion on the turbine blades. In Figure 4 the impact of the steam pressure is shown in a T-S diagram. Introducing reheat of steam enables to take advantage of high live steam pressures by helping to avoid low quality steam at the exit of the turbine. In Figure 5 it can be seen how reheating steam at an

---

[1] Live steam pressure is defined as the pressure of the steam which is exiting the boiler before it has been used to produce any work.

intermediate pressure contributes in maintaining high steam quality at lower exhaust pressures. Reheat will also contribute to raising the average temperature of heat addition. Modern power plants can have single or double reheat.
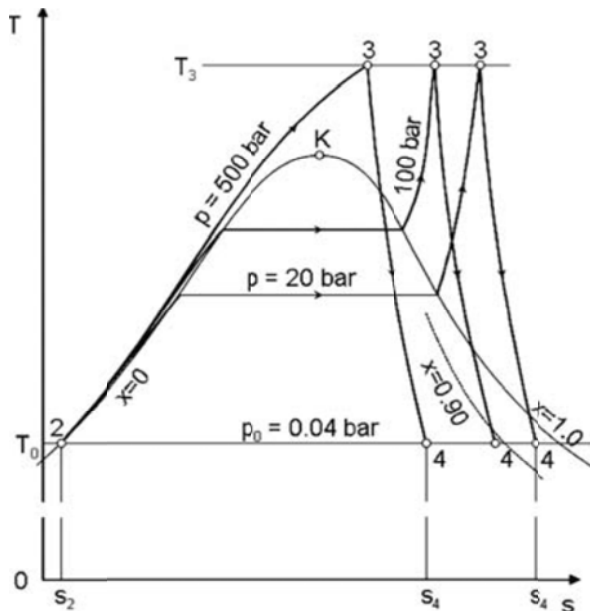
Figure 4 - Impact of increased pressure
(Baehr and Kabelac, 1996)
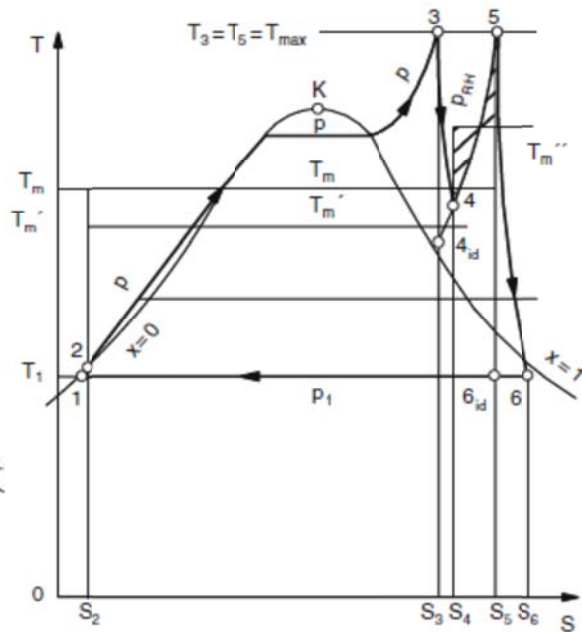
Figure 5 – Impact of reheat
(Baehr and Kabelac, 1996)
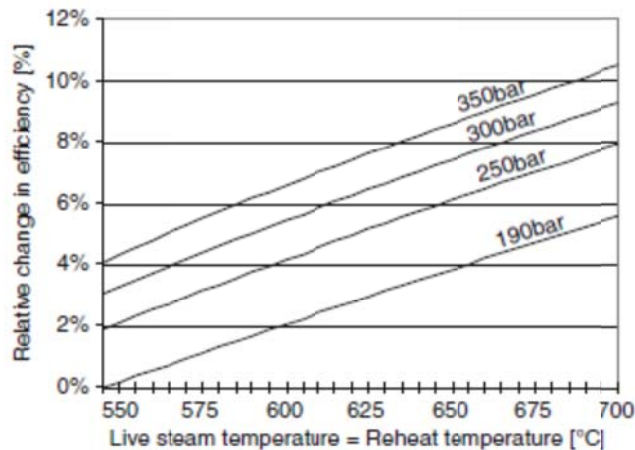
Figure 6 - Influence of live steam conditions on efficiency (Spliethoff, 2010)

In Figure 6 the impact of increased live steam pressure and reheat temperature on efficiency is shown. As can be seen the efficiency increases with higher pressures and temperatures. However the increment in increase of efficiency decreases as the pressure is raised. This effect cannot be seen on increases in temperature. Research projects are now focusing on development of new materials for future power plants that can withstand live steam pressures up to 350bar and

temperatures of up to 750°C (Spliethoff, 2011, p. 16). The steam cycle studied later in this report has live steam conditions of 242bar and 600°C and a reheat temperature of 620°C.

A third way of increasing the average temperature of heat addition is to introduce regenerative heating, commonly referred to as feedwater preheating. In a feedwater preheater the condensate is heated before entering the steam generator. The heat is supplied by steam extractions from the turbine. It is common to use at least one direct contact feedwater preheater operating above ambient pressure in order to vent out oxygen and other solved gases from the cycle. This is heater is commonly referred to as a deaerator, and is needed to maintain the purity of the working fluid in order to avoid corrosion (Moran and Shapiro, 2006, p. 352). Introducing more feedwater heaters will increase thermal efficiency, but will increase investment costs. Large power plants normally have six to nine feedwater heaters with feedwater outlet temperatures between 250°C and 300°C (Spliethoff, 2010, p.148).
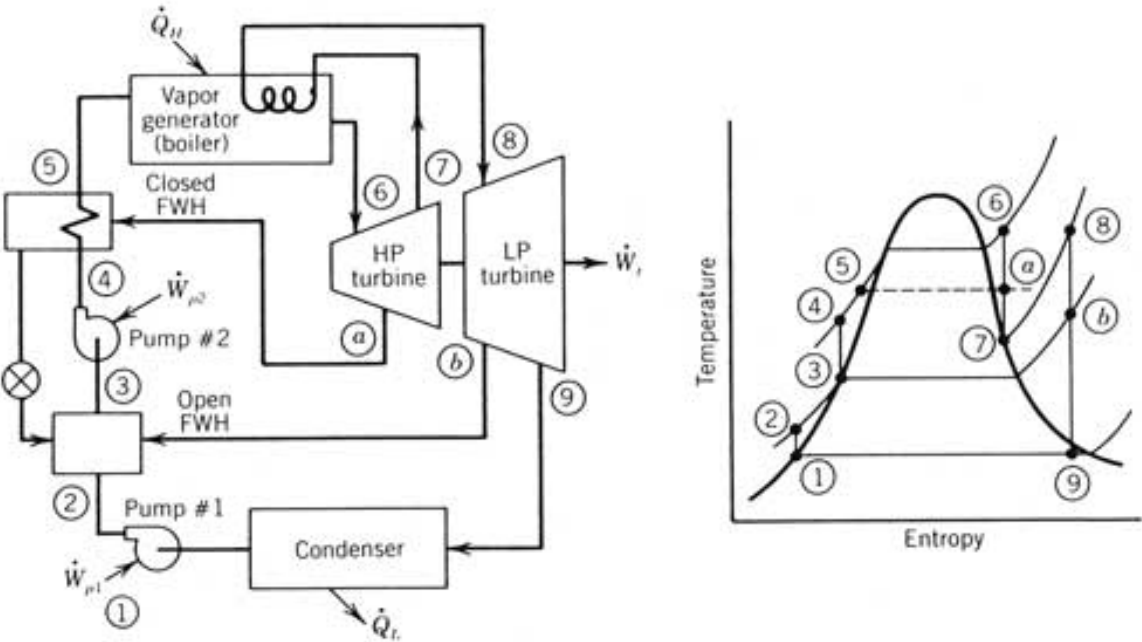
Figure 7 – Flow and T-S diagram of Regenerative Rankine Cycle with Single Reheat (Stine and Geyer, 2001)

In Figure 7 a flow sheet and T-S diagram of a Rankine cycle with one open and one closed feedwater heater and single reheat can be seen. The condensate exiting the condenser is lifted to a higher pressure in a pump from 1 to 2 before it enters an open feedwater heater where it is heated to its saturation temperature by a steam extraction from the LP turbine from 2 to 3. The feedwater is then pumped up to a higher pressure from 3 to 4 and heated in a closed HP feedwater heater from 4 to 5. The feedwater then enters the steam generator where it is superheated to state 6 and expanded in a HP turbine from 6 to 7. Some steam is extracted to the

closed feedwater heater where it rejects heat to the feedwater through condensation. The condensate is cascaded back into the open feedwater heater. The exhaust from the HP turbine enters re-enters the steam generator and is reheated to state 8 before entering an LP turbine where it is expanded from 8 to 9. The two-phase exhaust is thereby condensed in the condenser from 9 to 1. Real power plants have more turbine sections, steam extractions and feedwater heaters, but the principles remain the same.

Lower Temperature of Heat Rejection

The amount of work which is obtained from a Rankine cycle depends on the condenser pressure. Superheat and reheat have already been mentioned as modifications that can allow lower exhaust pressures due to the fact that they give higher steam quality at the outlet. Even though these modifications allows for low exhaust pressures and temperatures, the lack of heat sinks means that the exhaust temperature in a condensation power plant will normally not be below 30°C (Spliethoff, 2010, p. 151). The exhaust temperature is determined by the temperature and availability of the cooling medium and the temperature difference in the condenser. Low temperature differences in the condenser will permit lower exhaust temperatures at the expense of increased investment costs. It is therefore necessary to find the optimal trade-off between investment costs and exhaust temperature before designing a steam cycle. A review of condenser technologies can be found in Spliethoff (2011), p. 153-161.

2.2.4 Steam Generation

The following descriptions of steam generators are based on Spliethoff (2010), p. 81-93. Only pulverized coal fired steam generators are treated in this chapter.

The chemically bound energy in the fuel is released through combustion and transferred from the combustion flue gas to the steam production in a steam generator with steam-water heating surfaces. Steam generators for large scale power production utilize complex parallel tube systems for preheating, evaporating, superheating and reheating the water/steam. The different sections of the steam generator operate with different heat flux densities depending on the type of firing and the flue gas properties. Following the combustion, the flue gas temperature will be high, and heat transfer by radiation dominates. As the flue gas passes through the steam generator it rejects heat to the steam production and the temperature decrease gradually results in more convective heat transfer towards the end of the steam generator. The heat transfer coefficients achieved by evaporation are much higher than those of heating sub-cooled water or superheated steam. The

furnace walls immediately after combustion provide the highest heat flux densities on the gas side, and it is therefore standard practice to place the evaporator in the furnace wall.

There are several steam generator constructions available, with the main difference between them being the design of the evaporator. There are two main types of evaporator configuration, circulation systems and once through systems. In Figure 8 the configuration of a circulation (a) and a once through (b) evaporator can be seen. In a circulation evaporator water is partially evaporated before water and steam is separated in a drum. The water is reintroduced into the evaporator while the steam passes onwards to the superheaters for superheating. In a once-through system the water is completely evaporated and slightly superheated in the evaporator before it passes onwards to the superheaters. The power plant in Chapter 3 uses a once through evaporator configuration.
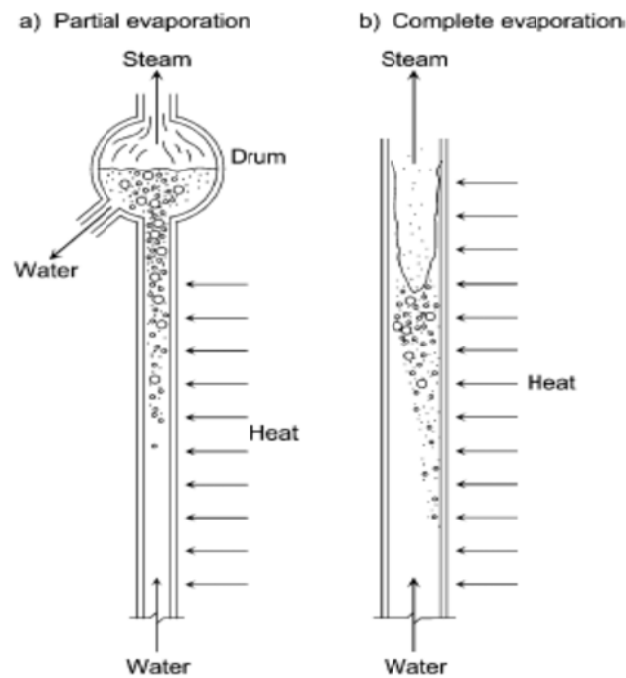
Figure 8 – evaporation processes for steam generation (Spliethoff, 2010)

In Figure 9 a typical configuration of a once through steam generator can be seen. The feedwater enters the economizer where it is preheated before entering the evaporator tubes in the the furnace walls. The steam is evaporated and slightly superheated in the evaporator before entering the radiant superheater. During part load operation the water may not be completely evaporated before exiting the evaporator. In this case the water is separated in a water separator and returned back to the evaporator by a circulation pump. In the radiant superheater the steam is further superheated before it enters the convection superheater for the final superheat. If the steam cycle has reheat, the reheaters will be placed in the same zones as the superheaters.

Due to modern steam cycles utilizing feedwater inlet temperatures of around 250°C-300°C, the outlet temperature of the flue gas in the steam generator will be high if the flue gas is only utilized for steam generation. It is therefore normal to use the remaining flue gas heat to preheat the combustion air. This raises the temperature of combustion and the fuel consumption can be reduced. In order to avoid corrosion and fouling in the preheater, the flue gas exit temperature should be above the acidic dew point of the flue gas (Spliethoff, 2010, p. 140). The acidic dew point depends on the sulfur content of the coal. In an oxy-combustion configuration the recycled flue gas and oxygen is preheated instead.

2.2.5 Losses in a Coal Based Condensation Plant

In Figure 10 the thermal losses of an air-fired coal based power plant with 39% thermal efficiency are shown. The biggest part of the losses is due to the thermal efficiency of the steam cycle, and constitutes about 44% of the total losses. The waste heat is removed from the cycle through the cooling water in the condenser. 44% of thermal loss may seem big, but the amount of thermal energy that can be transformed to mechanical energy is dictated by the exergy level of the steam, not the amount of heat it contains. Typical exergy efficiencies are in the region of 90% (Spliethoff, 2010, p. 70). Another significant loss is the power used to run the auxiliary systems of the power plant. Auxiliary systems include feedwater pumps, cooling water pumps, fans for combustion air and flue gas, coal preparation, flue gas clean-up systems, transformer losses, control systems etc. Around 6% of the heat input is also lost through the flue gas as the flue gas is only utilized above the acidic dew point. Moreover electrical generator losses, mechanical

losses from the turbine shafts and losses through unburned fuel and radiation in the steam generator constitute of less than 3% of the losses. The biggest loss from an exergetic point of view is found in the steam generator where the heat transfer, irreversible combustion and flue gas losses contribute to a high loss of exergy. While thermal efficiencies of steam generators are typically above 90%, exergy efficiencies are normally in the region of 50% (Spliethoff, 2010, p. 68)
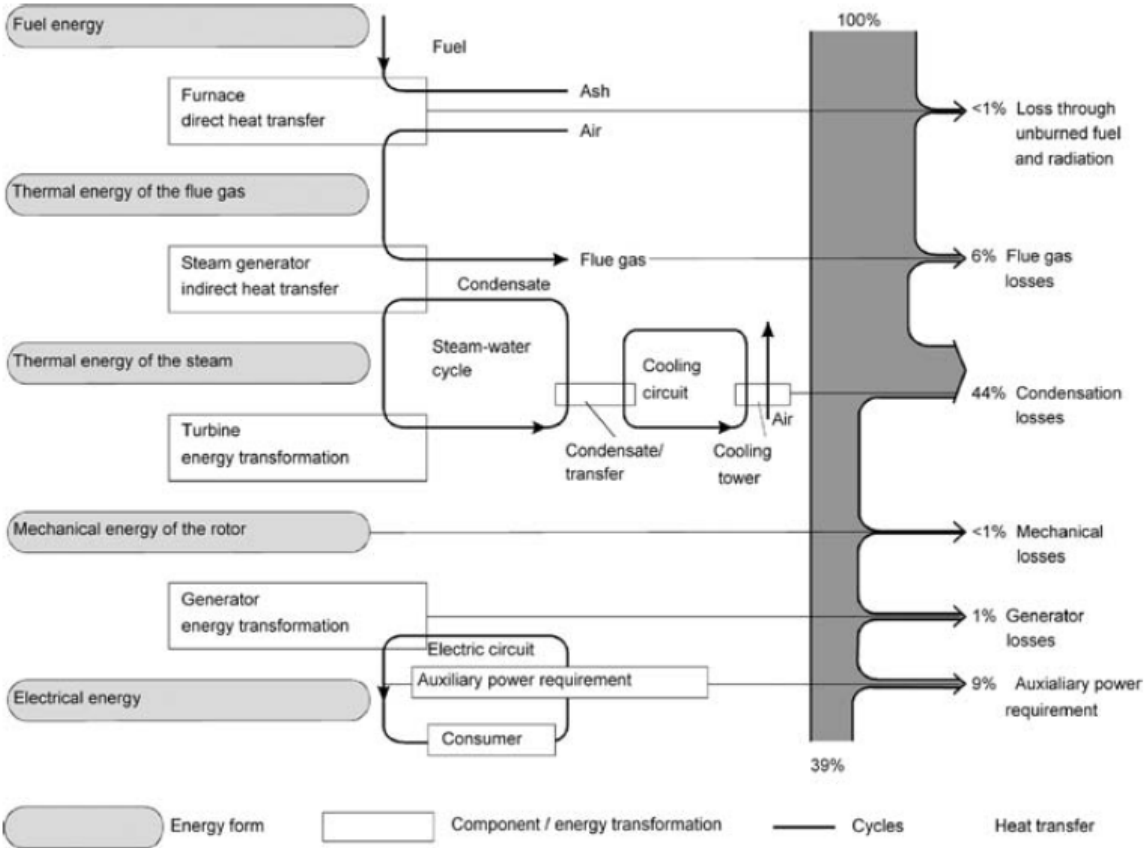
Figure 10 – Energy transformation or conversion, circulation and efficiency in a steam power plant (Spliethoff, 2010)

2.2.6 Calculating Performance of a Condensation Plant

Expansion Work
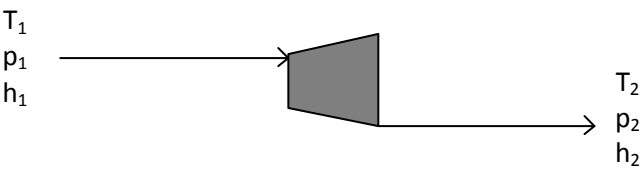
Figure 11 – Simple Expansion

By ignoring changes in kinetic and potential energy, the output from a turbine section in a steam cycle can be calculated from the following energy balance:

$$\dot{W}_T = \dot{m}\left[h_1(T_1, p_1) - h_2(T_2, p_2)\right] = \dot{m}\eta_{is}\left[h_1(T_1, p_1) - h_{2,is}(T_{2,is}, p_2)\right]$$

(2.3)

Where the isentropic efficiency, η_{is}, is used to account for the losses of the turbine and and $h_{2,is}$ and $T_{2,is}$ is the enthalpy and temperature resulting from an isentropic expansion to p_2.
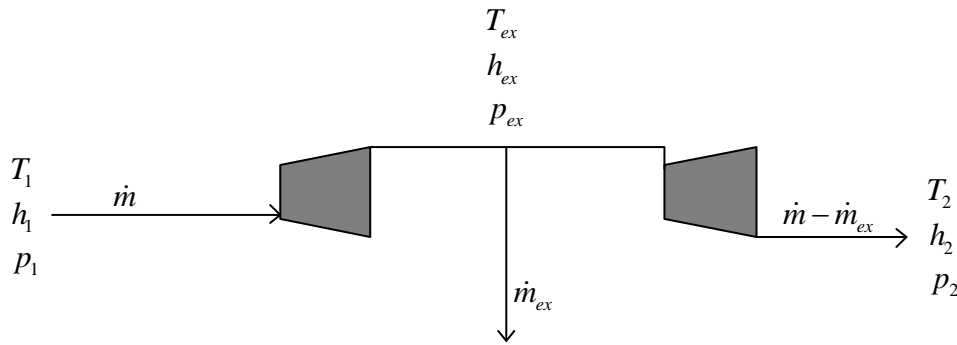
Figure 12 – Expansion with Extraction

If steam extractions are utilized as shown in Figure 12, the power output of the turbine can be calculated in the following way:

$$\dot{W}_T = \dot{m}(h_1 - h_{ex}) + (\dot{m} - \dot{m}_{ex})(h_{ex} - h_2)$$

(2.4)

Where the isentropic efficiency can be introduced in the same way as in (2.3). For a turbine with *n* extractions at *n* pressure levels the total turbine work can be expressed in the following way:

$$\dot{W}_T = \dot{m}(h_1 - h_{ex,1}) + \sum_{i=1}^{n-1}\left[(h_{ex,i} - h_{ex,i+1})(\dot{m} - \sum_{k=1}^{i}\dot{m}_{ex,k})\right] + (h_{ex,n} - h_2)(\dot{m} - \sum_{k=1}^{n}\dot{m}_{ex,k})$$

(2.5)

Where state 1 corresponds to the inlet and state 2 corresponds to the outlet. The isentropic efficiency can be introduced as in (2.3). It can be seen that a steam extraction will reduce the work output of all expansion stages downstream of the extraction.

Thermal Input and Combustion

The thermal input to the steam generator can be found by the fuel consumption and the lower or higher heating value of the fuel. In Spliethoff (2010) the lower heating value (LHV) is used for

efficiency calculations, and it will also be used here. The thermal input to the steam generator is calculated with the following equation:

$$\dot{Q} = \dot{m}_f \cdot LHV$$

(2.6)

In Spliethoff (2010), p. 64 the efficiency of the steam generator is defined in the following way:

$$\eta_{SG} = \frac{\sum \dot{m}_{S,j} \Delta h_j}{\dot{m}_f LHV}$$

(2.7)

Where $\dot{m}_{S,j}$ and Δh_j is the mass flow and change in specific enthalpy of the streams of the working medium (water or steam) of which heat is supplied to.

It is common practice to use a certain amount of excess oxygen in combustion in order to ensure complete combustion of the fuel. The excess oxygen on a mass basis can be calculated in the following way:

$$O_{2,excess} = \frac{\dot{m}_{O_2,air}}{\dot{m}_{O_2,stoi}}$$

(2.8)

Where $\dot{m}_{O_2,air}$ is the flowrate of oxygen in the combustion air, and $\dot{m}_{O_2,stoi}$ is the stoichiometric flowrate of oxygen required for complete combustion of the fuel. For an oxy-combustion steam generator the excess oxygen is defined in the following way:

$$O_{2,excess} = \frac{\dot{m}_{o_2,ASU} + \dot{m}_{o_2,AI} + \dot{m}_{o_2,RC}}{\dot{m}_{o_2,stoi}}$$

(2.9)

Where $\dot{m}_{o_2,ASU}$ is the flowrate of oxygen supplied from the ASU, $\dot{m}_{o_2,AI}$ is the flowrate of oxygen supplied to the combustion from air in-leakage and $\dot{m}_{o_2,RC}$ is the flowrate of oxygen supplied from the recycled flue gas.

Accounting for Auxiliaries and Losses

The mechanical losses in the turbines and the generator losses can be accounted for by introducing a mechanical efficiency of the turbines, η_{mech}, and mechanical efficiency of the generator, η_{gen}.

The pump and fan work in the steam cycle can be found through the energy balance of the respective pump. The energy balance for a pump or fan with inlet state 1 and outlet state 2 and a combined mechanical and isentropic efficiency, η_P, is the following:

$$\dot{W}_P = \dot{m}(h_2(T_2, p_2) - h_1(T_1, p_1)) = \frac{\dot{m}}{\eta_P}\left[h_{2,is}(T_{2,is}, p_2) - h_1(T_1, p_1)\right] \tag{2.10}$$

Where $h_{2,is}$ and $T_{2,is}$ is the enthalpy and temperature resulting from an isentropic compression to p_2.

In order to account for other auxiliaries an efficiency, η_{aux}, is introduced. This accounts for power consumption of coal preparation, cooling water pumps, flue gas cleanup systems, transformer losses, control systems etc.

Thermal Efficiency

The net power output of the power plant can be expressed in the following way:

$$\dot{W}_{net} = \eta_{gen}\eta_{mech}\eta_{aux}\sum\dot{W}_T - \sum\dot{W}_P - \sum\dot{W}_F \tag{2.11}$$

Where $\sum\dot{W}_F$ corresponds to the total fan work. If the power plant is an oxy-combustion plant the work required for the separation of oxygen and nitrogen in the ASU and the compression and separation work in the CPU will also be need to subtracted. The net power can then be written in the following way:

$$\dot{W}_{net} = \eta_{gen}\eta_{mech}\eta_{aux}\sum\dot{W}_T - \sum\dot{W}_P - \sum\dot{W}_F - \dot{W}_{ASU} - \dot{W}_{CPU} \tag{2.12}$$

The thermal, or LHV efficiency of an air-fired or oxy-combustion power plant, can be expressed in the following way:

$$\eta_{th} = \frac{\dot{W}_{net}}{\dot{m}_f LHV} \tag{2.13}$$

2.3   Thermodynamics of Compression

The main power consumers in the ASU and CPU of an oxy-combustion power plant are compressors, and integration of compression heat is one of the topics to be studied in this report. In this chapter the fundamentals of compression will be reviewed.

2.3.1   One-Stage Compression

T_1
p_1
h_1

T_2
p_2
h_2
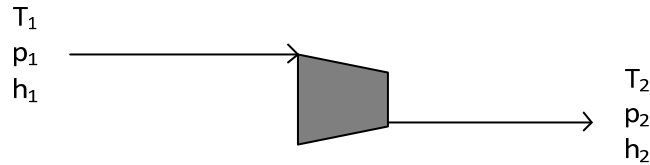
Figure 13 – Simple compression process

If kinetic and potential energy is neglected, the positive work in an internally reversible compression process can be expressed in the following way:

$$\left(\frac{\dot{W}_C}{\dot{m}}\right)_{\substack{int \\ rev}} = \int_{p_1}^{p_2} v\,dp \tag{2.14}$$

For a polytropic process the following relation can be used:

$$pv^n = const \tag{2.15}$$

n is the polytropic exponent and can be found with the following relation:

$$\frac{n-1}{n} = \frac{k-1}{k} \tag{2.16}$$

Where k is ratio between specific heat capacities (isentropic exponent). Since the heat capacities vary with temperature, the values of the isentropic and polytropic exponents will be temperature dependent. By assuming constant heat capacities, introducing (2.15) in (2.14) and following the procedure described in Moran and Shapiro (2006), p. 256, the following expression is obtained for the case of an ideal gas:

$$\left(\frac{\dot{W}}{\dot{m}}\right)_{\substack{int \\ rev}} = \frac{nRT_1}{n-1}\left[\left(\frac{p_2}{p_1}\right)^{\frac{n-1}{n}} - 1\right] \tag{2.17}$$

And:

$$\frac{T_2}{T_1} = \left(\frac{p_2}{p_1}\right)^{\frac{n-1}{n}} \tag{2.18}$$

If the polytropic efficiency, η_p, is introduced to account for irreversibilities the expressions in (2.17) and (2.18) can still be used to calculate the compression work and outlet temperature, but the isentropic exponent will then be given by the following relation:

$$\frac{n-1}{n} = \eta_p \left(\frac{k-1}{k}\right) \tag{2.19}$$

In this report the isentropic efficiency will be used. In Saravanamuttoo et al. (2009), p. 61, the relation between the polytropic and isentropic efficiencies is defined in the following way:

$$\eta_{is} = \frac{\left(\dfrac{p_2}{p_1}\right)^{\frac{k-1}{k}} - 1}{\left(\dfrac{p_2}{p_1}\right)^{\frac{k-1}{\eta_p k}} - 1} \tag{2.20}$$

For a real gas compressibility effects will need to be taken into account when calculating the compression work. Both for ideal and real gases k and n vary with temperature.

2.3.2 Multi-Stage Compression
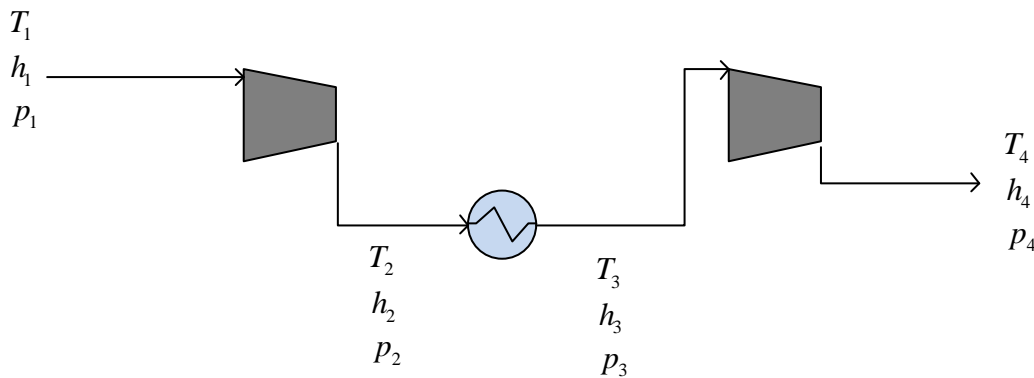
Figure 14 – Intercooled Compression

Intercooling in compression is utilized in order to minimize compression work. In Figure 14 the principle of intercooling is illustrated. The compression is split into two or more stages with a cooler in-between the stages. The work of an intercooled compression as shown in Figure 14, can be calculated with the following expression:

$$\left(\frac{\dot{W}}{\dot{m}}\right) = \frac{nR}{n-1}\left[T_1\left(\left(\frac{p_2}{p_1}\right)^{\frac{n-1}{n}}-1\right)+T_3\left(\left(\frac{p_4}{p_3}\right)^{\frac{n-1}{n}}-1\right)\right] \tag{2.21}$$

Since $p_2 \approx p_3$ and $T_2 > T_3$, it follows that the total compression work will be less for an intercooled compressor than for a compressor without intercooling as long as the total pressure ratio of the compressor is the same for the two. The outlet temperature of each compression stage can be found with (2.18).

Adiabatic compression is in this report used to refer to compression without intercooling as described in Chapter 2.3.1. From (2.18) it can be seen that adiabatic compression will give a higher outlet temperature that that of an intercooled compression, but (2.17) and (2.21) shows that the work of an adiabatic compression is higher.

2.4   Fundamentals of Process Integration

Process integration has since its development in the 1970s become a mature technology (Kemp, 2007, p. 2-4). The idea process integration is to design processes in order to conserve such as energy or material (Zhang and Lior, 2006). The design of a process should start with the reaction processes. The product composition and feed requirements to the reaction process will then determine the separation tasks to be performed. When these two steps have been completed the potential for heat integration can evaluated through pinch analysis. The integrated design will then determine the need for external heating and cooling (Kemp, 2007, p. 6). In this report the reaction and separation is already modeled, and pinch analysis will be used to set energy targets and evaluate the potential for heat integration between the different sections of the power plant. In the following chapters an introduction to pinch analysis is given.

2.4.1   Heat Exchange

In pinch analysis any flow that needs to be heated or cooled without changing in composition is defined as a stream (Kemp, 2007, p. 15). A stream which requires heating is defined as a cold stream, and a stream which requires cooling is defined as a hot stream. Heating and cooling can be supplied by an external utility such steam and cooling water in a utility heat exchanger or heat can be recovered within the process itself in a process heat exchanger.

The heat duty of a heat exchanger can be found with the following formula:

$$\dot{Q} = UA\Delta T_{LM} \tag{2.22}$$

Where U is the overall heat transfer coefficient of the heat exchange, A is the heat exchanger surface area and ΔT_{LM} is the logarithmic mean temperature difference. ΔT_{LM} is defined as:

$$\Delta T_{LM} = \frac{\Delta T_{HOT} - \Delta T_{COLD}}{\ln\left(\dfrac{\Delta T_{HOT}}{\Delta T_{COLD}}\right)}$$

(2.23)

Where ΔT_{HOT} is the temperature change of the hot side of the heat exchanger, and ΔT_{COLD} is the temperature change of the cold side of the heat exchanger.

Determining the overall heat transfer coefficient requires knowledge of the film heat transfer coefficients of the cold and hot stream and the thermal conductivity and thickness of the heat exchanger tube walls. By ignoring the heat transfer resistance from the heat exchanger material and fouling, the total heat transfer coefficient can be expressed in the following way:

$$\frac{1}{U} = \frac{1}{h_C} + \frac{1}{h_H}$$

(2.24)

Where h_C and h_H are the film heat transfer coefficients of the cold and hot stream respectively. The film heat transfer coefficient depends on flow regime, heat exchanger geometry, fluid properties, phase etc.

2.4.2 Composite Curves & Energy Targets

The temperature-heat content diagram (T-Q diagram) is a useful tool for representing heat exchange. If the specific heat capacity is assumed constant, the heat to be removed from or supplied to a stream can be found in the following way:

$$\dot{Q} = \int_{T_S}^{T_T} CP dT = CP(T_t - T_s)$$

(2.25)

Where CP is the heat capacity flow rate which is obtained by multiplying the flow rate of the stream with its specific heat capacity and T_t and T_s are the target and supply temperatures of the stream. For a system with several hot and cold streams the CPs existing over a given temperature range are added together to produce one single line for all the hot streams, and one single line for all the cold streams (Kemp, 2007). The two resulting curves are named the hot and cold composite curve respectively. By plotting the hot and cold composite curve in the same T-Q diagram and shifting the curves to obtain a specified minimum temperature difference, ΔT_{min}, between the curves, the heating and cooling requirements of the process can be seen. If streams have CP values which vary with temperature, the stream can be split into several linear segments.

An example of composite curves can be seen in Figure 15. The region where the curves are overlapping is the region where internal heat recovery between the process streams is possible. The cooling requirement can be found by looking at the region of the hot composite curve which does not overlap with the cold composite curve. The heating requirements are found by doing the same with the cold curve. The pinch is the point where the ΔT_{min} occurs.
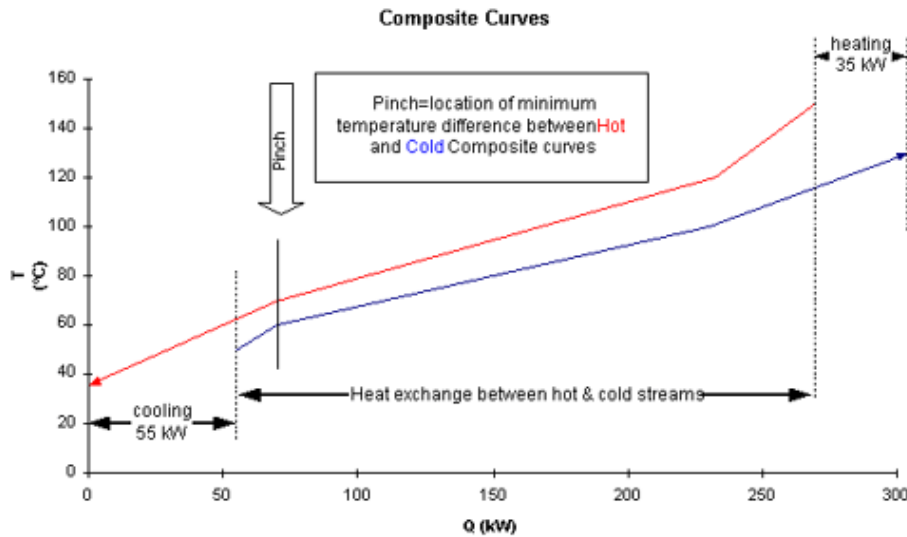
Figure 15 – Example of Composite Curves (PDC, 2012)

The pinch point divides the process in two. Above the pinch point the process is a heat sink where only heating from hot utility is required, and below pinch the process is a heat source where only cooling from cold utility is required. Using hot utility below the pinch point or cold utility above the pinch point will increase both the total hot and cold utility requirements with a size equal to the amount of the heating/cooling the utility adds. Furthermore a heat exchanger transferring heat across the pinch will add heating and cooling requirements equal to the amount heat which is transferred across the pinch.

Another useful representation is the Grand Composite Curve (GCC). The GCC is a graph of net heat flow against shifted temperature (Kemp, 2007, p. 26). The shifted temperature is found by adding $\Delta T_{min}/2$ to the temperature of all hot streams and subtracting $\Delta T_{min}/2$ from all the cold streams. The GCC represents the difference between available heat from the hot streams and the heat required by the cold streams relative to the pinch point at a given shifted temperature. It is useful for determining at which temperature levels heating and cooling from utilities needs to be supplied (Kemp, 2007, p. 26). An example of a GCC can be seen in Figure 16. The hot utility requirement can be seen at the top of the curve and the cold utility requirement can be seen at the bottom of the curve. In zones where the curve has a positive slope from right to left the

process acts as a heat sink, and where it has a negative slope the process acts as a heat source. The pockets where the curves overlapped are areas where heat recovery is possible, and are called self-sufficient pockets.
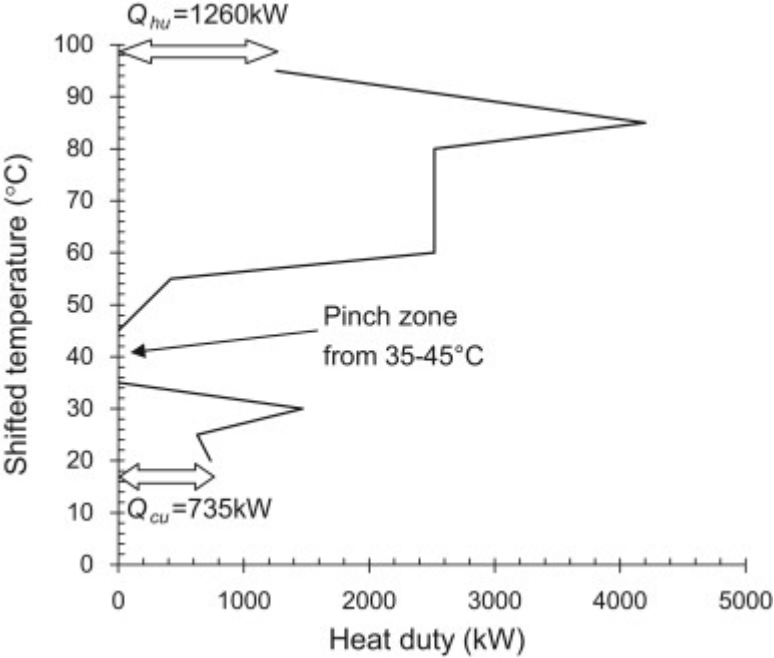
Figure 16 - Example of Grand Composite Curve (Sahu and Bandyopadhyay, 2010)

If the utility heating and cooling is included in the composite curves one obtains the balanced composite curves and balanced grand composite curve.

2.4.3 Deciding ΔT_{min}

It can be seen from the composite curves in Figure 15 that an increase in ΔT_{min} will increase the cooling and heating requirements. From an energetic point of view ΔT_{min} should therefore be kept as low as possible. However if (2.22) is rearranged to calculate the area, the following expression is obtained:

$$A = \frac{Q}{UA\Delta T_{LM}}$$

(2.26)

Since a reduction in ΔT_{min} will cause a reduction in ΔT_{LM}, the heat exchanger surface area requirement will increase if ΔT_{min} is reduced. With increasing area comes increasing costs. The ΔT_{min} should therefore be determined by finding the optimal trade-off between capital costs and energy savings. If the capital costs are annualized to the same timescale as the energy costs, the energy and capital can be summed to find the total costs. If the costs are plotted as a function of ΔT_{min}, the optimum value of ΔT_{min} can be found. This procedure is illustrated in Figure 17. Estimating capital costs and heat exchanger area properly requires knowledge of heat exchanger

costs and heat transfer coefficients, and is generally less exact than energy targeting (Kemp, 2007, p. 37). In this report the costs will only be discussed, not calculated.
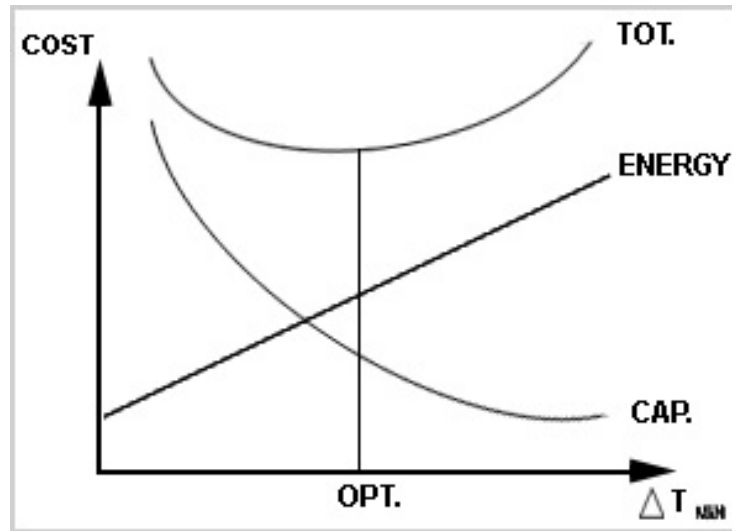
So far setting a global ΔT$_{min}$ has been discussed. In this report individual ΔT$_{min}$ contributions will be set for each stream to represent the variation in film heat transfer coefficient between streams. The minimum temperature difference of a match between two streams will then be the sum of the ΔT contribution of each stream.

2.4.4   Heat Exchanger Networks

In order to reach the energy targets for a process with multiple hot and cold streams, the heat exchange must be organized in a heat exchanger network (HEN). Kemp (2007), p. 34 describes the following procedure for creating a HEN design where the minimum energy requirement (MER) is met:

- Divide the problem at the pinch, and design each part separately.
- Start the design at the pinch and move away.
- Obey the following constraints immediately adjacent to the pinch:

  $CP_{HOT} \leq CP_{COLD}$ for all hot streams

  $CP_{HOT} \geq CP_{COLD}$ for all cold streams

- Maximize exchanger heat loads
- Supply external heating only above the pinch, and external cooling only below the pinch.

Creating a HEN design for reaching the MER may require a significant number of heat exchangers. A cost effective HEN design may therefore be a design which does not reach the MER. The minimum number of heat exchange units, u_{min}, required to reach the MER, can according to Kemp (2007), p. 70, in most cases be found by the following formula:

$$u_{min} = N - 1$$

Where N is the total number of streams, including utilities.

In this report a HEN design for the integrated cases will not be developed. However some basic considerations about the complexity of the system will be made on the basis of the minimum number of heat exchange units required.

3 Description and Performance of a Coal Fired Oxy-Combustion Power Plant

The power plant in this study is the same as described in Fu C. and Gundersen (2011). It is a 567MW (net) supercritical pulverized coal fired oxy-combustion power plant. The overall flowsheet of the power plant can be seen in Figure 18. Detailed flowsheets of the steam cycle and steam generator are available in Figure 19 and Figure 20 respectively. In the following chapters each section of the power plant is described in more detail before the performance of the power plant is evaluated through an Aspen Plus simulation. For detailed information on the streams consult the appendix where stream information extracted from the simulation model is given with reference to the stream names in Figure 18, Figure 19 and Figure 20.

3.1 The Steam Power Cycle

The steam cycle of the power plant is a supercritical cycle, and it is based on configuration 5C in DOE/NETL (2008). The steam turbines are arranged in one HP, one IP and one LP section and are designed to deliver 785,9MW at the generator terminals. In total there are six steam extractions. Along with the HP and IP exhaust these extractions supply four low-pressure feedwater heaters, the deaerator and three high-pressure feedwater heaters. The condensate from the low-pressure heaters is introduced to the condenser while the condensate from the high-pressure heaters is introduced to the deaerator. The turbine shafts are sealed against air in-leakage or steam blowout by a steam seal.

The steam exits the steam generator at 242bar and 600°C and enters the HP section of the turbine. After passing through the HP turbine the steam returns to the steam generator for reheating. The reheat steam enters the IP turbine at 620°C and passes successively through the IP and LP sections. The exhaust gas enters the condenser at a pressure of 6,8kPa. The fully condensed water is thereby pumped up to a pressure of 17,2bar before passing through the four low pressure feedwater heaters. After passing through the deaerator, the feedwater is pumped up to 278bar in the feedwater pumps. It is further heated in the three high pressure feedwater heaters before it is introduced to the steam generator. The feedwater pumps are powered by a turbine driver. The steam to this turbine is supplied from the exhaust of the IP turbine. Steam extractions to the ASU and CPU are taken from the IP exhaust, and the water to the flue gas recycle reheater (FG-H in Figure 18) is taken from the outlet of FWH 2 (stream F-5 in Figure 19).
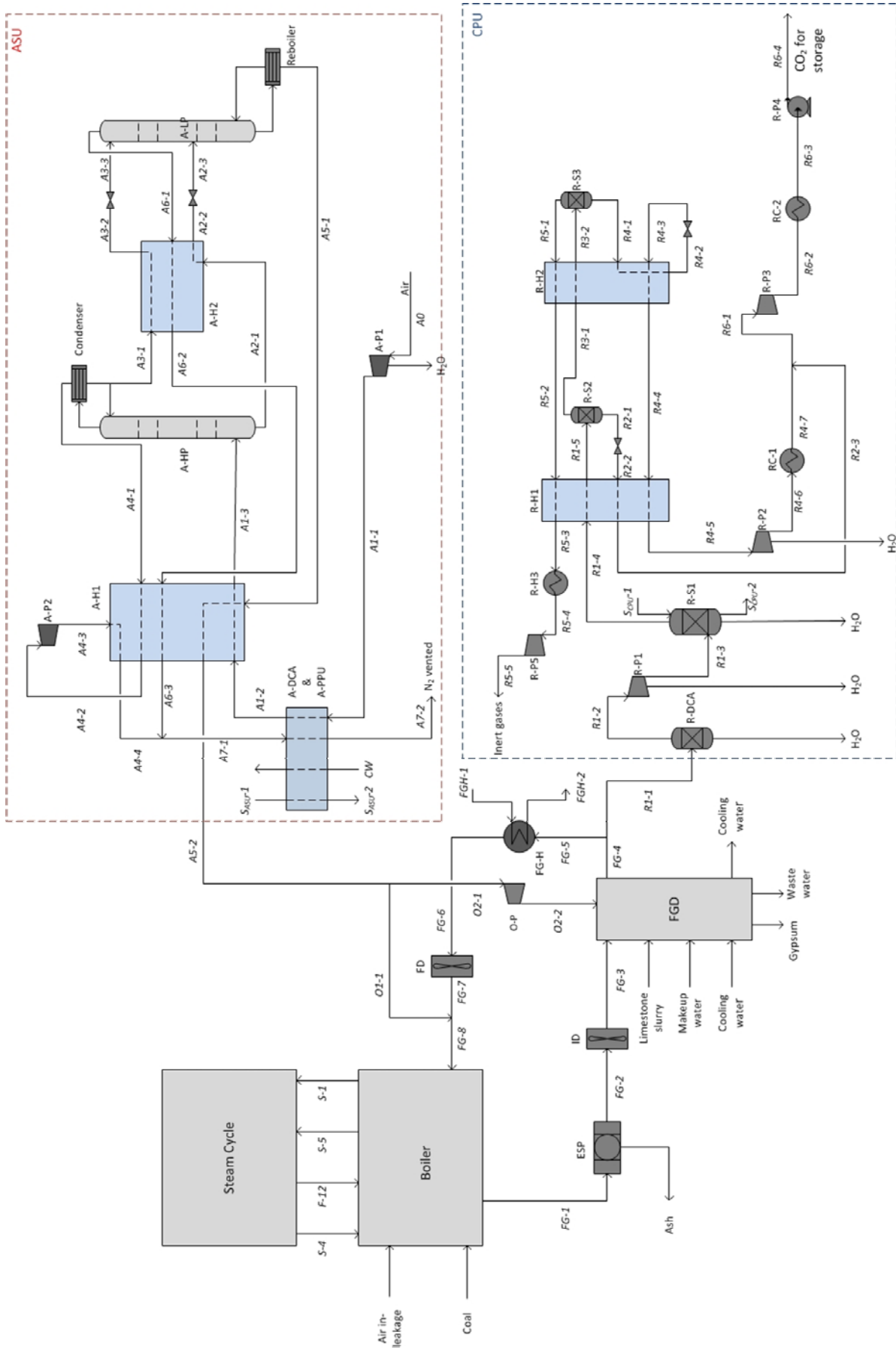
Figure 18 – Overall Flowsheet of Power Plant
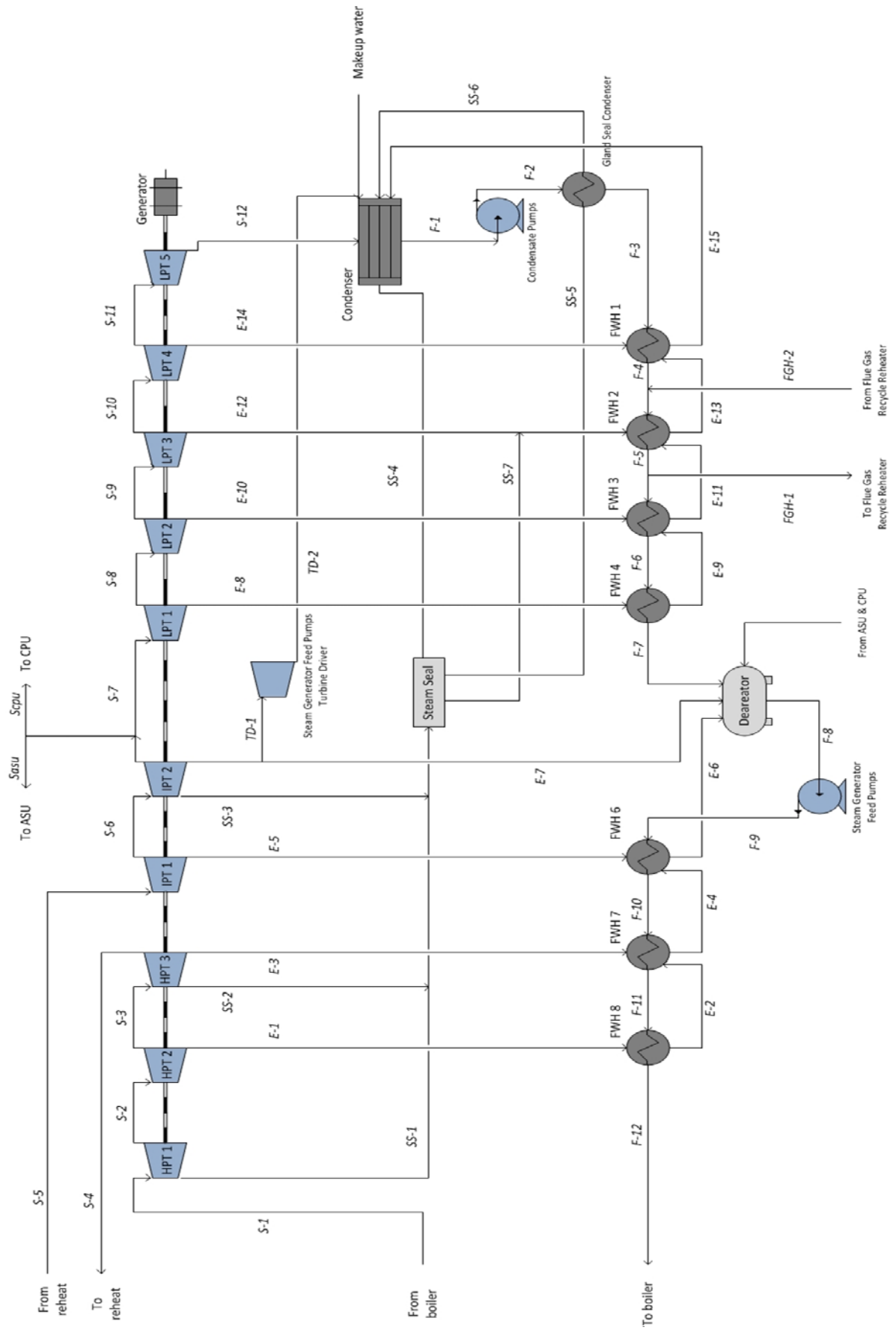
Figure 19 – Flowsheet of Steam Cycle
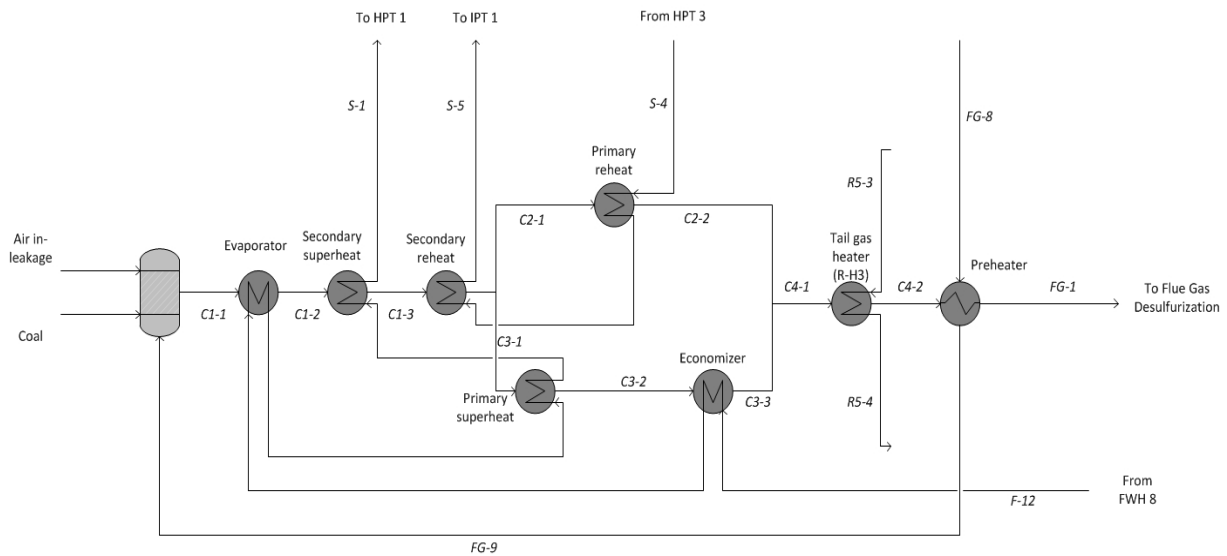
Figure 20 – Flowsheet of Steam Generator

3.2 The Steam Generator and Flue Gas Desulfurization

The steam generator is based on the Babcock & Wilkins supercritical once-through, spiral wound, Benson-boiler described in DOE/NETL (2008). A flowsheet of the heat exchange in the boiler can be found in Figure 20.

On the water/steam side feedwater enters the economizer and thereby passes through the evaporator in the furnace where it is evaporated and slightly superheated. The steam exiting the evaporator is further superheated in the primary and secondary superheaters successively before entering the HP turbine. The reheat steam enters in the primary reheater and goes through the secondary reheater before re-entering the steam cycle in the IP turbine.

On the gas side, recycled flue gas is fed to the forced draft fans (FD), mixed with oxygen from the ASU and preheated in the preheater before being distributed into the burner where the combustion of coal takes place. In the steam generating section, the hot flue gas passes successively across the furnace, the secondary superheater and the secondary reheater. The flue gas then turns downward and is split into one pass with the primary superheater and the economizer and one pass with the primary reheater. The flue gas from the two passes is then mixed used to provide heat to the tail gas heater in the CPU (RH-3 in Figure 18) before it goes through the preheater where it rejects heat to the oxygen and recycled flue gas.

The flue gas exiting the steam generator enters an electrostatic precipitator (ESP) in order to clean the gas of particles, and is thereby desulfurized in a wet limestone slurry process. The sulphur removal efficiency is 98%.

3.3 The Air Separation Unit

The following text is based on the description given by Chao and Gundersen (2011). The air separation unit is a double-column system which delivers O_2 of 95% molar purity at 1.5bar to the combustion process. Ambient air is compressed in two stages to a pressure of 5.6bar in A-P1 and consequently cooled down to 35°C by cooling water in a direct contact cooler (A-DCA). The compressor is intercooled with cooling water. After passing through the direct contact cooler, H_2O and CO_2 are removed in a front-end temperature swing adsorption-type pre-purification unit. The purified air is then cooled down to a temperature close to the dew point in the main heat exchanger, A-H1. The cooling duty is supplied by produced oxygen from the LP column and from the separated nitrogen. In the double distillation column O_2 is separated from N_2. The re-boiler in the low pressure column is integrated with the condenser in the high pressure column in A-H2. The waste N_2 is used to cool down the air in the pre-purification unit before it is vented to the atmosphere.

3.4 CO_2 Compression and Purification

The CO_2 compression and purification unit used by Chao and Gundersen (2011) is based on the process described in Pipitone and Bolland (2009). The part of the flue gas which is not recycled back to the combustion process, enters a direct contact cooler (R-DCA) to separate water from the gas. It is thereafter compressed in three stages with water cooling to a final pressure of 32bar in R-P1. In order to avoid formation of ice in sub-ambient heat exchangers, the compressed gas is dried in a molecular sieve twin-bed drier (R-S1). After drying the gas is partly condensed and cooled to 247,2K in a multi-stream heat exchanger (R-H1). The condensate is separated from the gas in a flash drum, expanded in a Joule Thompson valve and heated to provide cooling duty in R-H1. The vapour stream is further cooled to 219.2K in another multi-stream heat exchanger (R-H2) and separated in a second flash drum. The vapour stream consists mainly of inert gases and is heated to provide cooling duty in the two multi-stream heat exchangers. In order to recover pressure energy, it is further heated by combustion flue gas in the tail gas heater (R-H3) and expanded in a gas turbine to recover power. The liquid stream is first used to provide cooling in R-H2 at two pressure levels, and is then introduced to R-H1 to provide further cooling. R4-5 is compressed to the same pressure as R2-3 and the two streams are mixed and compressed to

78bar by a two-stage compressor with water intercooling. The compressed CO_2 is further cooled to 298,2K by seawater. The CO_2 is now in the dense phase and is pumped up to 150bar for transportation and storage.

3.5 Power Plant Performance

3.5.1 Simulation Model and Assumptions

In order to establish the performance of the power plant, the process is simulated by using Aspen Plus. The simulation model is based on a simulation model used by Fu Chao in Chao and Gundersen (2011), and the flowsheet of the simulation follows the flowsheets shown in Figure 18, Figure 19 and Figure 20. For the steam cycle the Steam NBS tables are used to calculate properties, while Peng-Robinson is being used for the rest of the process (ASU, CPU, Desulfurization, Steam generator). The computational specifications are listed in Table 1.

The power plant performance is compared to that of a reference air fired coal based power plant without CO_2 capture in order to establish the efficiency penalty related to CO_2 capture. Data on the reference plant performance is taken directly from Chao & Gundersen (2011).

Table 1 – Simulation Specifications (Extracted from Chao and Gundersen (2011))

Turbo-Machinery	
HP steam turbine isentropic efficiency	0,9
IP steam turbine isentropic efficiency	0,9
LP steam turbine isentropic efficiency	0,88
Steam turbines mechanical effiency	0,996
Generator mechanical efficiency	0,985
Compressor isentropic efficiency	0,82
Compressor mechancial efficiency	0,97
Fan isentropic efficiency	0,88
Fan mechanical efficiency	0,98
Tail gas turbine isentropic efficiency	0,9
Tail gas turbine mechanical efficiency	0,999
Pump efficiency (including motor driver)	0,736
Compression intercooler gas side outlet temperature, °C	35

ASU and CPU	
Minimum temperature difference in sub-ambient heat exchangers, K	2
Temperature difference of the condenser/reboiler, K	1,5
Pressure drop in the pre-purification unit, bar	0,1
Pressure drop in sub ambient heat exchangers, %	1-3
Pressure drop in HP column, bar	0,05

Pressure drop in LP column, bar	0,1
Inlet/outlet temperature of cooling water, K	298,2/308,2
Inlet/outlet temperature of seawater, K	288,2/298,2
Minimum temperature difference in cooling water heat exchangers, K	10
Cooling water pressure, bar	2

Steam Cycle	
Pressure drop in feed water heaters, bar	0,34
HP steam turbine inlet pressure, bar	242,3
IP steam turbine inlet pressure, bar	45,2
LP steam turbine inlet pressure, bar	9,5
Condenser pressure, bar	0,069
Minimum temperature difference in condenser, K	3,8
Auxiliary efficiency	0,968

3.5.2 Simulation of Steam Generation

Simulation Model

In order to fully evaluate integration possibilities for the power plant a detailed model of the steam generator is developed. In DOE/NETL (2008) there is not sufficient information to create an accurate model of the steam generator area. However the different sections of the steam generator are described and this forms the basis for the flowsheet in Figure 20. The different heat transfer sections in the steam generator are linked with the steam cycle through heat streams for ease of convergence. The split between stream C4 and C5 is specified so that stream C8 and C5 get equal temperatures through an Aspen Plus design specification.

Table 2 – Distribution of Heat Transfer in Steam Generator

Distribution of heat transfer to steam cycle	
Evaporator	36,49 %
Secondary superheat	21,97 %
Secondary reheat	4,89 %
Primary superheat	17,06 %
Primary reheat	14,68 %
Economizer	4,90 %

In order to specify the heat transfer inside the steam generator area, results from Hayashi et al. (2011) were used. They have produced a simulation model in order to determine the percentage of heat transferred in each section of a retrofit oxy-combustion steam generator. Based on their

results the distribution of heat transfer shown in Table 2 was used to specify the heat transfer in the different steam generator sections. It should be noted that this may give inaccurate results, especially since the steam generator configuration differs slightly between NETL (2009) and Hayashi et al. (2011), but it is the most accurate data that could be found on oxy-combustion steam generator heat transfer.

Coal Feed and Oxygen Requirements

The proximate and ultimate analysis of the coal feed to the combustion is shown in Table 3.

Table 3 – Proximate and Ulimate Analysis of Coal Feed (DOE/NETL, 2008)

	As received	Dry	
Proximate analysis			
Moisture	11,12	0,00	%
Volatile matter	34,99	39,37	%
Ash	9,70	10,91	%
Fixed carbon	44,19	49,72	%
Ultimate analysis			
Carbon	63,75	71,73	%
Hydrogen	4,50	5,06	%
Nitrogen	1,25	1,41	%
Sulfur	2,51	2,82	%
Chlorine	0,29	0,33	%
Ash	9,70	10,91	%
Moisture	11,12	0,00	%
Oxygen	6,88	7,74	%
Higher heating value	27135	30531	kJ/kg
Lower heating value	26171	29447	kJ/kg

Based on the information in Table 3, the theoretical oxygen requirement can be calculated. Oxygen will react with Carbon, Hydrogen and Sulfur. Depending on temperature some NO_x, HCl and SO_3 will be formed, and to calculate the actual concentrations chemical equilibrium calculations will have to be made. For simplicity it is however assumed that only the three following reactions take place with oxygen:

$$C + O_2 \rightarrow CO_2$$

(2.28)

$$H_2 + 0{,}5O_2 \rightarrow H_2O$$

(2.29)

$$S + O_2 \rightarrow SO_2$$

(2.30)

32

By introducing the molar weight of the substances, reactions are written on a mass basis below.

$$12\text{kg C} + 32\text{kg O}_2 \rightarrow 44\text{kg CO}_2 \qquad (2.31)$$

$$2\text{kg H}_2 + 0.5 \times 32\text{kg O}_2 \rightarrow 18\text{kg H}_2\text{O} \qquad (2.32)$$

$$32\text{kg S} + 32\text{kg O}_2 \rightarrow 64\text{kg SO}_2 \qquad (2.33)$$
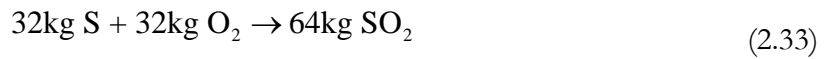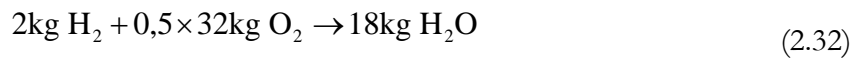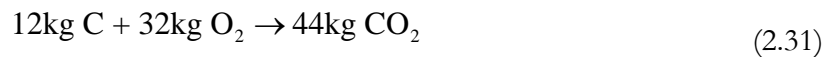
For the given feed in Table 3 this gives a theoretic oxygen requirement of $2,0163\text{kgO}_2/\text{kgCoal}$. With the stream information given in DOE/NETL (2008) and the procedure above, the excess O_2 in the combustion is determined to be 10,45% by using (2.9).

3.5.3   Simulation Results

Table 4 – Simulation Results for Air-Fired and Oxy-Combustion Case

	Air-Fired	Oxy-Combustion
Gross Power [kW]	591616	799760
Power Requirement		
ASU		
A-P1 [kW]	0	133720
A-P2 [kW]	0	-9705
CPU		
R-P1 [kW]	0	57605
R-P3 [kW]	0	16019
R-P2 [kW]	0	2015
R-P4 [kW]	0	-8862
R-P7 [kW]	0	2595
Other		
Fan Work [kW]	12127	12198
Auxilliaries [kW]	18932	25592
Condensate pumps [kW]	811	1099
Net Power	559746	567485
Fuel Consumption [kW]	51,32	69,23
LHV efficiency	41,68 %	31,32 %

The results of the Aspen Plus simulation of the oxy-combustion case are available in Table 4. It can be seen that compared to the air-fired case, the oxy-combustion case has a 10,36% decrease in efficiency. The balanced composite curves of the steam cycle and steam generator are available

in Figure 21 and the balanced GCC is available in Figure 22. The pinch point occurs in the inlet of the condenser.
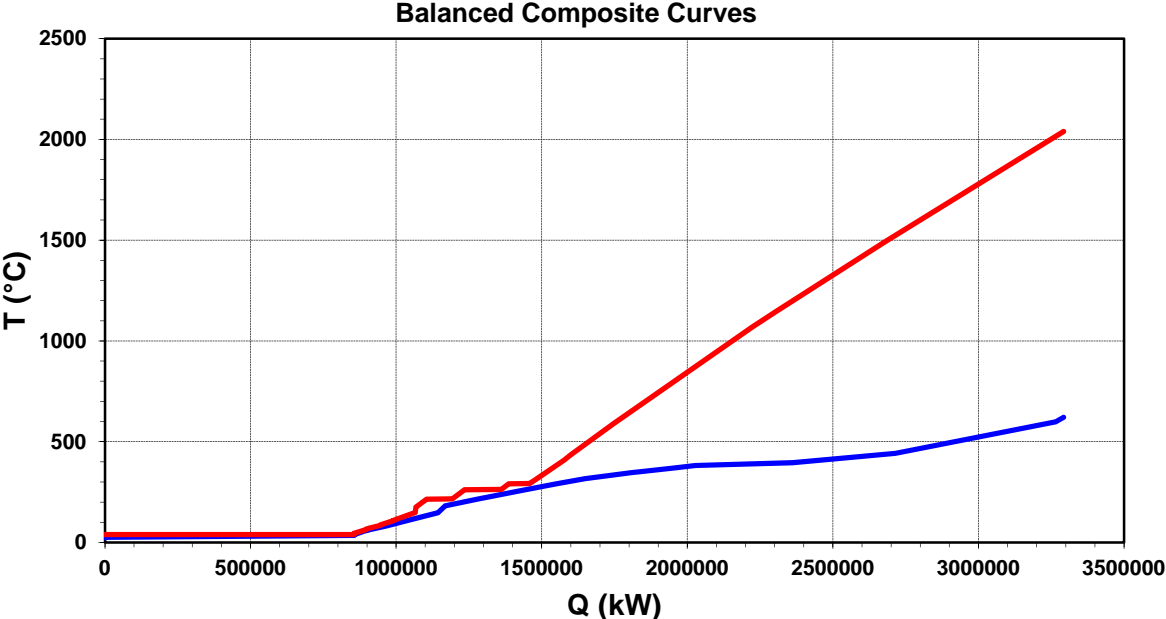
Figure 21 – Balanced Composite Curves of Steam Generator and Steam Cycle
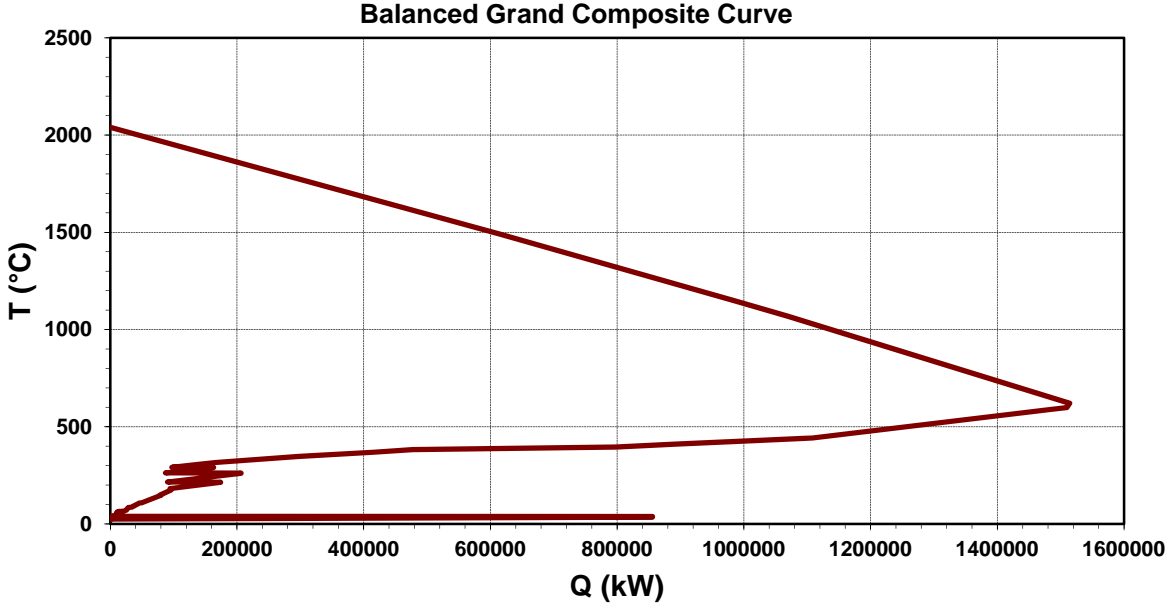
Figure 22 – Balanced Grand Composite Curve of Steam Generator and Steam Cycle

4 Integration Study

In this chapter the techniques described in Chapter 2.4 will be used in order to evaluate the potential for process integration in the power plant described in Chapter 3. The focus of this integration study will be heat integration of waste heat and this chapter will start with a review of the low temperature heat sources considered for integration before the possibilities for integration are discussed and the potential for integration is explored through simulations.

4.1 Heat Sources

4.1.1 Intercooling Heat

The heat rejected to cooling water in the compressor intercoolers can be utilized for integration. This can reduce the heating need of the process (steam extractions, fuel consumption etc.) at the same time as the need for cooling water is reduced. The suggested layout of the compression is shown Figure 23. The compressed gas is first cooled by a process stream and thereby if necessary by cooling water before entering the next compression stage. The stage inlet temperatures are the same as in the base case. In accordance with (2.21) the compression work will therefore remain the same as in the base case. In Table 5 the compression work, total cooling duty and stage outlet temperatures of the compressors in the ASU and CPU are shown.

Table 5 – Detailed Data on Intercooled Compressors in the Power Plant

A-P1			R-P1	
Stage 1 outlet temperature, °C	124,8		Stage 1 outlet temperature, °C	144,0
Stage 2 outlet temperature, °C	138,2		Stage 2 outlet temperature, °C	144,3
			Stage 3 outlet temperature, °C	146,0
Total work, kW	133720		**Total work, kW**	57605
Total cooling duty, kW	137464		**Total cooling duty, kW**	70040
R-P2			**R-P3**	
Stage 1 outlet temperature, °C	88,4		Stage 1 outlet temperature, °C	91,6
			Stage 2 outlet temperature, °C	104,5
Total work, kW	2082		**Total work, kW**	16019
Total cooling duty, kW	1894		**Total cooling duty, kW**	28729
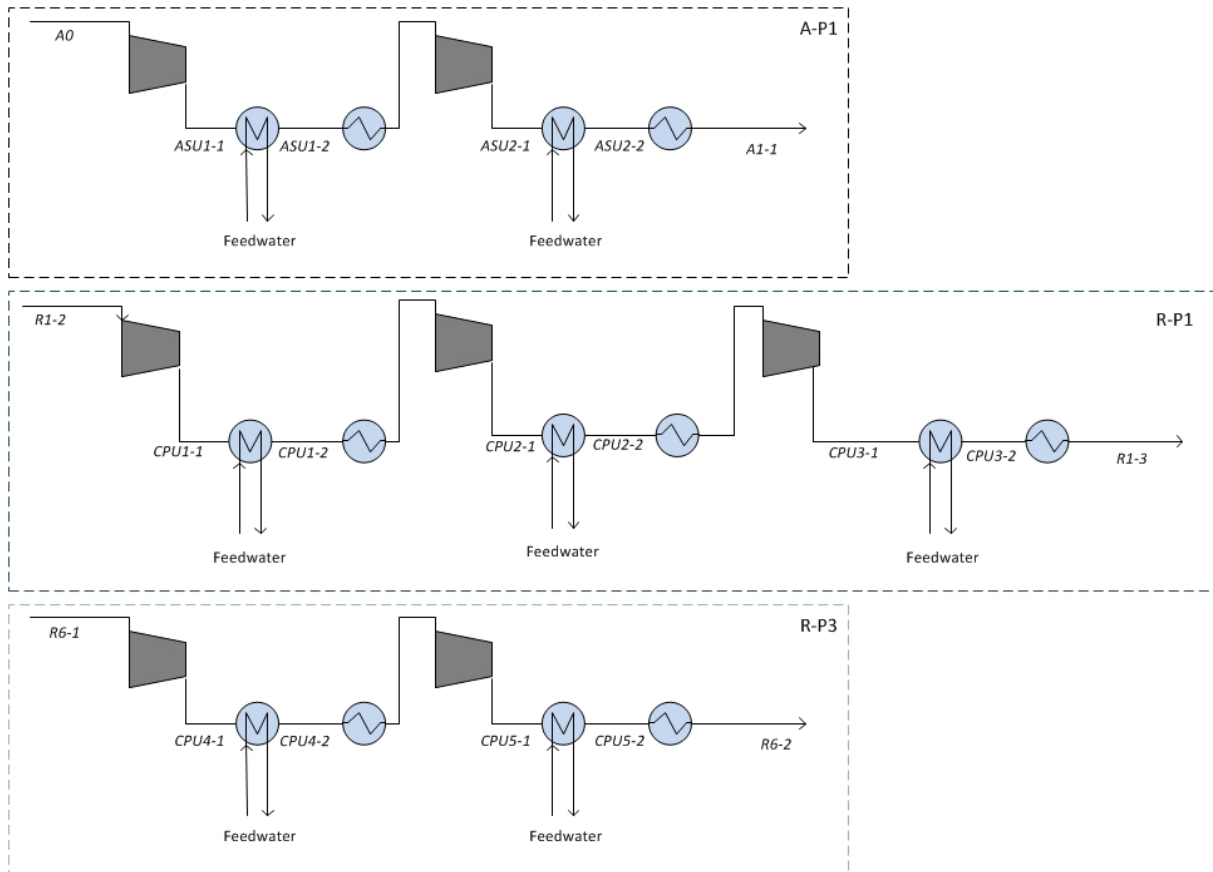
Figure 23 – Arrangement of Compressor Intercooling for Heat Integration

4.1.2 Adiabatic Compression Heat

Instead of integrating the heat removed in the intercoolers, the compression can be performed adiabatic (i.e. compression without intercooling). This will lift the heat to a higher temperature level and increase possibilities for integration. The compression work will increase, but heat integration may improve the overall efficiency of the power plant. There are three multi-stage compressors in the system. These are A-P1, R-P1 and R-P3. A-P1 and R-P3 will have pressure ratios of 5,6 and 4,41 respectively with adiabatic compression. This is considered feasible. R-P1 will on the other hand have a pressure ratio of 31,7. Gray (2011) describes a new compressor for use in a CPU where the compression ratio for one stage can reach 10:1 for one single stage. This compressor is named Ramgen, and is currently under development. This is the highest known compression ratio for use in a CPU, and therefore R-P1 is modified to a two stage compressor with heat integration in-between the stages. The pressure ratio of each stage will then be 5,63. The new arrangement of the compressors A-P1, R-P1 and R-P3 is shown in Figure 24, and the results on compressor performance with the illustrated design are shown in Table 6. The compression in R-P1 is not strictly adiabatic, but the term adiabatic compression will be used for referencing to the compressor configuration shown in Figure 24 later in this report.

36

A-P1		R-P1	
Stage 1 outlet temperature, °C	250,2	Stage 1 outlet temperature, °C	205,9
		Stage 2 outlet temperature, °C	207,6
Total work, kW	149754	Total work, kW	62219
Total cooling duty, kW	153016	Total cooling duty, kW	74923
R-P3			
Stage 1 outlet temperature, °C	165,8		
Total work, kW	17928		
Total cooling duty, kW	30459		
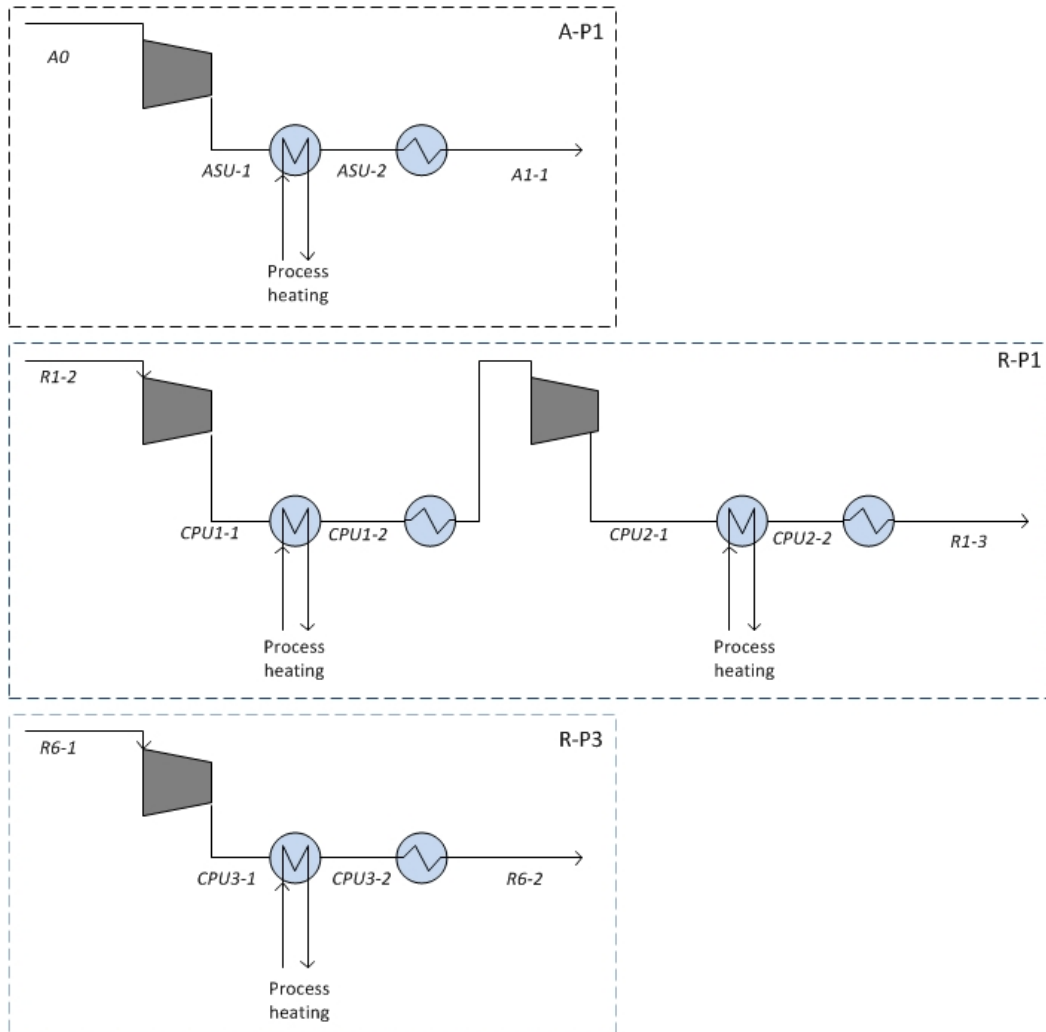
Figure 24 – Arrangement of Adiabatic Compression for Heat Integration

If the compressor performance for intercooled compression in Table 5 is compared with the performance for adiabatic compression Table 6, it can be seen that the increase in work with adiabatic compression, $\Delta \dot{W}_{AD}$, is 22557kW. For heat integration to be energy efficient any increase in work will need to be higher than this. Compared with the base case the temperatures are significantly higher at the stage outlets, something which will increase the possibilities for integration. Due to higher compression work it follows from the energy balance that the cooling duty is higher when adiabatic compression is utilized.

4.1.3 Flue Gas Heat

In addition to the compression heat, there is some potential for integration in the flue gas exiting the steam generator. The base case configuration has a steam generator exit temperature of 176.7°C. Spliethoff (2011) mentions flue gas temperatures of 130°C for modern air-fired steam generators and further discusses possibilities for utilizing the heat to transfer the residual heat to the low-temperature condensate or to combustion air which has not yet been preheated.

A lower limit must be imposed on the flue gas temperature in order to avoid the effects of gas-side acid condensation, i.e. corrosion of metal surfaces of air-preheaters, fouling and/or damage and increased maintenance expenses. In a thermo-economic analysis Espatolero et al. (2010) has concluded that it is profitable to introduce corrosion resistant plastic heat-exchangers to decrease the flue gas temperature down to 80-90°C in air fired cases. Stanger and Wall (2011) have estimated acidic dew points for three coal types in which the acidic dew point of oxy combustion flue gas is from 14-21,6°C higher than that of air-fired flue gas. Furthermore Spliethoff (2010), p.658, states that the acidic dew point for oxy-combustion flue gas may rise up to 160°C depending on the coal composition. It will therefore most likely be necessary to introduce the corrosion resistant material at a higher temperature than in an air-fired case, and more studies should be made to study the profitability of corrosion resistant heat exchangers for oxy-combustion power plants. Even though there is uncertainty surrounding the costs, the use of flue gas heat will be studied in this report in order to investigate the potential energy savings. The flue gas will be extracted from after the ID fans where the temperature is 187°C. If cooled to 85°C the flue gas will give 70955kW of heat available for integration, but the target temperature of the flue gas will depend on the utilization.

4.3   Possibilites for Integration

The utilization of the compression and flue gas heat is limited by the temperature levels. The highest temperature level of the heat is achieved with adiabatic compression in A-P1 as seen in Table 6. Depending on the compressor configuration several options are possible. Below the integration projects suggested in the project description for this master thesis are listed:

1. Integration of compression heat (from ASU and CPU) with the steam cycle (i.e. to use adiabatic compression).
2. Integration of compression heat with the regeneration of molecular sieves in the ASU and the CPU.
3. Using compression heat to preheat the recycled flue gas and oxygen prior to combustion.
4. Integration of compression heat and the low temperature heat from the flue gas with a new CO2 Rankine cycle.

Point 1 concerns integration of compression heat with the steam cycle by using adiabatic compression. There are two ways of integrating the compression heat with the steam cycle; producing more steam or use compression heat to preheat the feedwater. Producing more steam will change the entire configuration of the steam cycle. Due to the complexity this entails, this option has not been evaluated. Integration of the compression heat with the feedwater preheat will enable replacement of steam extractions to the feedwater heaters. This will result in a higher work output from the steam cycle. The additional work output will need to compensate for any increase in compression work. In addition to adiabatic compression heat, it will also be studied how heat from intercooled compressors and the flue gas can be integrated with the feedwater preheat. Integration with the feedwater preheat is studied in Chapter 5.

Point 2 concerns integration of compression heat with the regeneration of molecular sieves in the ASU and CPU. In the base case configuration the regeneration of molecular sieves is achieved through steam extractions from the IP turbine exhaust in the steam cycle. Replacing these steam extractions with compression heat is possible if the temperature level of the compression heat is higher than the condensation temperature of the extracted steam, which is 176,4°C. This can be achieved by adiabatic compression. The extraction steam has a mass flow of 2.27kg/s, and replacing it will result in a 2.95MW increase in work output. This is much lower than the extra work required to compress adiabatically, so this option can only be considered in combination with point 1. However the potential gain is small, and will not be studied further in this report.

Point 3 concerns increasing preheat of the recycled flue gas and oxygen. There are two ways of achieving increased preheat; utilizing compression heat or decreasing the exit temperature of the flue gas from the steam generator. This is further investigated in Chapter 6..

Point 4 is related to work on a CO_2 Rankine cycle by PhD student Amlaku Abie Lakew at NTNU. This cycle can be utilized to recover work from the flue gas exiting the steam generator. Integration with this power cycle is discussed in Chapter 7.

4.4 Assumptions and Constraints for Integration Projects

The integration study has many degrees of freedom, and exploring all possible interactions in the power plant will be very time consuming. In order to simplify the integration study and obtain a fair comparison between the integration projects, it is necessary to make some common assumptions and constraints for the integration projects. Below these assumptions and constraints are listed:

- Flue gas recirculation and excess O_2 will be set constant at 72% and 10,45% respectively for all integration projects.
- No changes are made to the ASU, CPU and FGD except for using adiabatic compression
- The steam extraction to the deareator is considered a process requirement and will not be modified.
- The inlet temperature of feedwater to the steam generator is the same for all cases.
- The heat rejected to water/steam in the steam generator is constant for all cases
- The pressure levels of steam extractions are the same for all cases
- Pressure drops and heat loss in heat exchangers are not taken into account
- Simulation specifications are as stated in Table 1 unless new specifications are proposed.
- No stream extractions should be replaced before the reheater. Replacing steam extraction upstream of the reheater will cause increased heat duty in the steam generator, and may affect its design.

The composite curves will be used to evaluate integration potential. In order to plot the composite curves the Aspen Plus output is entered into Pro_PI1. A ΔT contribution of each stream is entered. The values used can be found in Table 7. The reason for using a lower ΔT contribution for the flue gas in the reheater than for the flue gas exiting the steam generator is that the heat duty of the flue gas in the reheater is very low, and it is unwanted to constrain the integration projects due to this stream.

Table 7 – ΔT Contributions of Streams

Compressed gas	5	K
Flue gas	25	K
Feedwater	5	K
Condensing steam	-2	K
Flue gas in reheater (FG-H)	10	K

5 Integration with Feedwater Preheat

5.1 Motivation and Criterions for Integration

If heat is integrated with the feedwater, the reduced need for steam extractions will increase the work output from the turbines. The expression for the total work of a turbine with n extractions has already been given in (2.5). If $\Delta \dot{m}_{ex}$ is replaced by compression or flue gas heat, the total work will increase by $\Delta \dot{W}_T$. The total work from a turbine with n extractions will then be:

$$\dot{W}_T + \Delta \dot{W}_T = \dot{m}(h_1 - h_{ex,1}) + \sum_{i=1}^{n-1}\left[(h_{ex,i} - h_{ex,i+1})(\dot{m} - \sum_{k=1}^{i}(\dot{m}_{ex,k} - \Delta \dot{m}_{ex,k}))\right] + (h_{ex,n} - h_2)(\dot{m} - \sum_{k=1}^{n}\dot{m}_{ex,k} - \Delta \dot{m}_{ex,k}) \tag{4.1}$$

Thus the increase of work with integration can be found from the following equation:

$$\Delta \dot{W}_T = \sum_{i=1}^{n-1}\left[(h_{ex,i} - h_{ex,i+1})\sum_{k=1}^{i}\Delta \dot{m}_{ex,k}\right] + (h_{ex,n} - h_2)\sum_{k=1}^{n}\Delta \dot{m}_{ex,k} \tag{4.2}$$

From (4.2) it can be seen that replacing a steam extraction in section n will increase the turbine work in all turbine sections downstream of n. From this follows that steam extractions should be replaced at the highest possible pressure. If intercooled compression is utilized for integration with the feedwater preheat the temperature levels for integration are lower than if adiabatic compression is used, but the compression work of adiabatic compression is higher. For adiabatic compression to be implemented the following criteria should be met:

$$\Delta \dot{W}_{T,AD} > \Delta \dot{W}_{C,AD} \tag{4.3}$$

Where $\Delta \dot{W}_{C,AD}$ corresponds to the increase in compression work with adiabatic compression relative to that of the intercooled compression used in the base case and $\Delta \dot{W}_{T,AD}$ to the increased work output from the turbine when adiabatic compression heat is integrated.

For integration of adiabatic compression heat to be used instead of integration of intercooled compression heat the following criteria should be met:

$$\Delta \dot{W}_{T,AD} > \Delta \dot{W}_{T,IC} \tag{4.4}$$

Where $\Delta \dot{W}_{T,IC}$ is the work increase obtained by integrating intercooled compression heat.

The both (4.3) and (4.4) is met, integration of adiabatic is considered optimal from an energetic point of view.

5.2   Integration Projects

In Table 8 the temperature levels and heat duty of the cold streams in the feedwater preheaters is shown. The streams from FWH 1 to FWH 4 are a part of the low pressure condensate system, and the streams from FWH 6 to FWH 8 are a part of the high pressure feedwater system. From the temperature levels of the heat sources described in Chapter 4.2, it can be seen that intercooled compression heat and flue gas heat will only permit integration with the low pressure condensate system while adiabatic compression will permit some integration with the high pressure feedwater system.

Table 8 – Heat Duty and Temperature Levels of Cold Streams in Feedwater Preheaters

	FWH 1	FWH 2	FWH 3	FWH 4	FWH 6	FWH 7	FWH 8
Inlet Temperature, C	39,0	62,0	80,5	103,4	182,0	214,4	259,6
Outlet Temperature, C	60,1	80,5	103,4	144,1	214,4	259,6	289,8
Heat duty, kW	41188	43705	45149	81013	86531	125062	88923

Based on the temperature levels of the heat sources and in the feedwater system, the following integrations are suggested:

1.   Integration of intercooled compression heat with the low pressure condensate system.
2.   Integration of intercooled compression heat and flue gas heat with the low pressure condensate system.
3.   Integration of adiabatic compression heat with the low pressure condensate and the high pressure feedwater.
4.   Integration of adiabatic compression heat and flue gas heat with the low pressure condensate and high pressure feedwater

Point 1 and 2 is evaluated in order to study the potential gain of using adiabatic compression in 3 and 4, and to check whether the criterions stated in (4.3) and (4.4) are met. In order to evaluate the potential of integration options listed above, the Aspen Plus simulation model is modified to study the potential of the four different cases. In all the simulations SRK is used as equation of state for the heat exchange between the compression gas and flue gas and feedwater, and not Peng-Robinson. This is because Aspen Plus enables use of the Steam NBS tables for pure water

if SRK is applied. This makes the property calculations for the feedwater similar as in the base case simulation, and convergence problems in the steam cycle calculations are avoided.

5.3   Integration of Intercooling Heat

5.3.1   Integrated Design

The purpose of this integration is to recover heat from the compressor stage outlets for use with the low pressure condensate. This will replace some of the cooling water consumption in the compressor intercooling. The hot streams are the compression streams from the intercooled compressors shown in Figure 23 and the cold streams are the low pressure condensate and the recycled flue gas in the recycled flue gas reheater (FG-H in Figure 18). The hot and cold composite curves and GCC of these streams are available in Figure 25 and Figure 26. From the composite curves it can be seen that the temperature levels of the compression streams are insufficient to cover all of the heating needs of the low pressure condensate. The pinch is at 120°C, and the MER for heating is calculated to be 41196kW. The heating will have to be supplied by steam with a dew point temperature above pinch, which means that the steam should be extracted from the exhaust of IPT 2 where the pressure is 9,49bar and the dew point temperature is 176,8°C.
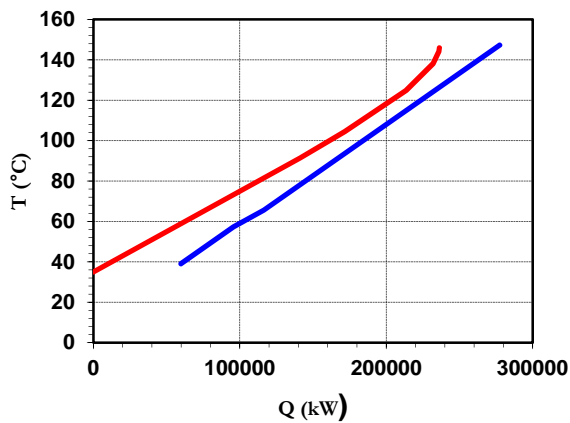
Figure 25 – Composite Curves of Integration   Figure 26 – GCC of Integration
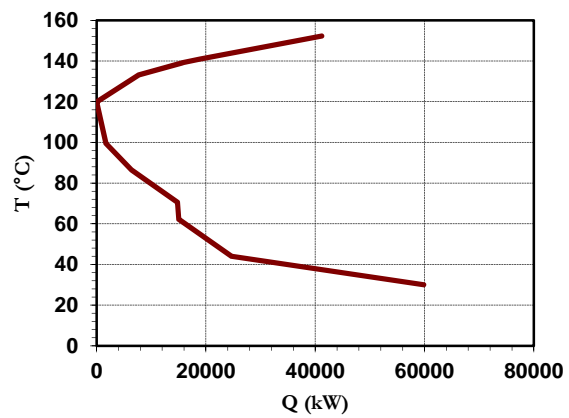
The suggested design of the steam cycle is shown in Figure 27. The compressors A-P1, RP-1 and R-P3 are operated as shown in Figure 23 with heat rejection to the low pressure condensate system and the recycled flue gas in-between the compressor stages. The integration of the intercooling heat with the low pressure condensate and recycled flue gas takes place in the heat exchanger network MHX in Figure 27.
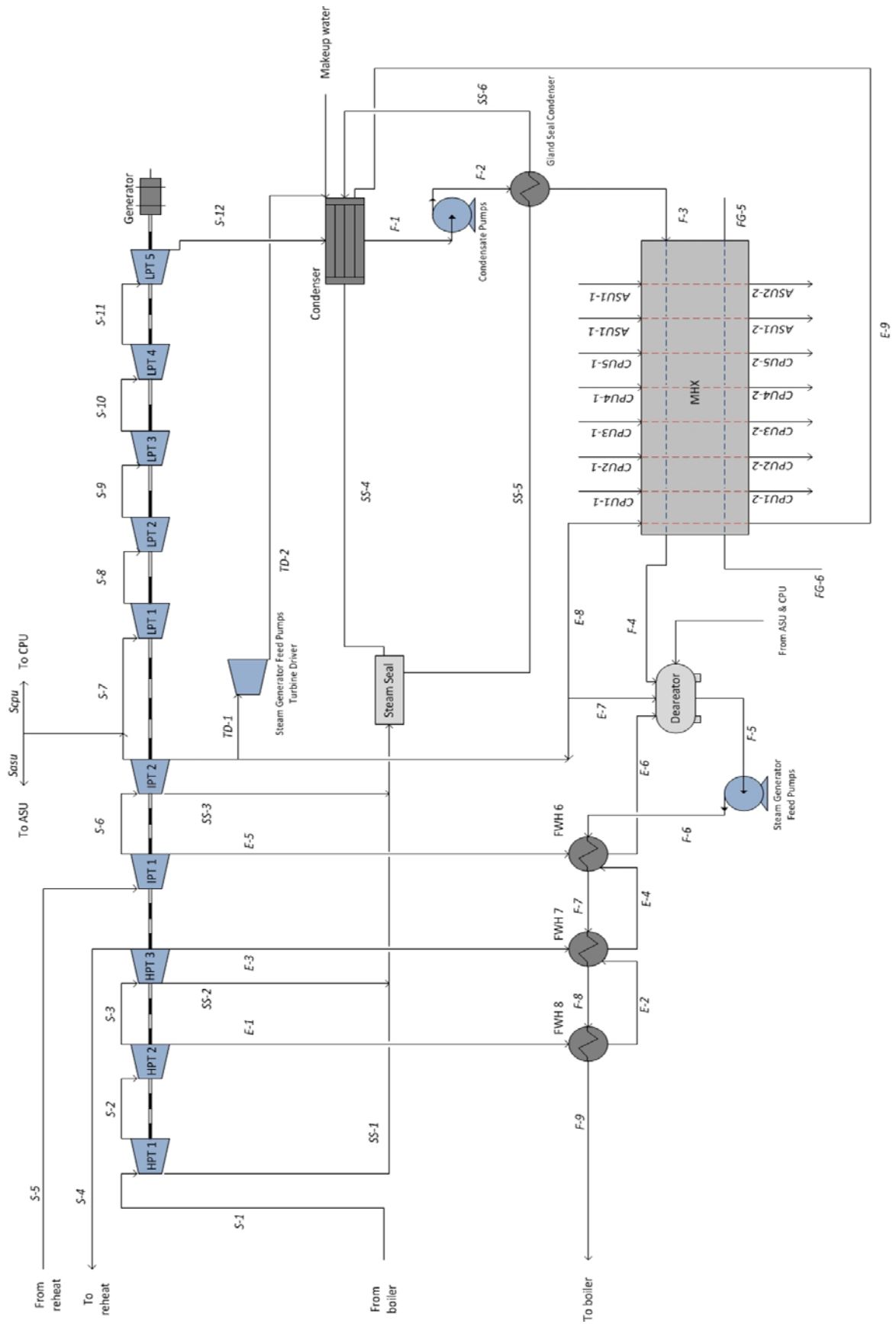
Figure 27 – Steam Cycle Integrated with Intercooling Heat

5.3.2 Integration Results

The results of the integration are summarized in Table 9. Full stream results are available in the appendix. From the results it can be seen that the integration of compression heat with the feedwater can improve the thermal efficiency by 1,19%. The net power output from the power plant will be increased by 21,5MW.

Table 9 – Comparison of performance between Air-Fired Case, Base Case and Integrated Case

	Air fired	Base Case	Integrated
Gross Power, kW	591616	799760	821999
Power Requirement			
ASU			
A-P1, kW	0	133720	133720
A-P2, kW	0	-9705	-9705
CPU			
R-P1, kW	0	57605	57605
R-P3, kW	0	16019	16019
R-P2, kW	0	2015	2015
R-P4, kW	0	-8862	-8862
R-P7, kW	0	2595	2595
Other			
Fan Work, kW	12127	12198	12198
Auxilliaries, kW	18932	25592	26304
Condensate pumps, kW	811	1099	1099
Net Power	559746	567485	589012
Fuel Consumption, kW	51,32	69,23	69,23
LHV efficiency	41,68 %	31,32 %	32,51 %

Table 10 – Comparison of Turbine Work Output for Oxy-Combustion With and Without Integration

	HPT 1	HPT 2	HPT 3	IPT 1	IPT 2	LPT 1	LPT 2	LPT 3	LPT 4	LPT 5
Extractions, kg/s[2]										
Integrated case	0,56	47,57	41,57	20,00	70,46	0,00	0,00	0,00	0,00	0,00
Base case	0,56	47,57	61,56	24,88	54,46	33,28	16,48	15,64	15,48	0,00
Power, MW[3]										
Integrated case	36,55	160,72	61,20	126,33	111,86	63,59	107,86	53,98	49,32	63,11
Base case	36,55	160,72	61,20	126,33	111,86	66,09	103,28	49,51	43,34	53,06
Work increase with integration, %	0,00	0,00	0,00	0,00	0,00	-3,78	4,43	9,03	13,80	18,94

---

[2] Extraction after turbine

[3] Turbine work does not take generator efficiency into account
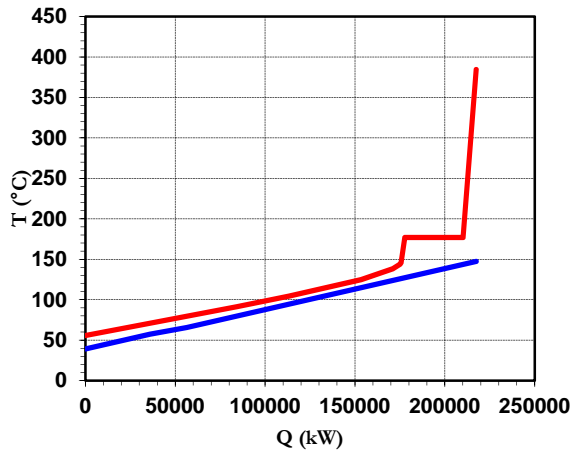
Figure 28 – Balanced Composite Curves   Figure 29 – Balanced GCC
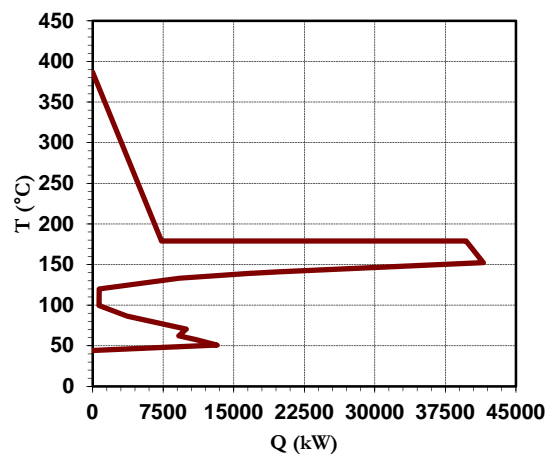
In Table 10 the steam extractions in the integrated is compared with the base case. The change in turbine work is also listed. The increase in steam extraction from the IPT 2 exhaust results in a reduction of the work in LPT 1, but from LPT 2 and onwards the work increases due to the elimination of extractions from downstream of LPT 1. The balanced composite curves of MHX are shown in Figure 28 and the balanced GCC in Figure 29. These show that the introduction of the steam extraction from the LPT 1 exhaust helps to overcome the pinch in Figure 25 and Figure 26.

5.3.3   Complexity and Costing

The integration of compression intercooling with feedwater increases the complexity of the system by adding additional heat exchangers and piping between the different sections of the power plant. From (2.27) it can be found that the heat exchanger network in MHX will require at least 9 heat exchanger units. In addition to this each stage of compression needs an intercooler where cooling water provides the final cooling of the gas to 35°C. This totals to 16 heat exchanger units compared to 11 in the base case scenario.

The main costs related to the integration of compression heat with the steam cycle are related to the investment in additional heat exchangers and the piping for the new interconnections. In addition it is probable that the overall heat exchanger area will be increased. The compression streams will give lower film heat transfer coefficients than the condensing steam they replace, and will therefore give higher area requirements. Replacing cooling water with feedwater in the compression intercooling should not significantly change the U-value of the heat exchange, but it can be seen from the balanced composite curves in Figure 28 that the feedwater has higher

temperature levels than cooling water. This will decrease the temperature differences in the heat exchange and increase the requirement for heat exchange area. The water coolers will however require significantly less heat exchange area as most of the intercooling will be provided by the feedwater. Since heat rejection to the feedwater replaces intercooling with cooling water it is uncertain how much the heat exchanger area requirements will grow, but an increase is likely.

The pressurized compression streams may also pose operational problems. In leakage of gases, in particular CO_2, into the feedwater system may lower the pH of the of the feedwater and cause corrosion in the steam cycle. Pipe ruptures may also cause leakages of CO_2 rich gas which can be a hazard to workers at the plant.

5.4   Integration Intercooling- and Flue Gas Heat

5.4.1   Integrated Design

The purpose of this integration is to recover heat from the flue gas and from the compression gas to use with the low pressure condensate system. The hot streams are the compression streams from the intercooled compressors shown in Figure 23 and the flue gas. The cold streams are the low pressure condensate and the recycled flue gas in the recycled flue gas reheater (FG-H in Figure 18). The composite curves and GCC of these streams are shown in Figure 30 and Figure 31. For making the curves the flue gas is set to be cooled to 85°C, but in the actual design it may have a different target temperature. From the composite curves it can be seen that the amount of heat that can be recovered from the hot streams is insufficient to cover all of the heating needs of the low pressure condensate system. The pinch temperature is 133°C and is the result of the ΔT contribution of the Flue Gas. The calculated minimum energy requirement for heating is 11124kW, and some steam extraction above pinch is necessary in order to achieve the target temperature of the low pressure condensate. The steam has to be utilized above then pinch, and will therefore be extracted from the IPT 2 exhaust where the pressure is 9,49bar and the dew point temperature is 176,8°C. The required cooling is high, so it is likely that the flue gas target temperature will be much less than 85°C.

The suggested integrated design of the steam cycle is shown in Figure 32. All compressors are operated as in the base case, but the intercooling with heat rejection to the feedwater and the recycled flue gas is performed as shown in Figure 23. In addition to integration of compression heat, the flue gas from the steam generator is integrated with the feedwater (streams FG-3-1 and FG-3-2). The flue gas is extracted from after the ID fan (stream FG-3 in Figure 18). It should be noted that MHX is a heat exchanger network and not one single heat exchanger.
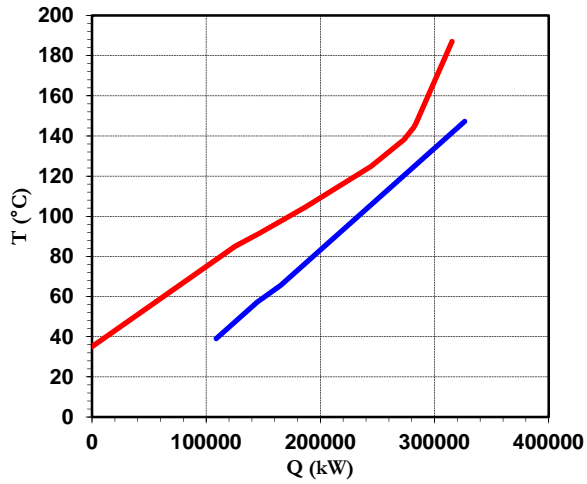
Figure 30 – Composite Curves of Integration

Figure 31 – GCC of Integration

Table 11 - Comparison of performance between Air-Fired Case, Base Case and Integrated Case

	Air fired	Base Case	Integrated
Gross Power, kW	591616	799760	832004
Power Requirement			
ASU			
A-P1, kW	0	133720	133720
A-P2, kW	0	-9705	-9705
CPU			
R-P1, kW	0	57605	57605
R-P3, kW	0	16019	16019
R-P2, kW	0	2015	2015
R-P4, kW	0	-8862	-8862
R-P7, kW	0	2595	2595
Other			
Fan Work, kW	12127	12198	12198
Auxilliaries, kW	18932	25592	26624
Condensate pumps, kW	811	1099	1099
Net Power	559746	567485	598696
Fuel Consumption, kW	51,32	69,23	69,23
LHV efficiency	41,68 %	31,32 %	33,04 %
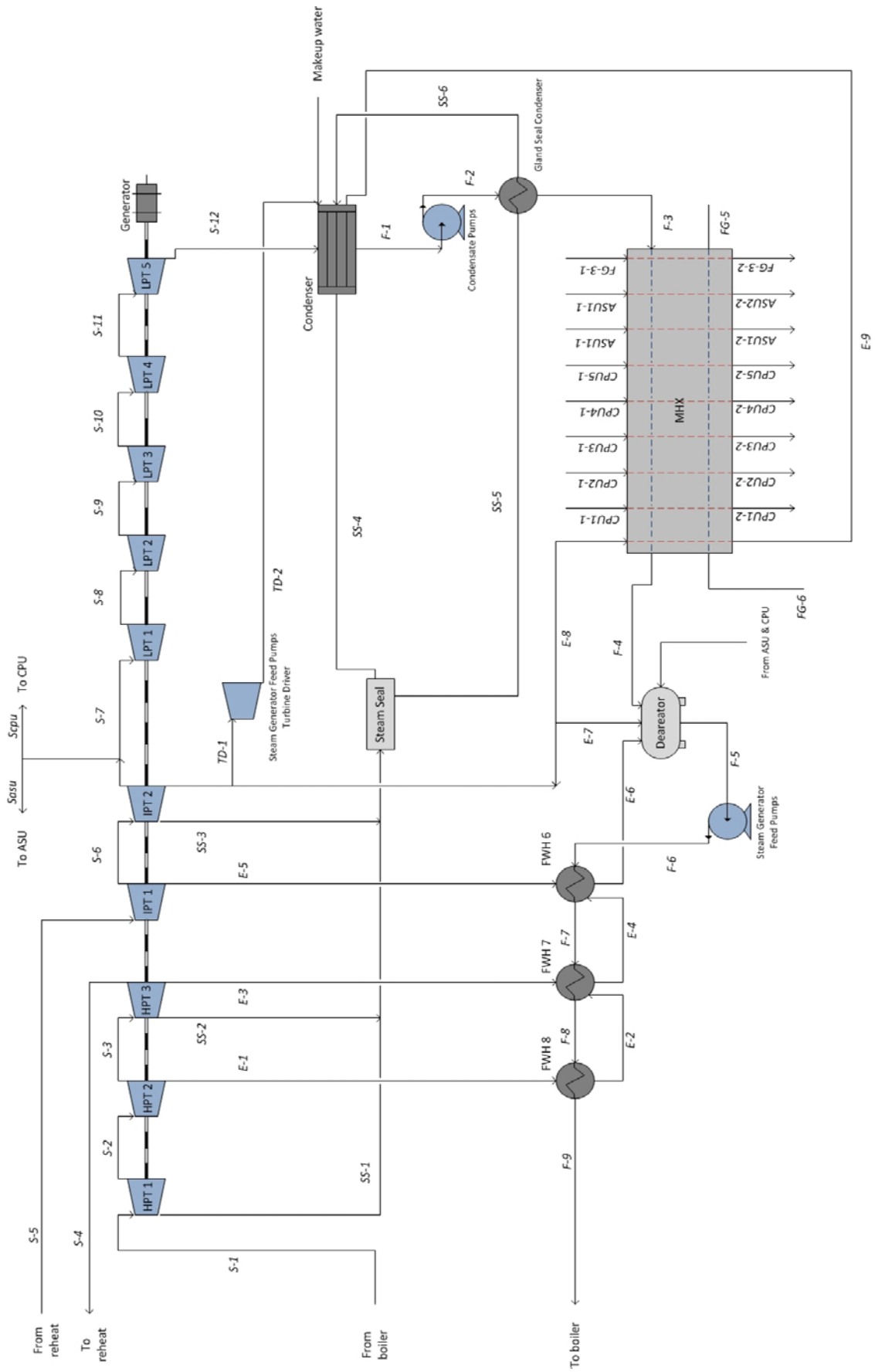
Figure 32 – Steam Cycle Integrated with Intercooling and Flue Gas Heat

5.4.2 Results

The results of the integration are summarized in Table 11. Full stream results are available in the appendix. From the results it can be seen that the integration of compression and flue gas heat can increase the thermal efficiency by 1,72%. The flue gas is only cooled to 150°C, and that there therefore still will be heat available for integration. Alternatively the flue gas could be cooled further reducing the heat duty of the compression streams and increase the driving force for heat exchange, but the reducing the heat duty of the flue gas is preferable in order to stay above the acidic dew point and minimize the need for corrosion resistant heat exchange surfaces. In Figure 33 and Figure 34 the balanced composite curves and the balanced GCC can be seen. It is now visible that the steam extraction helps to overcome the pinch. From the balanced GCC it can be seen that it is possible to reduce the steam extraction slightly in order to get closer to the minimum required driving force in the region around 140°C. This has however not been further investigated, but slight efficiency improvements are probable.
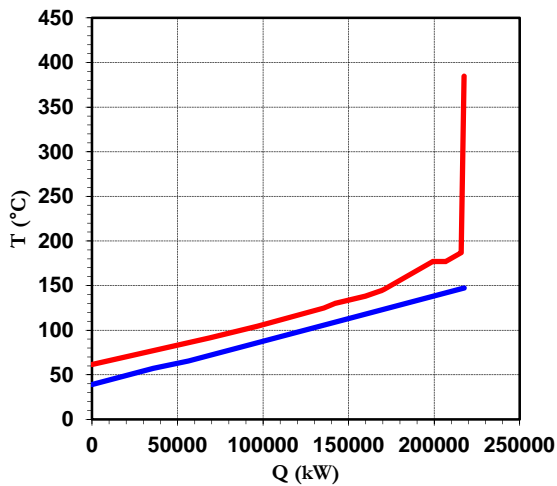
Figure 33 – Balanced Composite Curves
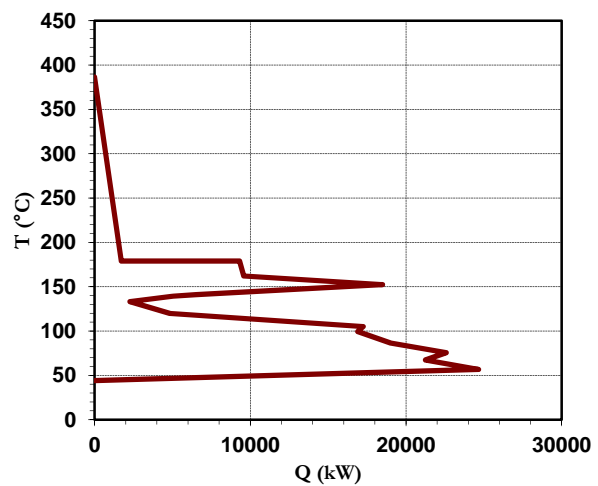
Figure 34 – Balanced GCC

Table 12 - Comparison of Turbine Work Output for Oxy-Combustion With and Without Integration

	HPT 1	HPT 2	HPT 3	IPT 1	IPT 2	LPT 1	LPT 2	LPT 3	LPT 4	LPT 5
Extractions, kg/s[4]										
Integrated case	0,56	47,57	61,56	24,88	58,21	0,00	0,00	0,00	0,00	0,00
Base case	0,56	47,57	61,56	24,88	54,46	33,28	16,48	15,64	15,48	0,00
Power, MW[5]										
Integrated case	36,55	160,72	61,20	126,33	111,86	65,50	111,1	55,60	50,80	65,01
Base case	36,55	160,72	61,20	126,33	111,86	66,09	103,28	49,51	43,34	53,06
Work increase with integration, %	0,00	0,00	0,00	0,00	0,00	-0,89	7,57	12,30	17,21	22,52

---

[4] Extraction after turbine

[5] Turbine work does not take generator efficiency into account

In Table 12 steam extractions after each turbine and the turbine work for each turbine is shown for the integrated design and the base case respectively. The results shows that the increase in turbine work is increasing downstream of LPT 1. The reason for the small decrease in work in LPT 1 is that the steam extraction here is increased by 3,75kg/s in order to overcome the pinch.

5.4.3 Complexity and Costing

The integration of compression intercooling with feedwater increases the complexity of the system by adding additional heat exchangers and piping between the different sections of the power plant. From (2.27) it can be found that the heat exchanger network in MHX will require 10 heat exchanger units. In addition each stage of compression needs an intercooler were cooling water cools the gas down to 35°C. This totals to 17 heat exchanger units compared to 11 in the base case scenario.

The considerations regarding heat exchanger surface area and operational issues are much like the ones for the case studied in Chapter 5.3, with the key difference being the introduction of flue gas heat. The flue gas is utilized prior to desulfurization, something which may necessitate in the use of corrosion resistant heat exchangers on the gas side when the flue gas is utilized. This applies if the acidic dew point of the flue gas is above 150°C. Flue gas normally gives low film heat transfer coefficients, so the overall heat exchanger surface area may be slightly higher for this case than for the case in Chapter 5.4. However if the balanced composite curves in Figure 28 and Figure 33 are compared, it can be seen that the average temperature difference is higher when the flue gas heat is introduced. This will decrease the heat exchanger surface area requirement. It is therefore difficult to compare the heat exchanger surface area of this integration and the one in Chapter 5.3 without performing a more detailed analysis.

5.5 Integration of Adiabatic Compression Heat with Feedwater

5.5.1 Integrated Design

The purpose of this integration is to integrate the heat from adiabatic compression with the feedwater system. The hot streams are the compression streams from adiabatic compression in Figure 24. The cold streams are the low pressure condensate, the high pressure feedwater and the recycled flue gas in the recycled flue gas reheater (FG-H in Figure 18). The composite curves and GCC of the integration are plotted in Figure 35 and Figure 36. From the composite curves it can be seen that it is necessary utilize steam extractions in order to reach the target temperature of the feedwater. The MER for heating is calculated to be 190081kW. It will be attempted to replace

steam extractions at as high pressure as possible, but not upstream of the reheat. When steam extractions to the high pressure feedwater heaters are replaced, the flow channeled back into the deaerator will be less. This will in turn result in a reduction of the flow through the turbines. In order to compensate for this more water needs to pass through the low pressure condensate system. This will increase the heat consumption before the deaerator, and the pump work of the condensate pumps while the temperature jump in the deaerator will decrease.
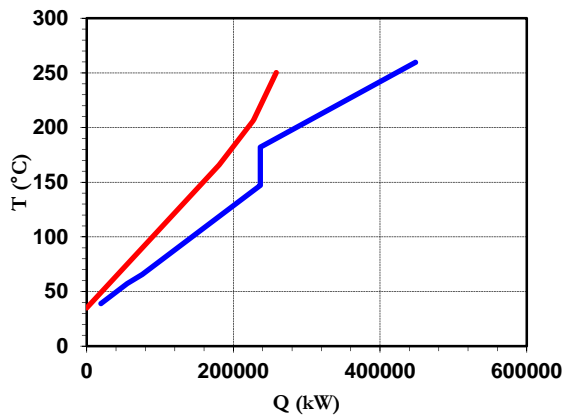
Figure 35 – Composite Curves of Integration
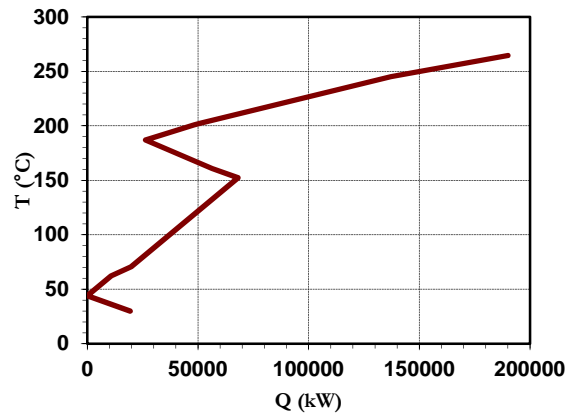
Figure 36 – GCC of Integration

The suggested layout for the modified steam cycle is shown in Figure 39. Note that the multi stream heat exchangers, MHX-1 and MHX-2, are representing heat exchanger networks and not actual heat exchangers. Steam extraction from IPT 1 will be used for heating in MHX 1. In MHX 2 steam extractions from LPT 1 to LPT 4 will be used for heating. In order to establish the performance, an Aspen Plus simulation was performed. The design point was established iteratively by varying the amount of steam extractions at the various pressure levels in order to reach the MER for heating.
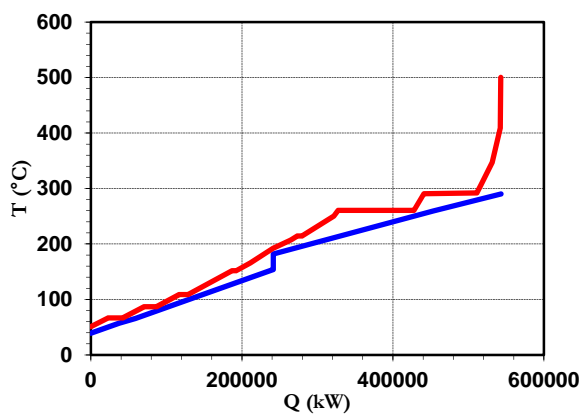
Figure 37 – Balanced Composite Curves
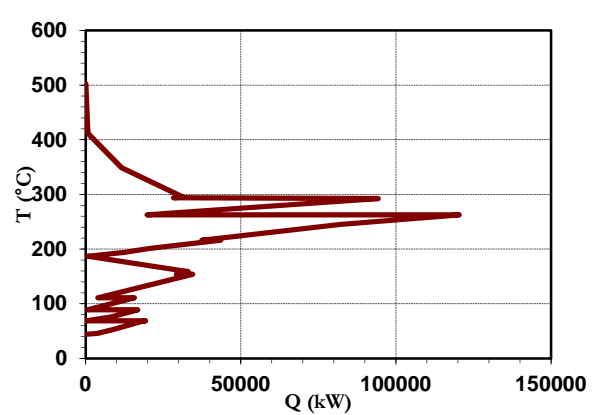
Figure 38 – Balanced GCC
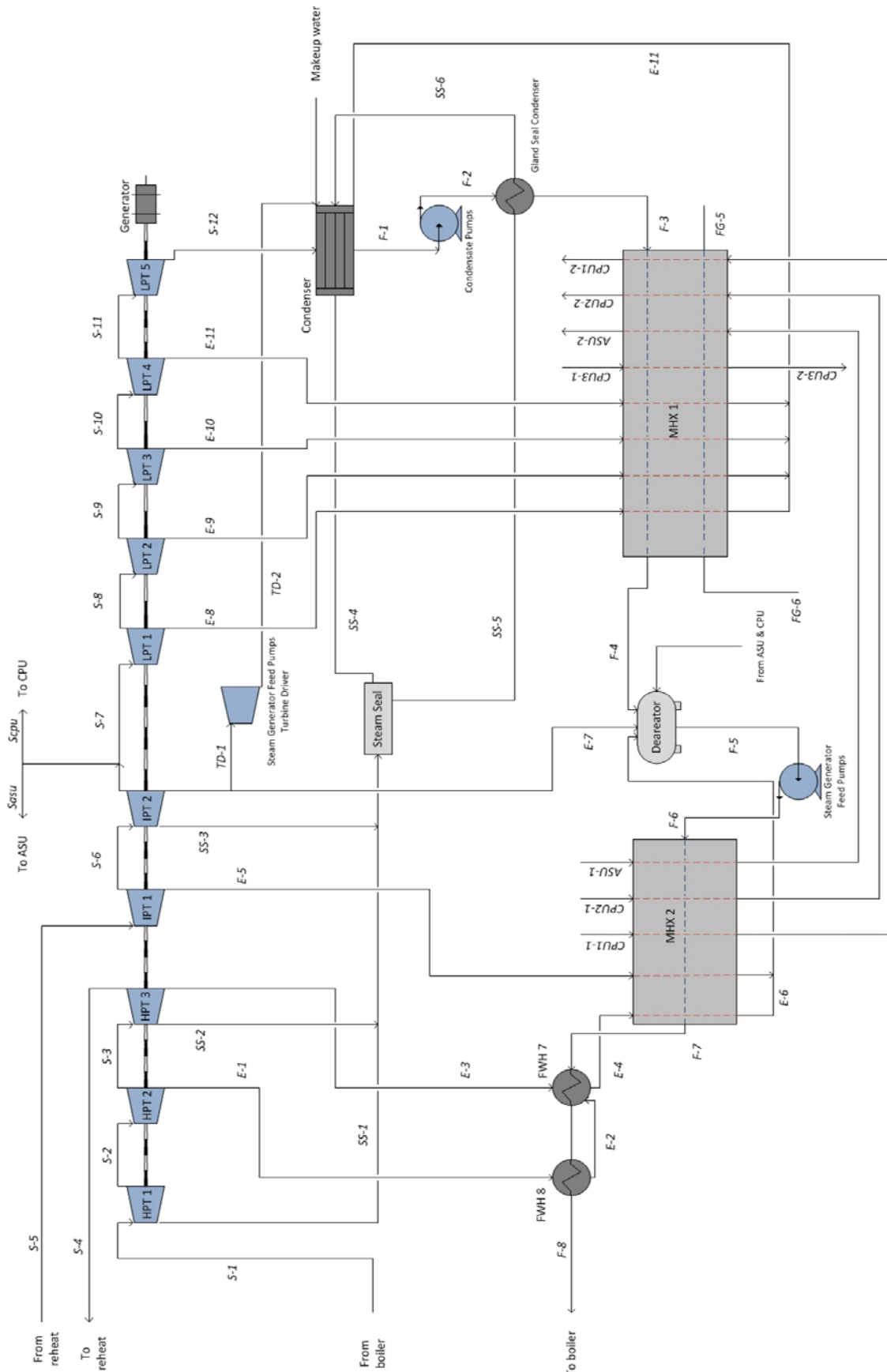
Figure 39 – Steam Cycle Integrated with Adiabatic Compression Heat

5.5.2 Results

A summary of the results of the integration can be seen in Table 13. Full stream results for the steam cycle are available in the appendix. The balanced composite curves and balanced GCC are available in Figure 37 and Figure 38.
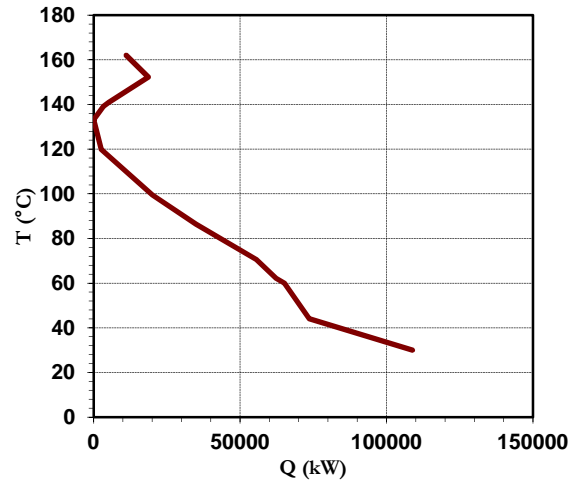
<div align="center">Table 13 – Comparison of performance between Air-Fired Case, Base Case and Integrated Case</div>

	Air fired	Base Case	Integrated
Gross Power, kW	591616	799760	850907
Power Requirement			
ASU			
A-P1, kW	0	133720	149754
A-P2, kW	0	-9705	-9705
CPU			
R-P1, kW	0	57605	62219
R-P3, kW	0	16019	17928
R-P2, kW	0	2015	2015
R-P4, kW	0	-8862	-8862
R-P7, kW	0	2595	2595
Other			
Fan Work, kW	12127	12198	12198
Auxilliaries, kW	18932	25592	27229
Condensate pumps, kW	811	1099	1150
Net Power	559746	567485	594386
Fuel Consumption, kW	51,32	69,23	69,23
LHV efficiency	41,68 %	31,32 %	32,81 %

From Table 13 it can be seen that the integration of Adiabatic Compression significantly increases the thermal efficiency. An improvement of 1,49% in thermal efficiency is obtained by integration. The results show that criterions for integration of adiabatic compression heat are fulfilled as (5.3) and (5.4) holds. The balanced composite curves and balanced GCC of the feedwater preheat shows that the temperature levels of the compression heat are well utilized with this configuration. The pinches are caused by the condensing steam, and the amount of steam added at each pressure level has been adjusted in order to respect the ΔT_{min} constraints specified earlier in this chapter. However it is probable that optimizing the amount of extractions will result in even further efficiency improvements as each steam extraction can be adjusted to

create a pinch. Doing this iteratively in Aspen Plus is time consuming, and has not been attempted.

In Table 14 the mass flows of the steam extractions in the integrated case and in the base case are shown along with the increase in work in each turbine section. From this it can see that the power output increases downstream of IPT 1.

Table 14 - Comparison of Turbine Work Output for Oxy-Combustion With and Without Integration

	HPT 1	HPT 2	HPT 3	IPT 1	IPT 2	LPT 1	LPT 2	LPT 3	LPT 4	LPT 5
Extractions, kg/s[6]										
Integrated case	0,56	47,57	61,56	3,10	54,46	2,50	5,00	7,00	8,50	0,00
Base case	0,56	47,57	61,56	24,88	54,46	33,28	16,48	15,64	15,48	0,00
Power, MW[7]										
Integrated case	36,55	160,72	61,20	131,35	116,93	69,47	117,17	57,98	52,13	65,39
Base case	36,55	160,72	61,20	131,35	111,86	66,09	103,28	49,51	43,34	53,06
Work increase with integration, %	0,00	0,00	0,00	0,00	4,53	5,11	13,45	17,11	20,28	23,24

5.5.3 Complexity and Costing

The integration of adiabatic compression heat will increase the complexity of the system by the addition of more heat exchangers and piping for interconnections. From (2.27) it can be seen that the minimum number of heat exchange units for this integration is 9 for MHX 1 and 4 for MHX 2. In total this will give 15 units for the feedwater system (Including FWH 7 and 8). In addition there will be a total of 4 coolers supplied by cooling water in the compressors A-P1, R-P1 and R-P3. This totals to 19 units compared to 14 in the base case.

The integration will cause an increase in the heat exchange surface area requirement for the feedwater preheaters as condensing steam is replaced by compressed gas with much lower film heat transfer coefficients. However, since the heating of the feedwater is used to cool compression gases and replacing cooler area, it is uncertain if the total area requirement will increase compared to the base case. The feedwater holds a higher temperature than the cooling water, so the decrease in temperature differences in heat exchange will result in higher area requirements. Compared with the integration case in Chapter 5.3, the area requirement for the

---

[6] Extraction after turbine
[7] Turbine work does not take generator efficiency into account

heat exchangers utilizing compression heat to preheat the feedwater is likely to be lower since the average pressure of heat rejection is higher due to the use of adiabatic compression. However, since steam is extracted at several pressure levels, this configuration will require more heat exchanger units than the one in Chapter 5.3. It is possible that the most cost efficient solution will be to extract more steam at higher pressure levels in order to eliminate some of the low pressure extractions.

As for the integration, the same safety and operational issues mentioned in Chapter 5.3.3 apply here when it comes to integration of the compression streams.

5.6 Integration of Adiabatic Compression Heat and Flue Gas Cooling with Feedwater

5.6.1 Integrated Design

This integration shares many similarities with the integration described in Chapter 5.5, with the only difference being that the flue gas is added as a hot stream. The composite curves and GCC of the streams can be seen in Figure 40 and Figure 41 with the flue gas set to be cooled to 85°C. The MER for heating is calculated to be 163758kW. The pinch point is in the start of the high pressure feedwater system, and all steam extractions will be introduced above this point. As in Chapter 5.5 it will be attempted to utilize steam extractions at the lowest possible pressures, but not upstream of the reheat. In Figure 42 the proposed process layout can be seen. The compressor layout is as in Figure 24. Also here MHX1 and MHX2 represent heat exchanger networks and not actual heat exchangers.
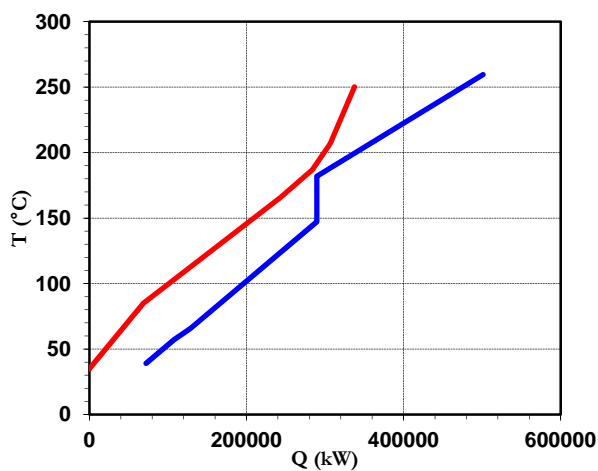
Figure 40 – Composite Curves of Integration
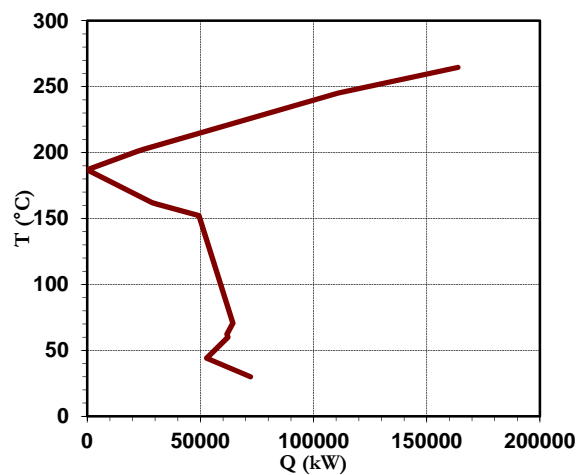
Figure 41 – GCC of Integration
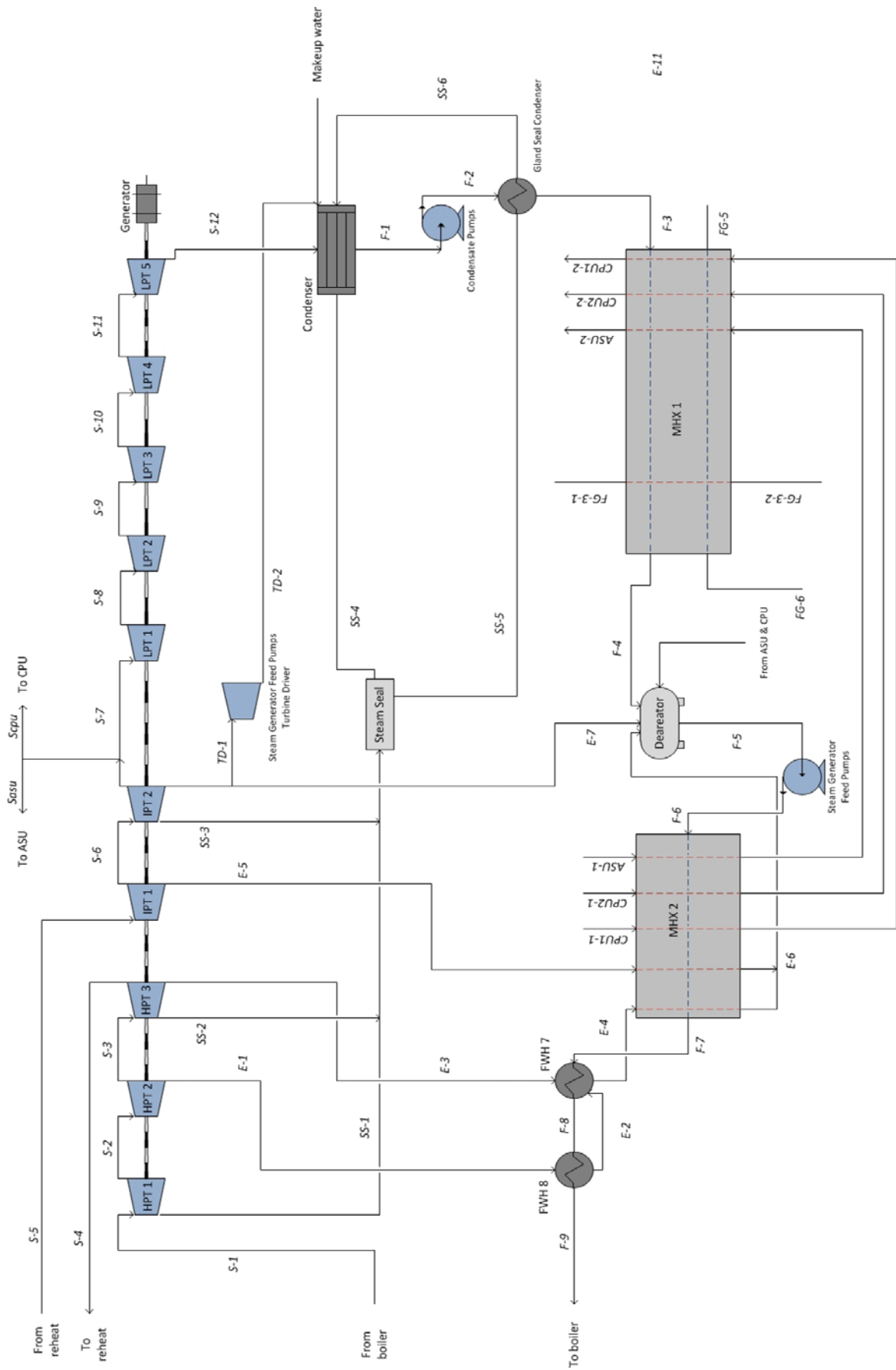
Figure 42 – Steam Cycle Integrated with Adiabatic Compression Heat and Flue Gas

5.6.2 Results

A summary of the results from the Aspen Plus simulation can be seen in Table 15. It can be seen that this integration increases the net power output by 35,6MW, resulting in an increase in the thermal efficiency of 1.96%. Also here the criterions for integration stated in (5.3) and (5.4) holds. The flue gas needs to be cooled to 85,2°C for this design, and it is not necessary to use adiabatic compression in R-P3. The balanced composite curves and GCC of the heat exchange in MHX 1, MHX 2, FWH 7 and 8 are shown in Figure 42 and Figure 43. These shows an even distribution in temperature differences in the heat exchange in the low pressure condensate system where only compression and flue gas heat is utilized. It can be seen that the steam extractions do not reach the ΔT_{min}, so the steam extractions can be slightly reduced. From Table 16 it can be seen that the reduction of steam extractions give an increase in expansion work from IPT 2 to LPT 5. The increase in work is highest in the low pressure turbines.

Table 15 - Comparison of performance between Air-Fired Case, Base Case and Integrated Case

	Air fired	Base Case	Adiabatic
Gross Power, kW	591616	799760	857880
Work Requirement			
ASU			
A-P1, kW	0	133720	149754
A-P2, kW	0	-9705	-9705
CPU			
R-P1, kW	0	57605	62219
R-P3, kW	0	16019	16019
R-P2, kW	0	2015	2015
R-P4, kW	0	-8862	-8862
R-P7, kW	0	2595	2595
Other			
Fan Work, kW	12127	12198	12198
Auxilliaries, kW	18932	25592	27452
Condensate pumps, kW	811	1099	1150
Net Work	559746	567485	603045
Fuel Consumption, kW	51,32	69,23	69,23
LHV efficiency	41,68 %	31,32 %	33,28 %
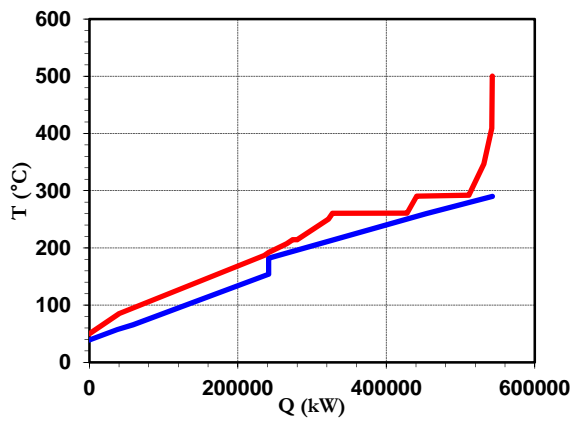
Figure 43 – Balanced Composite Curves
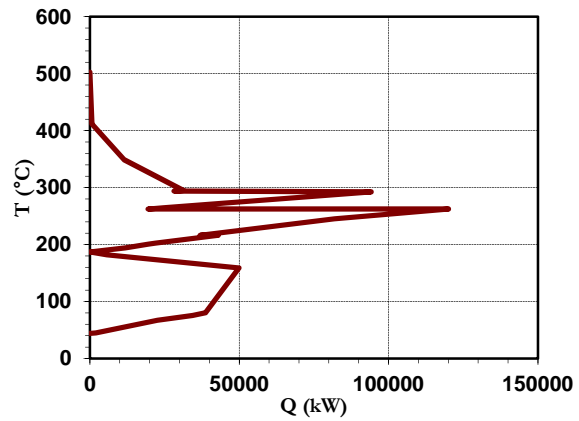
Figure 44 – Balanced GCC

Table 16 - Comparison of Turbine Work Output for Oxy-Combustion With and Without Integration

	HPT 1	HPT 2	HPT 3	IPT 1	IPT 2	LPT 1	LPT 2	LPT 3	LPT 4	LPT 5
Extractions, kg/s[8]										
Integrated case	0,56	47,57	61,56	3,10	54,46	0,00	0,00	0,00	0,00	0,00
Base case	0,56	47,57	61,56	24,88	54,46	33,28	16,48	15,64	15,48	0,00
Work, kW[9]										
Integrated case	36,55	160,72	61,20	131,35	116,95	69,49	117,86	58,98	53,89	68,96
Base case	36,55	160,72	61,20	126,33	111,86	66,09	103,28	49,51	43,34	53,06
Increase with integration, %	0,00	0,00	0,00	0,00	4,55	5,14	14,12	19,13	24,34	29,97

5.6.3 Complexity and Costing

The complexity and costing of this integration will be much like in 5.5. However the replacement of all steam extractions to the low pressure condensate system results in a lower number of heat exchange units required. The minimum number of units for this integration is 5 for MHX 1 and and 4 for MHX 2. In addition there will be 5 coolers supplied by cooling water in the compressors A-P1, R-P1 and R-P3. This gives a total of 16 heat exchange units (Including FWH 7 and 8) which two more than the base case. It is likely that there will be an increase in total heat exchanger area as steam extractions are replaced by flue gas at close to ambient pressure. The flue gas is cooled to 85,2°C, something which will most likely make it necessary to use corrosion resistant surfaces where the flue gas is utilized. The flue gas will give significantly lower film heat transfer coefficients than condensing steam, and the corrosion resistant surfaces will also increase the thermal resistance. However the reduced complexity and higher thermal efficiency than in 5.5 creates incentive for integrating the flue gas heat.

---

[8] Extraction after turbine

[9] Turbine work does not take generator efficiency into account

The same safety and operational issues mentioned in Chapter 5.3.3 apply here when it comes to integration of the compression streams with the feedwater.

6 Recycled Flue Gas Preheat

6.1 Background

In the base case, preheating of the recycled flue gas is already performed in the preheater in the steam generator. In the composite curves of the steam generator in Figure 45, the preheating is the part which stretches from 0 to around 180MW. The pinch in the steam generator occurs in the hot end of the preheater, and any additional preheat below the pinch will therefore reduce the ΔT_{min} of the steam generator, which will in turn increase the required heat exchange area. However, the fuel consumption and consequently the steam generator efficiency will increase due to the higher temperature of the recycled flue gas and oxygen entering the steam generator. A decrease in fuel consumption will also slightly reduce the O_2 requirement and thereby the work required in the ASU. The decrease in fuel consumption and in the O_2 requirement will in turn result in a reduction in the flow rate of flue gas, resulting in a reduction of the work in the CPU.
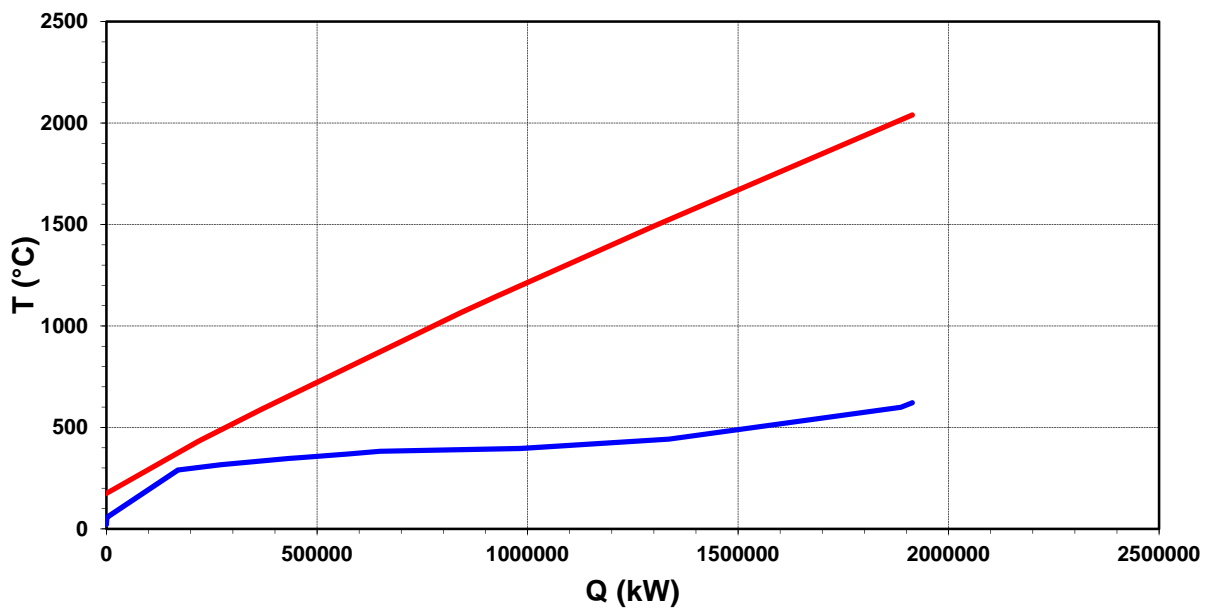
Figure 45 – Composite Curves of Steam Generator

6.2 Possibilities for Integration

It is possible to utilize all of the heat sources described in Chapter 4.1 to increase preheat of the recycled flue gas. However the pinch at the hot end of the preheater seen in Figure 44 limits the

amount that can be integrated. From the composite curves in it can be seen that the temperature of recycled flue gas and oxygen exiting the preheater is too high for any of the heat sources considered in Chapter 4.1 to be utilized for providing further preheat after the preheater. Replacing the preheater with other heat sources does not make sense since the feedwater enters the steam generator at 290°C and consequently the flue gas would have to exit from the steam generator at a temperature above 290°C. The only remaining option is then to preheat the recycled flue gas and oxygen before it is entering the preheater in the steam generator. Heat of the flue gas can be utilized by lowering the steam generator exit temperature and thereby increasing the heat duty in the preheater or compression heat can be utilized by introducing a new heat exchanger in which the recycled flue gas and oxygen enters before entering the preheater in the steam generator. In this heat exchanger the recycled flue gas will be heated by compression heat.

6.3   Simulation Model

The simulation model used to evaluate the base case performance is sensitive to variations in operating conditions, and to evaluate the effects of increased preheat it is therefore necessary to develop a new and more simple simulation model. A flow diagram of the new simulation model is shown in Figure 46. The simulation model only models the combustion, heat rejection to the steam generation and reheat, preheat and the flue gas treatment. The simulation specifications are the same as for the other simulations. In order to estimate the work in the ASU and CPU the specific work per kg of O_2 produced and the specific work in the CPU per kg CO_2 entering the CPU from the base case simulation is used. These are determined to be 0,242kWh/kgO_2 and 0,117kWh/kgCO_2 respectively. Heat transfer to the steam cycle is modeled through a cooler which removes the same amount of heat from the combustion product which is transferred to the steam cycle and tail gas heater in the base case. The excess oxygen is kept constant at 10,45% for all simulations. In order to obtain good comparisons between the integration scenarios, the mass flow of the coal feed is varied in order to obtain the same outlet temperature from the steam generation and reheat for all simulations. The outlet from the steam generation and reheat block is therefore fixed to 399,9°C for all integration cases.

In order to validate the model, the results of this simulation model with base case operation are compared with those of the base case simulation model. In Table 17 the two models are compared. The equilibrium calculations of the combustion are very sensitive to changes in the composition of the streams, so obtaining completely similar results is difficult, but the two

simulation models give very similar results. It will therefore be assumed that the simulation model gives credible results.
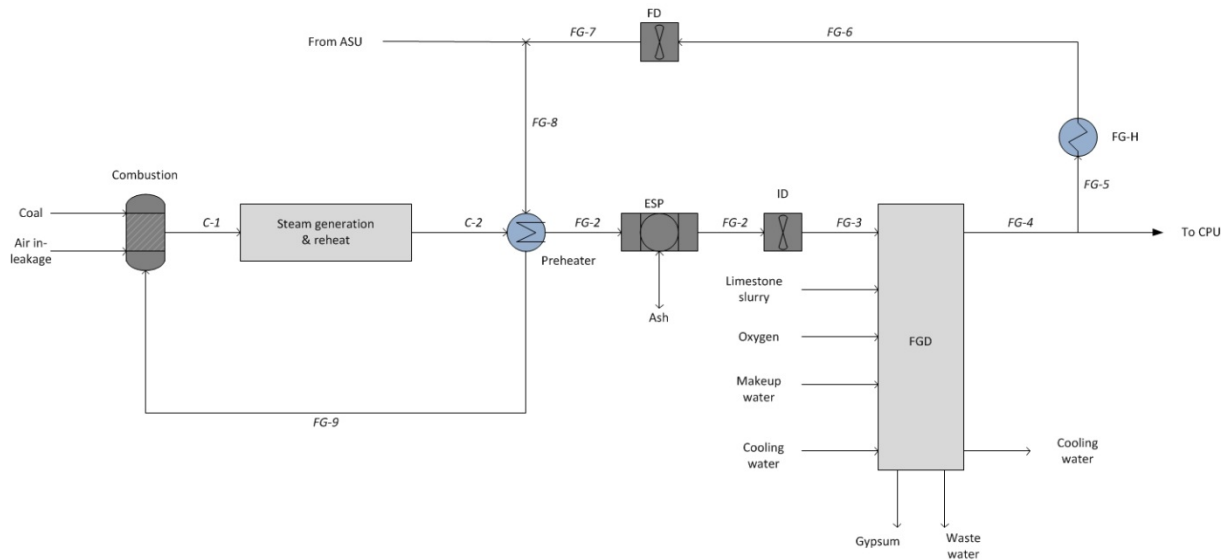
Figure 46 – New Simulation Model for Preheat Calculations

Table 17 – Comparison of Original and New Simulation for Base Case

	Original simulation	New simulation	Difference
Gross work steam cycle, kW	799760	799760	0
O2 consumption, kg/s	142,2	142,7	0
Work ASU, kW	124014	124285	-270
CO2 to CPU, kg/s	164,1	164,1	0
Work CPU, kW	69372	71466	268
Auxilliary work, kW	25592	25592	0
Fan work, kW	12198	12517	-319
Condensate pump, kW	1099	1099	0
Net work, kW	567485	564802	321
Fuel Consumption, kg/s	69,23	69,22	0
LHV efficiency	30,3 %	30,3 %	0

6.4   Decreasing Steam Generator Exit Temperature

The exit temperature of the flue gas from the steam generator in the base case is 176,7°C. By decreasing this temperature more heat will be transferred to the recycled flue gas and oxygen, and less fuel will be needed. In order to evaluate the effects of this a sensitivity analysis is performed. In the sensitivity analysis the ΔT_{min} is varied from 70 to 40°C. The results are available in Table 18.

Table 18 – Reducing ΔT_{min} by Decreasing Flue Gas Outlet Temperature

ΔT_{min} of preheater, °C	70	60	50	40
Flue gas outlet temperature, °C	177,6	168,4	159,2	149,8
Gross work steam cycle, kW	799760	799760	799760	799760
O_2 consumption, kg/s	142,7	142,1	141,5	140,9
Work ASU, kW	124329	123801	123273	122752
CO_2 to CPU, kg/s	164,1	163,5	162,8	162,1
Work CPU, kW	69131	68855	68569	68287
Auxilliary work, kW	25592	25592	25592	25592
Fan work, kW	12539	12321	12101	11883
Net work, kW	568169	569191	570225	571246
Fuel Consumption, kg/s	69,25	68,97	68,68	68,40
LHV efficiency	30,3 %	30,5 %	30,7 %	30,9 %

From the results it can be seen that reducing the ΔT_{min} of the preheater from 70 to 40 can improve the higher heating value efficiency of the power plant by 0,6%. The correlation between ΔT_{min} and thermal efficiency is close to linear; it is therefore likely that further decreases will give a similar improvement in efficiency. The improvement in efficiency originates from a decrease in fuel consumption, oxygen requirement, mass flow of flue gas into the CPU and fan work. A decrease in ΔT_{min} of the preheater will increase the heat exchange area. If the outlet temperature is below the acidic dew point of the flue gas it may also be necessary to introduce corrosion resistant coatings in parts of the preheater. The increased investment costs of the preheater should be lower than the savings of the increased efficiency for the decreased ΔT_{min} to be

profitable. In order to make a decision on the ΔT_{min} a thermo-economic analysis should be performed to find the optimal ΔT_{min}.

6.5   Increase Preheat with Compression Heat

In this chapter it will be studied how using compression heat to preheat the recycled flue and oxygen gas before it enters the preheater will affect the performance of the power plant. The layout of the steam generator will then be as shown in Figure 47. The only modification to the process is that a new heater is introduced to preheat the recycled flue gas and oxygen prior to entering the preheater in the steam generator. The outlet temperature of the flue gas, FG-2, remains as in the base case, but the temperature of the recycled flue gas and oxygen entering the preheater will be increased. In the base case the temperature of the recycled flue gas and oxygen prior to entering the preheater is 56,7°C. In order to evaluate the effect of increasing this temperature, a sensitivity analysis where the temperature of stream FG-9 is varied from 60 to 100°C is performed. The results are available in Table 19.
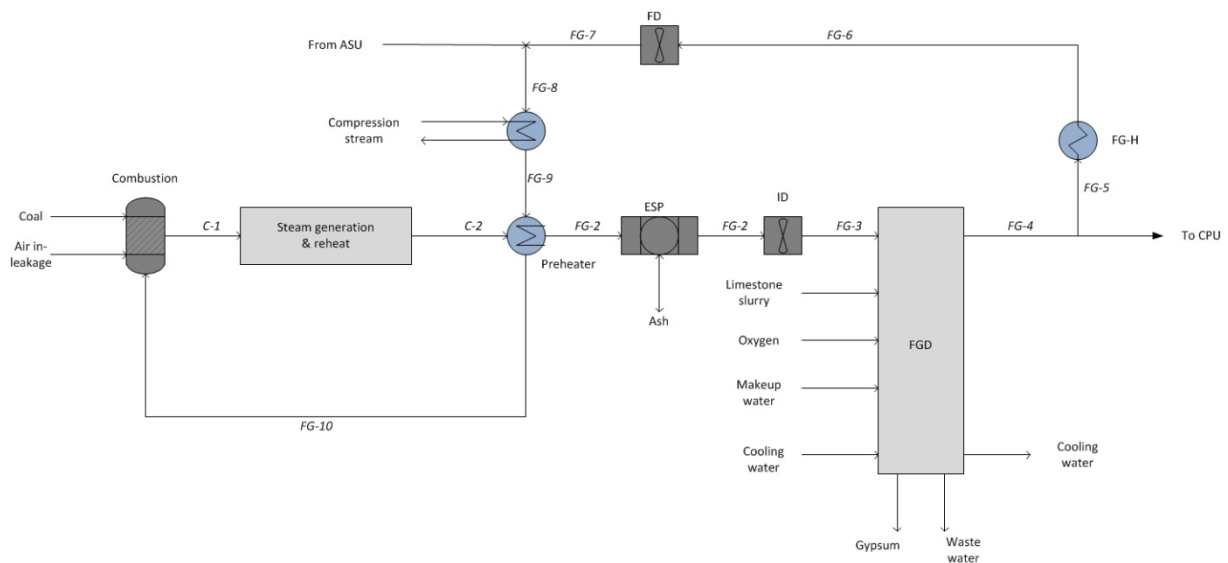
Figure 47 – Increasing Preheat by Utilizing Compression Heat

Table 19 – Results of Increasing Preheat by Utilizing Compression Heat

Preheat to, °C	60	70	80	90	100
Heat duty, kW	2349	8683	15019	21356	27691
ΔT_{min} in preheater, °C	65,8	57,1	48,4	39,6	30,8
Gross work steam cycle, kW	799760	799760	799760	799760	799760
O2 consumption, kg/s	142,7	141,9	141,4	140,9	140,4
Work ASU, kW	124339	123645	123191	122728	122274

CO2 to CPU, kg/s	163,8	163,3	162,7	162,1	161,5
Work CPU, kW	69013	68769	68526	68290	68036
Auxilliary work, kW	25592	25592	25592	25592	25592
Fan work, kW	12502	12462	12423	12384	12344
Net work, kW	568314	569292	570028	570766	571514
Fuel Consumption, kg/s	69,13	68,88	68,64	68,39	68,15
LHV efficiency	30,3 %	30,5 %	30,6 %	30,8 %	30,9 %

From the results of the sensitivity analysis it can be seen that the results of the simulations are close to the results of increased utilization of flue gas heat in Chapter 6.4. By adding 27691kW and thus heating the recycled flue gas and oxygen from 56,6°C to 100°C, the thermal efficiency can be increased by 0,6%. This will however decrease the ΔT_{min} of the steam generator and decrease the overall temperature differences in the preheater. The consequence of this is an increased heat exchanger area requirement for the preheater. Compared with Chapter 6.4 this integration gives a lower ΔT_{min} in the preheater for the same improvements in efficiency. In addition there will be investment costs related to the new heat exchanger which utilizes compression heat. It will not be necessary to use adiabatic compression in order to introduce this integration as the temperature as the stage outlet temperatures of R-P1 and A-P1 with intercooled compression are sufficient to supply the heat. For getting the best available heat transfer coefficients it would be advantageous to utilize streams at high pressures, notably the stream into the second intercooler and/or the aftercooler of R-P1. As for the integration in Chapter 6.4, a thermo-economic analysis should be performed before deciding the operational point of this integration, but it seems likely that the proposal in Chapter 6.4 will give lower investment costs for a similar improvement in efficiency.

7   CO$_2$ Rankine Cycle

At the Department of Energy and Process Engineering at NTNU, PhD student Amlaku Abie Lakew has been working on a super-critical Rankine Cycle with CO$_2$ as the working medium. In Lakew et al. (2011) a thermodynamic analysis comparing a CO$_2$ Rankine Cycle with a mechanical pump with a CO$_2$ Rankine Cycle with a thermally driven pump is performed. For this report the case of a mechanical pump will be considered.

7.1   Process Description

The process and the description in this chapter is taken from Lakew et al. (2011). The layout of the CO$_2$ Rankine Cycle can be seen in Figure 47.
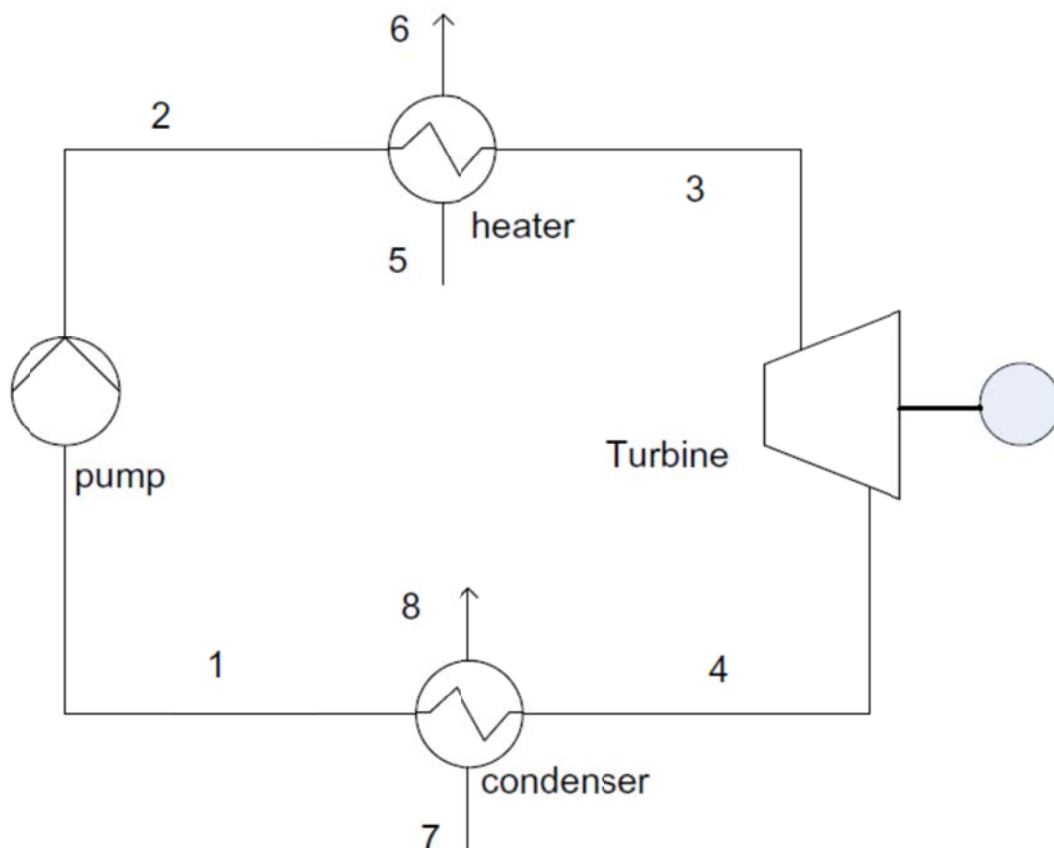
Figure 48 – Flowsheet of CO$_2$ Rankine Cycle (Lakew et al., 2011)

CO$_2$ is raised to a higher pressure by a mechanical pump from 1 to 2. It is thereby heated by a heat source in a heater from 2 to 3 before it expands in a turbine from 3 to 4. The CO$_2$ is then condensed by cooling water in a condenser from 4 to 1. As can be seen the layout of this process is almost identical to the ideal Rankine cycle described in Chapter 2.2.2, and the same equations as presented in Chapter 2.2.6 can be used to evaluate the performance.

7.2   Discussion of Integration

The purpose of integrating a CO_2 Rankine Cycle with the power plant is to convert waste heat into work. Integrating the CO_2 Rankine Cycle with adiabatic compression heat is not considered as preliminary calculations showed that the work increase of adiabatic compression was very close to the power output of the CO_2 Rankine Cycle. Integrating with heat from the intercooler was not attempted either as replacing the water intercoolers with a CO_2 Rankine Cycle seems unrealistic. The only remaining heat source for integration is then the flue gas heat. The flue gas will be utilized after the ID fans (stream FG-3 in Figure 18).

In order to investigate the potential of integrating the CO_2 the stream information on the flue gas stream was sent to Amlaku Abie Lakew for him to use his simulation model to estimate the potential for integration. The flue gas is set to be cooled from 187°C to 85°C, giving a heat duty of 79MW in Aspen Plus simulations. Unfortunately, due to an error in the simulations, the simulation model gave a heat output more than 5 times higher than that of Aspen Plus under similar conditions. However it is believed that the work output will be in the region of 8,8 to 9,6MW (Lakew, 2011). This will increase thermal efficiency of the power plant by 0,47-0,51%.

The costs related to the integration of a CO_2 Rankine Cycle are mainly related to the investment costs of the two heat exchangers and the pump and the turbine. The cycle operates at high pressures, so the equipment will have to be designed to withstand high pressure.

8 Discussion of Integration Results

8.1 Potential Efficiency Improvements

Of the integration projects studied in this report, the integration projects concerning integration with the feedwater preheat gives the highest efficiency improvements. By integrating the heat obtained from intercooling the compression streams of the base case without any modifications on the pressure ratios compression processes, an improvement of 1,19% in the thermal efficiency can be obtained. By adding flue gas heat, the amount of heat and temperature level of heat addition is increased and steam extractions can be further reduced. This gives a 1,72% increase in the thermal efficiency. Both of these integrations utilize one steam extraction to the low pressure condensate system, and all extractions downstream of IPT 2 are eliminated. If adiabatic compression is introduced in the three compressors A-P1, R-P1 and R-P3, the temperature level of the compression heat is increased. The higher temperature levels of the adiabatic compression heat allow for some integration with the high pressure feedwater downstream of the deaerator. The effects of this integration is a 1,49% increase in thermal efficiency without flue gas heat integration, and a 1,96% increase in thermal efficiency if the flue gas heat is integrated. If the cases of intercooled and adiabatic compression are compared, it can be seen that adiabatic compression increases the thermal efficiency by 0,30% if the flue gas heat is not utilized and by 0,24% if the flue gas heat is utilized. It should be noted that the case of adiabatic compression with flue gas heat utilizes much more of the flue gas heat than the case of intercooled compression with flue gas heat. However, the results presented in this report shows that using adiabatic compression is the best option from an energetic point of view as the increase in compression work is clearly offset by the increased power output from the steam cycle.

The other two integrations considered are increasing the preheat of recycled flue gas and oxygen and utilization of flue gas heat in a CO_2 rankine cycle. Both of these give similar results, but it is likely that increasing the preheat of the recycled flue gas and oxygen will be the most cost efficient option as it only involves adding more heat exchanger area in the preheater if the flue gas is further cooled or adding one more heat exchanger and more heat exchange area in the preheater if compression heat is used for the first part of the preheat. Of these two options decreasing the flue gas exit temperature seems to be the best. The increase in efficiency by introducing further cooling of the flue gas depends on the flue gas exit temperature. Since the addition of more heat will increase investment costs of heat exchanger, a final decision should not be made before an economic analysis is performed. However it is unlikely that the improvement in thermal efficiency will exceed 0,6-0,7%.

8.2 Possible Interactions Between Integration Cases

It is possible to combine several of the integration options considered in this report. For the cases of integration of intercooling heat or adiabatic compression heat with the feedwater without integration of flue gas heat, it will be possible to use the flue gas heat with a CO_2 rankine cycle or use it to further preheat the recycled flue gas and oxygen. Furthermore for the case of fully intercooled compression and flue gas heat integration with the feedwater preheat, the temperature of the flue gas after heat rejection to the feedwater is still 150°C, something which will enable use of a CO_2 rankine cycle or more preheat. If more preheat is added to the recycled flue gas and oxygen, the flow rates in the ASU and CPU compressors will be slightly reduced, something which will reduce the amount of compression heat available for integration with the feedwater. However the change in flow rate is small, so the effect is not likely to be significant. If compression heat is used to preheat recycled flue gas and oxygen, less heat will be available for integration with the feedwater preheat, but the flue gas will have the same temperature as in the base case, and can still be used with either a CO_2 rankine cycle or with the feedwater preheat.

As the paragraph above illustrates, there are many possible interactions between the integration cases studied in this report. However, many of them affect each other, and quantifying the gain of combining them will need more studies. However it does not seem likely that the increase in efficiency will be much higher than the 1,98 % which is obtained by using adiabatic compression heat and flue gas heat with the feedwater preheat. Higher efficiency improvements may be obtained if the CPU, ASU, steam cycle and steam generator are adapted for heat integration, but this will require re-design of the power plant.

8.3 Costs of Integration

As for all process improvements, the costs will be a deciding factor when choosing whether to use integration in this power plant. Some comments on the costs have already been made in the presentation of each integration case, but for this discussion the most important aspects will be repeated.

For the cases with integration of compression heat with the feedwater preheat it will be necessary to introduce more heat exchangers in the feedwater system. The total area of these heat exchangers will also be higher than if steam is used, as the compressed gases will give much lower film heat transfer coefficients than the condensing steam. However much of the area requirement of the compressor intercoolers will be removed. If adiabatic compression is used the complexity of the compression will be reduced, but the size of the compressor may increase. If the flue gas is

used, it may be necessary to introduce corrosion resistant coating if it is cooled below the acidic dew point. This will increase investment costs. In order to estimate the costs, a heat exchanger network design should be made for each integration case. A good design will have to incorporate the overall heat transfer coefficients of the stream matches, investment costs of the heat exchangers and the potential income of the energy savings in order to find an optimal solution. It is possible that the most cost efficient designs do not meet the energy saving targets set in this report.

The case of increasing preheating of recycled flue gas and oxygen will increase investments in heat exchangers. The area requirement of the preheater in the steam generator will increase both if further cooling of the flue gas or compression heat is used to add further preheating to the flue gas. If corrosion resistant materials have to be used to cool the flue gas, this is likely to increase costs. The flow rates on the gas side of the steam generator, in the CPU and in the ASU will be slightly reduced due to the lower fuel consumption. It is however, not certain if this decrease in flow rate is big enough to have a significant effect on the size of the equipment and investment costs. In order to determine the amount of preheat to be used a thermo-economic analysis should be made to find the most cost efficient solution.

As for the CO_2 Rankine cycle, the investment costs will only be related to the components of the rankine cycle itself. The investment costs over the lifetime of the Rankine cycle should be lower than the income of the additional power output it provides for the integration to be implemented.

8.4   Operational and Safety Concerns

The integration will increase the complexity of the system, and there are some possible obstacles. The cost is likely to be the decisive factor when deciding to use integration or not, but safety and operational issues may also pose problems. When integrating compression heat with the feedwater, there is a danger that there will be in-leakage of gases into the feedwater. Especially gases like CO_2 and SO_x may cause serious problems if they leak into the feedwater. These compounds may lower the pH of the water and cause corrosion and damage to equipment within the steam cycle. It is therefore vital that all heat exchangers are sealed to such an extent that this is avoided.

The complexity of having heat rejection to other process applications from compressor intercoolers may also pose problems as it will be more complicated to regulate the operation of

the compressors than it would with cooling water. This problem can be solved by using adiabatic compression.

8.5 Ranked List of Integration Projects

The aim of this work has been to evaluate the potential for process integration of low temperature heat within a coal fired oxy-combustion power plant. Special attention has been given to compression heat and the potential for using adiabatic compression. The simulations performed in this study has shown that there is a significant potential for improvement in efficiency if the compression heat is used with the feedwater preheat, and that the potential is even higher if adiabatic compression is used. Increasing preheat of recycled flue gas and oxygen and integration of a CO_2 Rankine cycle with the flue gas, has also been shown to give improvements in the thermal efficiency. Costs and operational issues have been briefly discussed in the previous chapters, but further studies are needed to quantify the costs related to the integrations proposed in this report. On the basis of what has been discussed in this report, the integration cases are ordered from the most promising to the least promising. The list is as follows:

1. Integration of adiabatic compression heat and flue gas heat with the low pressure condensate and high pressure feedwater.
2. Integration of adiabatic compression heat with low pressure condensate and high pressure feedwater combined with increased preheat of recycled flue gas and oxygen. The increase in preheating should be supplied by the flue gas itself.
3. Use heat from intercooling and flue gas heat for integration with low pressure condensate.
4. Use heat from intercooling for integration with low pressure condensate combined with increased preheat of recycled flue gas and oxygen. The increase in preheating should be supplied by the flue gas itself.
5. Point 2 and 4 without more preheating of recycled flue gas and oxygen.
6. Increased preheat of recycled flue gas and oxygen by lowering steam generator exit temperature
7. Increased preheat of recycled flue gas by use of compression heat
8. Using heat in flue gas with a CO_2 Rankine cycle

Adiabatic compression has been prioritized as it gives fewer streams for integration, heat available at higher temperatures and less complicated compression. If the flue gas is not used

with the feedwater preheat, it should if practical and profitable, be used to increase the preheat of the recycled flue gas and oxygen. Increased preheat of recycled flue gas and oxygen should preferably be done by lowering the steam generator exit temperature, and not by using compression heat. The CO_2 rankine cycle is ranked last as it is likely that the costs will be higher than that of increasing preheat of recycled flue gas and oxygen.

9 Conclusion & Suggestions for Further Work

In this report it has been shown that integration of compression heat from the ASU and CPU can significantly improve the efficiency of the studied oxy-combustion power plant if the heat is integrated with the feedwater preheat of the steam cycle in order to replace steam extractions from the turbines. Furthermore it has been shown that due to higher temperature level of the heat, adiabatic compression will give higher efficiency improvements than integrating heat from intercooled compressors. The reason behind this is that higher temperature levels allow for replacing steam extractions from the turbines at higher pressure levels, and the work increase from replacing steam extractions is higher than the increase of work in the compressors. If the flue gas exiting the steam generator is integrated along with the compression heat, further efficiency improvements can be obtained. Increasing preheat of the recycled flue gas and oxygen entering the combustion has been shown to improve efficiency, but to a smaller extent than integration with the feedwater preheating. In addition the flue gas heat can be cooled by rejecting heat to an external CO_2 rankine cyle to improve the thermal efficiency of the power plant.

The integrated designs considered in this report will increase the complexity of the system, and may increase capital costs. Further studies should therefore be made in order to properly estimate the cost and operability issues which arise with the integration projects suggested in this report. In Chapter 8.5 a ranked list of process integration projects has been suggested. This list can be used as a basis deciding which integration projects to pick for further studies.

The extent of the efficiency improvements obtained in this report has shown that possibilities for process integration should be considered when designing an oxy-combustion power plant. In this report the study has been performed on the oxy-combustion power plant modeled in Chapter 3, and the various parts of the power plant are not designed specifically for heat integration. It is likely that even higher improvements in the thermal efficiency of oxy-combustion power plants can be obtained if the steam cycle, ASU and CPU are designed and adapted for heat integration. Future developments of ASUs, CPUs and steam cycles for oxy combustion should therefore also focus on the opportunities for heat integration.

Based on the remarks above two suggestions for further work can be given:
- Develop new concepts for the ASU, CPU and steam cycle where opportunities for heat integration of compression heat are considered.

- Make further studies of the integration projects proposed in this report. These studies may include heat exchanger network designs, cost calculations and optimization. The focus should be placed on the projects with integration of adiabatic compression heat.

References

BAEHR, H. D. & KABELAC, S. 1996. *Thermodynamik: Grundlagen und technische Anwendungen,* Berlin, Heidelberg, Springer.

BOLLAND, O. 2010. Power Generation: CO_2 Capture and Storage. Norwegian University of Science and Technology.

CHAO, F. & GUNDERSEN, T. 2011. Exergy analysis of an oxy-combustion process for coal-fired power plants with CO2 capture. Trondheim: NTNU.

DOE/NETL 2008. Pulverized Coal Oxycombustion Power Plants. 2007/1291.

ESPATOLERO, S., CORTÉS, C. & ROMEO, L. M. 2010. Optimization of boiler cold-end and integration with the steam cycle in supercritical units. *Applied Energy,* 87**,** 1651-1660.

GRAY, M. A. 2011. CO_2 compression. *In:* SCHERER, V. & STOLTEN, D. (eds.) *Efficient Carbon Capture for Coal Power Plants.* Weinheim: Wiley-VCH Verlag.

IEAGHG. 2007. *Capturing CO_2* [Online]. http://www.ieaghg.org/docs/general_publications/cocapture.pdf.

KANNICHE, M., GROS-BONNIVARD, R., JAUD, P., VALLE-MARCOS, J., AMANN, J.-M. & BOUALLOU, C. 2010. Pre-combustion, post-combustion and oxy-combustion in thermal power plant for CO2 capture. *Applied Thermal Engineering,* 30**,** 53-62.

KATHER, A. & KLOSTERMANN, M. 2011. CO_2 Capture via the Oxyfuel Process with Cryogenic Air Separation. *In:* SCHERER, V. & STOLTEN, D. (eds.) *Efficient Carbon Capture for Coal Power Plants.* Weinheim: Wiley-VCH Verlag.

KBR. 2010. *Pinch Studies: Heat and Mass Integration* [Online]. http://www.kbr.com/Services/Advanced-Chemical-Engineering-Services/Advanced-Simulation/Pinch-studies/. [Accessed 23.01 2012].

KEMP, I. C. 2007. *Pinch analysis and process integration: a user guide on process integration for the efficient useof energy,* Amsterdam, Butterworth-Heinemann.

LAKEW, A. A. 2011. *RE: RE: Compression stream data.* Type to ZEINER, T. H.

LAKEW, A. A., BOLLAND, O. & LADAM, Y. 2011. Theoretical thermodynamic analysis of Rankine power cycle with thermal driven pump. *Applied Energy,* 88**,** 3005-3011.

LÉANDRI, J.-F., PAELINCK, P., SKEA, A. & BOHTZ, C. 2011. Cost assessment of foosil power plants equipped with CCS under typical scenarios. Alstom Power.

MORAN, M. J. & SHAPIRO, H. N. 2006. *Fundamentals of engineering thermodynamics,* Hoboken, N.J., Wiley.

PDC. 2012. *Energy pinch technology* [Online]. http://www.keuken.com/3.2.1-enpinch-techn.htm. [Accessed 22.01 2012].

PIPITONE, G. & BOLLAND, O. 2009. Power generation with CO2 capture: Technology for CO2 purification. *International Journal of Greenhouse Gas Control,* 3**,** 528-534.

SAHU, G. C. & BANDYOPADHYAY, S. 2010. Energy conservation in water allocation networks with negligible contaminant effects. *Chemical Engineering Science,* 65**,** 4182-4193.

SARAVANAMUTTOO, H. I. H., COHEN, H., ROGERS, G. F. C. & STRAZNICKY, P. V. 2009. *Gas turbine theory,* Harlow, Prentice Hall.

SPLIETHOFF, H. 2010. *Power Generation from Solid Fuels,* Berlin, Heidelberg, Springer-Verlag Berlin Heidelberg.

SPLIETHOFF, H. 2011. Advanced Power Plant Technology. *In:* SCHERER, V. & STOLTEN, D. (eds.) *Efficient Carbon Capture for Coal Power Plants.* Weinheim: Viley-VCH Verlag.

STANGER, R. & WALL, T. 2011. Sulphur impacts during pulverised coal combustion in oxy-fuel technology for carbon capture and storage. *Progress in Energy and Combustion Science,* 37**,** 69-88.

STINE, W. B. & GEYER, M. 2001. *Power from the Sun* [Online]. http://www.powerfromthesun.net/book.html. [Accessed 20.01 2012].

TRANIER, J.-P. & PERRIN, N. Impurities management in an Oxy-Combustion Power Plant. 2nd International Oxyfuel Combustion Conference, 2011 Yeppoon, Queensland, Australia.

ZHANG, N. & LIOR, N. 2006. Proposal and Analysis of a Novel Zero CO_2 Emission Cycle With Liquid Natural Gas Cryogenic Exergy Utilization. *Journal of Engineering for Gas Turbines and Power,* 128**,** 81-91.

Appendix

In the following tables stream information with reference to stream names in Figure 18, 19, 20, 27, 32, 39, 42 is given.

Stream Information from Figure 18									
		FG-1	**FG-2**	**FG-3**	**FG-4**	**FG-5**	**FG-6**	**FG-7**	**FG-8**
Mass flow	kg/sec	751,255	744,540	744,540	724,491	521,633	521,633	521,633	669,433
Temperature	C	176,667	176,667	187,018	57,222	57,222	65,572	73,083	56,311
Pressure	Bar	1,000	1,000	1,100	1,030	1,030	1,010	1,100	1,100
Component mass flows									
O2	kg/sec	18,523	18,523	18,523	20,230	14,566	14,566	14,566	154,187
N2	kg/sec	45,091	45,091	45,091	45,134	32,497	32,497	32,497	34,847
AR	kg/sec	21,641	21,641	21,641	21,748	15,658	15,658	15,658	21,481
H2O	kg/sec	71,815	71,815	71,815	51,286	36,926	36,926	36,926	36,927
CO2	kg/sec	583,653	583,653	583,653	586,021	421,935	421,935	421,935	421,940
SO2	kg/sec	3,521	3,521	3,521	0,071	0,051	0,051	0,051	0,051
NO2	kg/sec	0,001	0,001	0,001	0,000	0,000	0,000	0,000	0,000
H2	kg/sec	0,087	0,087	0,087	0,000	0,000	0,000	0,000	0,000
HCL	kg/sec	0,206	0,206	0,206	0,000	0,000	0,000	0,000	0,000
SO3	kg/sec	0,002	0,002	0,002	0,000	0,000	0,000	0,000	0,000
ASH	kg/sec	6,715	0,000	0,000	0,000	0,000	0,000	0,000	0,000
		A0	**A1-1**	**A1-2**	**A1-3**	**A2-1**	**A2-2**	**A2-3**	**A3-1**
Mass flow	kg/sec	627,288	618,248	618,248	618,248	335,959	335,959	335,959	169,461
Temperature	C	25,000	35,000	9,835	-173,678	-173,746	-179,351	-188,975	-177,960
Pressure	Bar	1,013	5,600	5,500	5,450	5,450	5,400	1,450	5,400
Component mass flows									
O2	kg/sec	143,474	143,474	143,474	143,474	141,976	141,976	14,566	1,172
N2	kg/sec	466,815	466,815	466,815	466,815	187,304	187,304	32,497	167,341
AR	kg/sec	7,959	7,959	7,959	7,959	6,679	6,679	15,658	0,947
H2O	kg/sec	8,715	7,909	0,000	0,000	0,000	0,000	0,000	0,000
CO2	kg/sec	0,324	0,324	0,000	0,000	0,000	0,000	0,000	0,000
		A3-2	**A3-3**	**A4-1**	**A4-2**	**A4-3**	**A4-4**	**A5-1**	**A5-2**
Mass flow	kg/sec	169,461	169,461	112,828	112,828	112,828	112,828	150,512	150,512
Temperature	C	-181,458	-192,740	-177,960	-6,209	-90,210	-6,209	-179,490	-6,209
Pressure	Bar	5,350	1,400	5,400	5,350	1,200	1,170	1,500	1,470
Component mass flows									
O2	kg/sec	1,172	1,172	0,326	0,326	0,326	0,326	142,189	142,189
N2	kg/sec	167,341	167,341	112,169	112,169	112,169	112,169	2,394	2,394
AR	kg/sec	0,947	0,947	0,332	0,332	0,332	0,332	5,929	5,929
H2O	kg/sec	0,000	0,000	0,000	0,000	0,000	0,000	0,000	0,000
CO2	kg/sec	0,000	0,000	0,000	0,000	0,000	0,000	0,000	0,000
		A6-1	**A6-2**	**A6-3**	**A7-1**	**A7-2**	**O1-1**	**O2-1**	**O2-2**
Mass flow	kg/sec	354,908	354,908	354,908	467,736	618,248	147,793	2,719	2,719
Temperature	C	-192,709	-178,383	-6,209	-6,209	25,000	-6,209	-6,209	71,268
Pressure	Bar	1,400	1,380	1,350	1,170	1,013	1,470	1,470	3,103

Component mass flows								
O2	kg/sec	0,959	0,959	0,959	1,285	1,285	139,620	2,569	2,569
N2	kg/sec	352,252	352,252	352,252	464,421	464,421	2,350	0,043	0,043
AR	kg/sec	1,697	1,697	1,697	2,029	2,029	5,822	0,107	0,107
H2O	kg/sec	0,000	0,000	0,000	0,000	0,000	0,000	0,000	0,000
CO2	kg/sec	0,000	0,000	0,000	0,000	0,000	0,000	0,000	0,000
		R1-1	R1-2	R1-3	R1-4	R1-5	R2-1	R2-2	R2-3
Mass flow	kg/sec	202,857	192,515	192,515	188,496	188,496	123,746	123,746	123,746
Temperature	C	57,222	35,000	35,000	35,103	-26,000	-26,000	-33,844	21,817
Pressure	Bar	1,030	1,010	32,000	31,700	31,400	31,400	18,000	17,700

Component mass flows								
O2	kg/sec	5,664	5,664	5,664	5,662	5,662	0,691	0,691	0,691
N2	kg/sec	12,638	12,638	12,638	12,638	12,638	1,266	1,266	1,266
AR	kg/sec	6,089	6,089	6,089	6,089	6,089	1,029	1,029	1,029
H2O	kg/sec	14,360	4,019	4,019	0,000	0,000	0,000	0,000	0,000
CO2	kg/sec	164,086	164,086	164,086	164,087	164,087	120,741	120,741	120,741
SO2	kg/sec	0,020	0,020	0,020	0,020	0,020	0,019	0,019	0,019
		R3-1	R3-2	R4-1	R4-2	R4-3	R4-4	R4-5	R4-6
Mass flow	kg/sec	64,750	64,750	35,808	35,808	35,808	35,808	35,808	35,808
Temperature	C	-26,000	-54,000	-54,000	-43,150	-55,766	-44,209	21,817	88,751
Pressure	Bar	31,400	31,100	31,100	30,800	9,000	8,700	8,400	18,000

Component mass flows								
O2	kg/sec	4,972	4,972	0,329	0,329	0,329	0,329	0,329	0,329
N2	kg/sec	11,372	11,372	0,577	0,577	0,577	0,577	0,577	0,577
AR	kg/sec	5,060	5,060	0,531	0,531	0,531	0,531	0,531	0,531
H2O	kg/sec	0,000	0,000	0,000	0,000	0,000	0,000	0,000	0,000
CO2	kg/sec	43,346	43,346	34,371	34,371	34,371	34,371	34,371	34,371
SO2	kg/sec	0,001	0,001	0,001	0,001	0,001	0,001	0,001	0,001
		R4-7	R5-1	R5-2	R5-3	R5-4	R5-5	R6-1	R6-2
Mass flow	kg/sec	35,808	28,942	28,942	28,942	28,942	28,942	159,554	159,554
Temperature	C	35,000	-54,000	-44,209	21,817	351,000	20,829	24,766	35,000
Pressure	Bar	17,700	31,100	30,800	30,500	30,200	1,050	17,700	78,000

Component mass flows								
O2	kg/sec	0,329	4,643	4,643	4,643	4,643	4,643	1,019	1,019
N2	kg/sec	0,577	10,795	10,795	10,795	10,795	10,795	1,843	1,843
AR	kg/sec	0,531	4,529	4,529	4,529	4,529	4,529	1,560	1,560
H2O	kg/sec	0,000	0,000	0,000	0,000	0,000	0,000	0,000	0,000
CO2	kg/sec	34,371	8,975	8,975	8,975	8,975	8,975	155,112	155,112
SO2	kg/sec	0,001	0,000	0,000	0,000	0,000	0,000	0,020	0,020
		R6-3	R6-4	Air in-leakage					
Mass flow	kg/sec	159,554	159,554	12,603					
Temperature	C	25,000	44,626	25,000					
Pressure	Bar	78,000	150,000	1,013					

Component mass flows				
O2	kg/sec	1,019	1,019	2,883
N2	kg/sec	1,843	1,843	9,379

AR	kg/sec	1,560	1,560	0,160	
H2O	kg/sec	0,000	0,000	0,175	
CO2	kg/sec	155,112	155,112	0,007	
SO2	kg/sec	0,020	0,020	0,000	

		Coal	Limestone slurry	Gypsum	Waste water
Mass flow	kg/sec	69,230	17,967	10,302	59,600
Temperature	C	25,000	25,000	57,200	57,200
Pressure	Bar	1,000	1,013	1,050	1,030

Stream Information from Figure 19								
		S-1	S-2	S-3	S-4	S-5	S-6	S-7	S-8
Mass flow	kg/sec	612,541	611,977	564,407	502,848	502,848	477,963	423,481	390,200
Temperature	C	598,889	563,864	409,652	346,901	621,111	500,238	384,535	305,459
Pressure	Bar	242,330	199,948	76,877	49,008	45,216	21,381	9,494	5,012
		S-9	S-10	S-11	S-12	F-1	F-2	F-3	F-4
Mass flow	kg/sec	373,723	358,081	342,600	342,600	467,850	467,850	467,850	467,850
Temperature	C	167,814	97,516	64,192	38,726	38,389	38,541	39,056	60,850
Pressure	Bar	1,324	0,579	0,241	0,069	0,069	17,237	16,892	16,547
		F-5	F-6	F-7	F-8	F-9	F-10	F-11	F-12
Mass flow	kg/sec	564,860	467,850	467,850	612,541	612,541	612,541	612,541	612,541
Temperature	C	81,428	103,494	147,257	176,378	181,965	214,791	259,735	290,118
Pressure	Bar	15,858	15,513	15,168	9,211	289,580	289,235	288,890	288,546
		E-1	E-2	E-3	E-4	E-5	E-6	E-7	E-8
Mass flow	kg/sec	47,570	47,570	60,995	108,565	24,885	133,450	15,343	33,281
Temperature	C	409,652	290,395	346,901	260,843	500,238	214,262	384,535	305,459
Pressure	Bar	76,877	74,808	49,008	47,539	21,381	20,739	9,494	5,012
		E-9	E-10	E-11	E-12	E-13	E-14	E-15	TD-1
Mass flow	kg/sec	33,281	16,477	49,757	15,642	66,324	15,481	81,805	36,304
Temperature	C	108,872	167,814	86,817	97,516	66,619	64,192	45,129	384,535
Pressure	Bar	1,379	1,324	0,621	0,579	0,269	0,241	0,097	9,494
		TD-2	SS-1	SS-2	SS-3	SS-4	SS-5	SS-6	SS-7
Mass flow	kg/sec	36,304	0,564	0,564	0,564	0,416	0,352	0,352	0,924
Temperature	C	52,249	563,864	346,901	384,535	389,700	389,700	100,009	389,700
Pressure	Bar	0,138	199,948	49,008	9,494	9,494	9,494	1,014	9,494
		FGH-1	FGH-2	TO ASU	TO CPU	From ASU & CPU		Makeup water	
Mass flow	kg/sec	97,010	97,010	2,230	0,041	2,271		6,373	
Temperature	C	81,428	71,111	384,535	384,535	176,378		25,000	
Pressure	Bar	15,858	15,858	9,494	9,494	9,211		1,014	

		C1-1	**C1-2**	**C1-3**	**C2-1**	**C2-2**	**C3-1**	**C3-2**	**C3-3**

| | | **Stream Information from Figure 20** | | | | | | | |

Stream Information from Figure 20

		C1-1	**C1-2**	**C1-3**	**C2-1**	**C2-2**	**C3-1**	**C3-2**	**C3-3**
Mass flow	kg/sec	751,254	751,254	751,254	301,073	301,073	450,181	450,181	450,181
Temperature	C	2013,297	1461,593	1116,729	1037,867	402,692	1037,867	554,120	402,687
Pressure	Bar	1,100	1,090	1,080	1,070	1,050	1,070	1,060	1,050
Component mass flows									
O2	kg/sec	18,516	18,516	18,516	7,420	7,420	11,095	11,095	11,095
N2	kg/sec	45,091	45,091	45,091	18,071	18,071	27,021	27,021	27,021
AR	kg/sec	21,640	21,640	21,640	8,673	8,673	12,968	12,968	12,968
H2O	kg/sec	71,816	71,816	71,816	28,781	28,781	43,035	43,035	43,035
CO2	kg/sec	583,658	583,658	583,658	233,907	233,907	349,751	349,751	349,751
SO2	kg/sec	3,521	3,521	3,521	1,411	1,411	2,110	2,110	2,110
NO2	kg/sec	0,001	0,001	0,001	0,000	0,000	0,000	0,000	0,000
H2	kg/sec	0,086	0,086	0,086	0,035	0,035	0,052	0,052	0,052
CL2	kg/sec	0,000	0,000	0,000	0,000	0,000	0,000	0,000	0,000
C	kg/sec	0,000	0,000	0,000	0,000	0,000	0,000	0,000	0,000
S	kg/sec	0,000	0,000	0,000	0,000	0,000	0,000	0,000	0,000
HCL	kg/sec	0,206	0,206	0,206	0,083	0,083	0,124	0,124	0,124
SO3	kg/sec	0,002	0,002	0,002	0,001	0,001	0,001	0,001	0,001
ASH	kg/sec	6,715	6,715	6,715	2,691	2,691	4,024	4,024	4,024

		C4-1	**C4-2**	**FG-9**					
Mass flow	kg/sec	751,254	751,254	669,425					
Temperature	C	402,689	392,293	321,800					
Pressure	Bar	1,050	1,050	1,100					
Component mass flows									
O2	kg/sec	18,516	18,516	154,182					
N2	kg/sec	45,091	45,091	34,847					
AR	kg/sec	21,640	21,640	21,480					
H2O	kg/sec	71,816	71,816	36,926					
CO2	kg/sec	583,658	583,658	421,939					
SO2	kg/sec	3,521	3,521	0,051					
NO2	kg/sec	0,001	0,001						
H2	kg/sec	0,086	0,086						
CL2	kg/sec	0,000	0,000						
C	kg/sec	0,000	0,000						
S	kg/sec	0,000	0,000						
HCL	kg/sec	0,206	0,206						
SO3	kg/sec	0,002	0,002						
ASH	kg/sec	6,715	6,715						

Stream information from Figure 27

		S-1	S-2	S-3	S-4	S-5	S-6	S-7	S-8
Mass flow	kg/sec	612,541	611,977	564,407	502,848	502,848	477,963	407,481	407,481
Temperature	C	598,889	563,864	409,652	346,901	621,111	500,238	384,535	305,459
Pressure	Bar	242,330	199,948	76,877	49,008	45,216	21,381	9,494	5,012

		S-9	S-10	S-11	S-12	F-1	F-2	F-3	F-4
Mass flow	kg/sec	407,481	407,481	407,481	407,481	467,850	467,850	467,850	467,850
Temperature	C	167,814	97,516	64,192	38,726	38,389	38,541	39,056	147,257
Pressure	Bar	1,324	0,579	0,241	0,069	0,069	17,237	16,892	15,168

		F-5	F-6	F-7	F-8	F-9	E-1	E-2	E-3
Mass flow	kg/sec	612,541	612,541	612,541	612,541	612,541	47,570	47,570	60,995
Temperature	C	176,378	181,965	214,791	259,735	290,118	409,652	290,395	346,901
Pressure	Bar	9,211	289,580	289,235	288,890	288,546	76,877	74,808	49,008

		E-4	E-5	E-6	E-7	E-8	E-9	TD-1	TD-2
Mass flow	kg/sec	108,565	24,885	133,450	15,343	16,000	16,000	36,304	36,304
Temperature	C	260,843	500,238	214,262	384,535	384,535	55,769	384,535	52,249
Pressure	Bar	47,539	21,381	20,739	9,494	9,494	9,494	9,494	0,138

		SS-1	SS-2	SS-3	SS-4	SS-5	SS-6	To ASU	To CPU
Mass flow	kg/sec	0,564	0,564	0,564	1,340	0,352	0,352	2,230	0,041
Temperature	C	563,864	346,901	384,535	389,700	389,700	100,009	384,535	384,535
Pressure	Bar	199,948	49,008	9,494	9,494	9,494	1,014	9,494	9,494

		From ASU & CPU		Makeup water					
Mass flow	kg/sec	2,271		6,373					
Temperature	C	176,378		25,000					
Pressure	Bar	9,211		1,014					

		CPU1-1	CPU1-2	CPU2-1	CPU2-2	CPU3-1	CPU3-2	CPU4-1	CPU4-2
Mass flow	kg/sec	192,515	192,515	192,515	192,515	192,515	192,515	158,449	158,449
Temperature	C	144,014	59,355	144,293	59,355	145,955	59,355	91,359	59,355
Pressure	Bar	3,196	3,196	10,113	10,113	32,000	32,000	37,156	37,156

Component mass flows

		CPU1-1	CPU1-2	CPU2-1	CPU2-2	CPU3-1	CPU3-2	CPU4-1	CPU4-2
O2	kg/sec	5,664	5,664	5,664	5,664	5,664	5,664	0,691	0,691
N2	kg/sec	12,638	12,638	12,638	12,638	12,638	12,638	1,266	1,266
AR	kg/sec	6,089	6,089	6,089	6,089	6,089	6,089	1,029	1,029
H2O	kg/sec	4,019	4,019	4,019	4,019	4,019	4,019	0,000	0,000
CO2	kg/sec	164,086	164,086	164,086	164,086	164,086	164,086	120,741	120,741
SO2	kg/sec	0,020	0,020	0,020	0,020	0,020	0,020	0,019	0,019

		CPU5-1	CPU5-2	ASU1-1	ASU1-2	ASU2-1	ASU2-2	FG-5	FG-6
Mass flow	kg/sec	158,449	192,515	627,288	627,288	627,288	627,288	521,633	521,633
Temperature	C	104,483	59,355	124,858	59,355	138,169	59,355	57,222	65,572
Pressure	Bar	78,000	37,156	2,382	2,382	5,600	5,600	1,030	1,010

Component mass flows

		CPU5-1	CPU5-2	ASU1-1	ASU1-2	ASU2-1	ASU2-2	FG-5	FG-6
O2	kg/sec	0,691	0,691	143,474	143,474	143,474	143,474	14,566	14,566
N2	kg/sec	1,266	1,266	466,815	466,815	466,815	466,815	32,497	32,497
AR	kg/sec	1,029	1,029	7,959	7,959	7,959	7,959	15,658	15,658
H2O	kg/sec	0,000	0,000	8,715	8,715	8,715	8,715	36,926	36,926
CO2	kg/sec	120,741	120,741	0,324	0,324	0,324	0,324	421,935	421,935
SO2	kg/sec	0,019	0,019	0,000	0,000	0,000	0,000	0,000	0,000

Stream information from Figure 32

		S-1	S-2	S-3	S-4	S-5	S-6	S-7	S-8
Mass flow	kg/sec	612,541	611,977	564,407	502,848	502,848	477,963	419,731	419,731
Temperature	C	598,889	563,864	409,652	346,901	621,111	500,238	384,535	305,459
Pressure	Bar	242,330	199,948	76,877	49,008	45,216	21,381	9,494	5,012
		S-9	S-10	S-11	S-12	F-1	F-2	F-3	F-4
Mass flow	kg/sec	419,731	419,731	419,731	419,731	467,850	467,850	467,850	467,850
Temperature	C	167,814	97,516	64,192	38,726	38,389	38,541	39,056	147,257
Pressure	Bar	1,324	0,579	0,241	0,069	0,069	17,237	16,892	15,168
		F-5	F-6	F-7	F-8	F-9	E-1	E-2	E-3
Mass flow	kg/sec	612,541	612,541	612,541	612,541	612,541	47,570	47,570	60,995
Temperature	C	176,378	181,965	214,791	259,735	290,118	409,652	290,395	346,901
Pressure	Bar	9,211	289,580	289,235	288,890	288,546	76,877	74,808	49,008
		E-4	E-5	E-6	E-7	E-8	E-9	TD-1	TD-2
Mass flow	kg/sec	108,565	24,885	133,450	15,343	3,750	3,750	36,304	36,304
Temperature	C	260,843	500,238	214,262	384,535	384,535	65,039	384,535	52,249
Pressure	Bar	47,539	21,381	20,739	9,494	9,494	9,494	9,494	0,138
		SS-1	SS-2	SS-3	SS-4	SS-5	SS-6	To ASU	To CPU
Mass flow	kg/sec	0,564	0,564	0,564	1,340	0,352	0,352	2,230	0,041
Temperature	C	563,864	346,901	384,535	389,700	389,700	100,009	384,535	384,535
Pressure	Bar	199,948	49,008	9,494	9,494	9,494	1,014	9,494	9,494
		From ASU & CPU		Makeup water					
Mass flow	kg/sec	2,271		6,373					
Temperature	C	176,378		25,000					
Pressure	Bar	9,211		1,014					
		CPU1-1	CPU1-2	CPU2-1	CPU2-2	CPU3-1	CPU3-2	CPU4-1	CPU4-2
Mass flow	kg/sec	192,515	192,515	192,515	192,515	192,515	192,515	158,449	158,449
Temperature	C	144,014	65,039	144,293	65,039	145,955	65,039	91,359	65,039
Pressure	Bar	3,196	3,196	10,113	10,113	32,000	32,000	37,156	37,156
Component mass flows									
O2	kg/sec	5,664	5,664	5,664	5,664	5,664	5,664	0,691	0,691
N2	kg/sec	12,638	12,638	12,638	12,638	12,638	12,638	1,266	1,266
AR	kg/sec	6,089	6,089	6,089	6,089	6,089	6,089	1,029	1,029
H2O	kg/sec	4,019	4,019	4,019	4,019	4,019	4,019	0,000	0,000
CO2	kg/sec	164,086	164,086	164,086	164,086	164,086	164,086	120,741	120,741
SO2	kg/sec	0,020	0,020	0,020	0,020	0,020	0,020	0,019	0,019
		CPU5-1	CPU5-2	ASU1-1	ASU1-2	ASU2-1	ASU2-2	FG-5	FG-6
Mass flow	kg/sec	158,449	192,515	627,288	627,288	627,288	627,288	521,633	521,633
Temperature	C	104,483	65,039	124,858	59,355	138,169	59,355	57,222	65,572
Pressure	Bar	78,000	37,156	2,382	2,382	5,600	5,600	1,030	1,010
Component mass flows									
O2	kg/sec	0,691	0,691	143,474	143,474	143,474	143,474	14,566	14,566
N2	kg/sec	1,266	1,266	466,815	466,815	466,815	466,815	32,497	32,497
AR	kg/sec	1,029	1,029	7,959	7,959	7,959	7,959	15,658	15,658
H2O	kg/sec	0,000	0,000	8,715	8,715	8,715	8,715	36,926	36,926
CO2	kg/sec	120,741	120,741	0,324	0,324	0,324	0,324	421,935	421,935

SO2	kg/sec	0,019	0,019	0,000	0,000	0,000	0,000	0,000	0,000
		FG3-1	**FG3-2**						
Mass flow	kg/sec	751,712	751,712						
Temperature	C	187,023	150,000						
Pressure	Bar	1,100	1,100						

Component mass flows

O2	kg/sec	0,730	0,730
N2	kg/sec	2,149	2,149
AR	kg/sec	0,509	0,509
H2O	kg/sec	8,244	8,244
CO2	kg/sec	11,260	11,260
SO2	kg/sec	0,032	0,032
NO2	kg/sec	0,000	0,000
H2	kg/sec	0,761	0,761
CL2	kg/sec	0,000	0,000
C	kg/sec	0,000	0,000
S	kg/sec	0,000	0,000
HCL	kg/sec	0,006	0,006
SO3	kg/sec	0,000	0,000

Figure 39

		S-1	S-2	S-3	S-4	S-5	S-6	S-7	S-8
Mass flow	kg/sec	612,541	611,977	564,407	502,848	502,848	499,648	445,165	442,665
Temperature	C	598,889	563,864	409,652	346,901	621,111	500,238	384,535	305,459
Pressure	Bar	242,330	199,948	76,877	49,008	45,216	21,381	9,494	5,012
		S-9	S-10	S-11	S-12	F-1	F-2	F-3	F-4
Mass flow	kg/sec	437,665	430,665	422,165	422,165	489,534	489,534	489,534	489,534
Temperature	C	167,814	97,516	64,192	38,726	38,389	38,541	39,034	154,000
Pressure	Bar	1,324	0,579	0,241	0,069	0,069	17,237	16,892	15,168
		F-5	F-6	F-7	F-8	F-9	E-1	E-2	E-3
Mass flow	kg/sec	612,541	612,541	612,541	612,541	612,541	47,570	47,570	60,995
Temperature	C	176,378	181,965	214,791	259,735	290,052	409,652	290,395	346,901
Pressure	Bar	9,211	289,580	289,235	288,890	288,546	76,877	74,808	49,008
		E-4	E-5	E-6	E-7	E-8	E-9	E-10	E-11
Mass flow	kg/sec	108,565	3,200	111,765	15,343	2,500	5,000	7,000	8,500
Temperature	C	260,843	500,238	192,000	384,535	305,459	167,814	97,516	64,192
Pressure	Bar	47,539	21,381	21,381	9,494	5,012	1,324	0,579	0,241
		E-12	SS-1	SS-2	SS-3	SS-4	SS-5	SS-6	TD-1
Mass flow	kg/sec	23,000	0,564	0,564	0,564	1,340	0,352	0,352	36,304
Temperature	C	50,000	563,864	346,901	384,535	389,700	389,700	100,009	384,535
Pressure	Bar	0,241	199,948	49,008	9,494	9,494	9,494	1,014	9,494
		TD-2	To ASU	To CPU	From ASU & CPU		Makeup water		
Mass flow	kg/sec	36,304	2,230	0,041	2,271		6,373		
Temperature	C	52,249	384,535	384,535	176,378		25,000		
Pressure	Bar	0,138	9,494	9,494	9,211		1,014		

		CPU1-1	CPU1-2	CPU2-1	CPU2-2	CPU3-1	CPU3-2	ASU-1	ASU-2
Mass flow	kg/sec	192,423	192,423	192,423	192,423	158,449	158,449	627,288	627,288
Temperature	C	205,913	50,000	207,594	50,000	165,777	50,000	250,190	50,000
Pressure	Bar	5,685	5,685	32,000	32,000	78,000	78,000	5,600	5,600
Component mass flows									
O2	kg/sec	6,379	6,379	6,379	6,379	1,114	1,114	143,474	143,474
N2	kg/sec	12,633	12,633	12,633	12,633	1,787	1,787	466,815	466,815
AR	kg/sec	6,090	6,090	6,090	6,090	1,521	1,521	7,959	7,959
H2O	kg/sec	4,022	4,022	4,022	4,022	0,000	0,000	8,715	8,715
CO2	kg/sec	163,280	163,280	163,280	163,280	154,008	154,008	0,324	0,324
SO2	kg/sec	0,020	0,020	0,020	0,020	0,020	0,020	0,000	0,000

		FG-5	FG-6						
Mass flow	kg/sec	521,633	521,633						
Temperature	C	57,222	65,572						
Pressure	Bar	1,030	1,010						
Component mass flows									
O2	kg/sec	14,566	14,566						
N2	kg/sec	32,497	32,497						
AR	kg/sec	15,658	15,658						
H2O	kg/sec	36,926	36,926						
CO2	kg/sec	421,935	421,935						
SO2	kg/sec	0,000	0,000						

Stream information from Figure 42

		S-1	S-2	S-3	S-4	S-5	S-6	S-7	S-8
Mass flow	kg/sec	612,541	611,977	564,407	502,848	502,848	499,648	445,165	445,165
Temperature	C	598,889	563,864	409,652	346,901	621,111	500,238	384,535	305,459
Pressure	Bar	242,330	199,948	76,877	49,008	45,216	21,381	9,494	5,012
		S-9	S-10	S-11	S-12	F-1	F-2	F-3	F-4
Mass flow	kg/sec	445,165	445,165	445,165	445,165	489,534	489,534	489,534	489,534
Temperature	C	167,814	97,516	64,192	38,726	38,389	38,541	39,034	154,000
Pressure	Bar	1,324	0,579	0,241	0,069	0,069	17,237	16,892	15,168
		F-5	F-6	F-7	F-8	F-9	E-1	E-2	E-3
Mass flow	kg/sec	612,541	612,541	612,541	612,541	612,541	47,570	47,570	60,995
Temperature	C	176,378	181,965	214,791	259,735	290,052	409,652	290,395	346,901
Pressure	Bar	9,211	289,580	289,235	288,890	288,546	76,877	74,808	49,008
		E-4	E-5	E-6	E-7	SS-1	SS-2	SS-3	SS-4
Mass flow	kg/sec	108,565	3,200	111,765	15,343	0,564	0,564	0,564	1,340
Temperature	C	260,843	500,238	192,000	384,535	563,864	346,901	384,535	389,700
Pressure	Bar	47,539	21,381	21,381	9,494	199,948	49,008	9,494	9,494
		SS-5	SS-6	TD-1	TD-2	To ASU	To CPU	From ASU & CPU	
Mass flow	kg/sec	0,352	0,352	36,304	36,304	2,230	0,041	2,271	
Temperature	C	389,700	100,009	384,535	52,249	384,535	384,535	176,378	
Pressure	Bar	9,494	1,014	9,494	0,138	9,494	9,494	9,211	

		Makeup water							
Mass flow	kg/sec	6,373							
Temperature	C	25,000							
Pressure	Bar	1,014							
		CPU1-1	**CPU1-2**						
Mass flow	kg/sec	192,423	192,423	192,423	192,423	627,288	627,288	521,633	521,633
Temperature	C	205,913	50,000	207,594	50,000	250,190	50,000	57,222	65,572
Pressure	Bar	5,685	5,685	32,000	32,000	5,600	5,600	1,030	1,010
Component mass flows									
O2	kg/sec	6,379	6,379	6,379	6,379	143,474	143,474	14,566	14,566
N2	kg/sec	12,633	12,633	12,633	12,633	466,815	466,815	32,497	32,497
AR	kg/sec	6,090	6,090	6,090	6,090	7,959	7,959	15,658	15,658
H2O	kg/sec	4,022	4,022	4,022	4,022	8,715	8,715	36,926	36,926
CO2	kg/sec	163,280	163,280	163,280	163,280	0,324	0,324	421,935	421,935
SO2	kg/sec	0,020	0,020	0,020	0,020	0,000	0,000	0,000	0,000
		FG3-1	**FG3-2**						
Mass flow	kg/sec	751,712	751,712						
Temperature	C	187,023	85,250						
Pressure	Bar	1,100	1,100						
Component mass flows									
O2	kg/sec	0,730	0,730						
N2	kg/sec	2,149	2,149						
AR	kg/sec	0,509	0,509						
H2O	kg/sec	8,244	8,244						
CO2	kg/sec	11,260	11,260						
SO2	kg/sec	0,032	0,032						
NO2	kg/sec	0,000	0,000						
H2	kg/sec	0,761	0,761						
CL2	kg/sec	0,000	0,000						
C	kg/sec	0,000	0,000						
S	kg/sec	0,000	0,000						
HCL	kg/sec	0,006	0,006						
SO3	kg/sec	0,000	0,000						